Atomistic Simulation of Hydroxyethyl Cellulose (HEC) for Enhanced Oil recovery applications

BY

Mohammed Omar Bazaid

A Thesis Presented to the

DEANSHIP OF GRADUATE STUDIES

KING FAHD UNIVERSITY OF PETROLEUM & MINERALS

DHAHRAN, SAUDI ARABIA

In Partial Fulfillment of the
Requirements for the Degree of

MASTER OF SCIENCE

In

Materials Science and Engineering

April 2020

KING FAHD UNIVERSITY OF PETROLEUM & MINERALS

DHAHRAN- 31261, SAUDI ARABIA

DEANSHIP OF GRADUATE STUDIES

This thesis, written by Mohammed Bazaid under the direction of his thesis advisor and approved by his thesis committee, has been presented and accepted by the Dean of Graduate Studies, in partial fulfillment of the requirements for the degree of **MASTER OF SCIENCE IN MATERIALS SCIENCE & ENGINEERING.**

24/11/2020

Dr. Abduljabar Alsayoud
(Advisor)

25-11-2020

Dr. Safwat Abdelazeim
(Co-Advisor)

Dr. Zuhair Gasem
Department Chairman

Dr. Abdullah Sultan
(Member)

Prof. Suliman Saleh Al-Homidan
Dean of Graduate Studies

Dr. Wail Falath
(Member)

20/12/2020
Date

Dr. Abdelsalam Al-Sarkhi
(Member)

To my parents who taught me that nothing of real value comes the easy way

ACKNOWLEDGMENTS

I would like to Thank my parents for their continuous support and encouragement

My Thesis advisors, Dr. Abduljabar Al-Sayoud and Dr. Safwat Abdelazeim, for their guide and patience, without whom this study wouldn't be possible

My fiends Gaith Nadreen and Ridwan Ahmed for the rich and informative discussions and Arguments

And all professors and friends who helped me during my MS.

TABLE OF CONTENTS

LIST OF TABLES

LIST OF FIGURES

LIST OF ABBREVIATIONS

MD	:	Molecular Dynamics
EOR	:	Enhanced Oil Recovery
cEOR	:	Chemical Enhanced Oil Recovery
HEC	:	Hydroxyethyl Cellulose
HMHEC	:	Hydrophobically Modified Hydroxyethyl Cellulose
IFT	:	Interfacial Tension
RDF	:	Radial Distribution Function

ABSTRACT

Full Name : Mohammed Omar Bazaid

Thesis Title : Atomistic Simulation of Hydroxyethyl Cellulose (HEC) for Enhanced Oil recovery applications

Major Field : Material Science and Engineering

Date of Degree : April 2020

The increasing global energy consumption along with the oil being the main source of energy worldwide emphasizes the need to develop better techniques in oil extraction. One of the most efficient technique is the chemical enhanced oil recovery (cEOR) that based on water-flooding with specific additives such as polymers and surfactants. Partially hydrolyzed polyacrylamide polymer (HPAM) is the most widely used polymer in the cEOR formulations. However, HPAM sensitivity to a high salinity brines limits its applicability in most oil fields. Herein, we study HEC, a non-ionic alternative to HPAM for cEOR application, and because of its non-ionic nature that is more salinity tolerant, and being environmentally friendly, are the most attractive features. We employed Molecular Dynamics Simulation (MD) to examine Cellulose, HEC and the Hydrophobic modification of HEC (HMHEC) it terms of back-bone chain dynamic, aggregation, interfacial properties, and the interaction with the surfactant. These simulations were done at three different conditions, which are relevant for cEOR activities; freshwater, seawater and reservoir connate water. The latter was investigated at 373K to mimic the reservoir harsh conditions. Most of the examined polymers do not show significant dynamics at the backbone level, and support that the biopolymers are somehow have rigid backbone chain. However, a significantly different aggregation behavior was observed for some systems at

reservoir conditions. In one-hand, HEC appears to aggregate even at 1wt% with the HMHEC shows a significant aggregation tendency. In the other hand, Cellulose does have the minimum aggregation tendency. Concerning the ion interactions with the biopolymers, we found that these polymers do not show any interactions with cations in the examined brines. As regard the interfacial properties of the biopolymers, they do not show a significant modification of the IFT of oil-water system.

ملخص الرسالة

الاسم الكامل: محمد عمر بازيد

عنوان الرسالة: محاكاة ذرية لأداء مركب هيدروكسي إيثايل سيلليلوز من أجل استخدامه في مجال استخراج النفط

التخصص: علم وهندسة مواد

تاريخ الدرجة العلمية: أبريل 2020

تزامنا من زيادة استهلاك الطاقة عالميا، وتربع النفط في صدارة المواد المستخدمة لإنتاج الطاقة – يليه الغاز والفحم- كان لزاما على الدول المنتجة للنفط ابتكار طرق وأساليب جديدة لاستخراج النفط المتبقي في البئر والذي لا يمكن استخراجه بالطرق التقليدية. إحدى الطرق لفعل ذلك هي استخدام مواد بوليمر وخلطها مع الماء لزيادة كثافته ثم ضخه في البئر. HPAM يعتبر حاليا البوليمر الأكثر استخداما لاستخراج النفط بالطريقة سالفة الذكر، لكن مشكلة HPAM هي حساسيته الشديدة في البيئة عالية الملوحة، وهو حال أكثر الآبار الموجودة في الخليج العربي. . في هذه الرسالة نقدم بديلا لـ HPAM وهو مركب هيدروكسي إيثايل سيلليلوز HEC وهو مركب لا أيوني، وكونه لا أيوني يعني عدم تأثره بالأملاح والأيونات في البيئة المحيطة به. لكن هناك عيب في هذا المركب وهو قدرته المنخفضة نسبيا على زيادة لزوجة الماء مقارنة بـ HPAM. الحل الذي نعرضه لهذه المشكلة هو إضافة مجموعة كيميائية لا تختلط بالماء Hydrophobic group لجعل المركب أكثر تمددا عند خلطه بالماء، وهو ما سيزيد اللزوجة. استخدمنا طريقة محاكاة الحركة الجزيئية Molecular Dynamics Simulation لنستكشف أداء هذا المركب إذا وضع في بيئات مختلفة، وهل هذا الأداء مناسب لاستخدام المركب في بيئة أبار النفط عالية الملوحة. نتائج المحاكاة الجزيئية تظهر تأييدا لاستخدام HEC في بيئة عالية الملوحة. لكن في وجود أكثر من سلسلة من هذا المركب في نفس المكان تظهر النتائج ميله للتجمع وتكوين الروابط بين سلاسل المركب نفسه، وهو سلوك يضعف زيادة اللزوجة للماء بشكل كبير. نتائج المحاكاة لأداء المركب لتقليل التوتر السطحي بين الماء والنفط يظهر أن التوتر لا يتأثر بهذا المركب، وهو ما يستلزم استخدام مادة كيميائية تسمى Surfactant مع HEC لتقليل هذا التوتر بين الماء والنفط. نتائج محاكاة الأداء لـHEC في وجود Surfactant في نفس المكان تظهر ميل HEC أكثر للتجمع بين سلاسل المركب في بيئات الملوحة المختلفة.

Chapter 1

INTRODUCTION

In 2018, “The Annual Report of Statistical Energy Consumption and Statues” by British Petroleum (BP) reported that 34% of the energy consumed worldwide comes from oil, followed by coal and natural gas with 27% and 24% respectively [1]. It is also notable to mention that renewables (Solar power, wind turbines, hydroelectricity) account for almost 11% of the energy consumption. These numbers indicate that our dependency on oil and natural gas as a major energy source is a fact, and a fact that will last for years before renewables take the lead.

Knowing these facts about oil, there is no surprise that big countries such as the US are highly investing in technologies to improve their oil production. According to Energy Information Administration (EIA)[2], the oil production in the US took a massive leap from 2012 to 2019 to make the US a net oil exporter rather than importer. This was done by applying hydraulic fracturing and horizontal drilling in shale basins to extract oil in low permeability areas. Thus, it is highly demanding for Saudi Arabia to develop better oil extraction techniques to utilize the reservoir as much as possible. This Thesis study is an attempt to expand our knowledge to achieve this.

In this chapter, an introduction about the oil extraction methods including primary, secondary and tertiary methods are briefly explained, with a bit more statics on the tertiary methods part since this is a hotspot research area nowadays. Afterwards, a deeper explanation of the chemical enhanced oil recovery (cEOR) is presented. We discuss the

method principles, currently used chemicals, more elaboration on HPAM - Hydrolyzed Polyacrylamide -literature because it is the most widely used polymer nowadays. The advantages and limitations of HPAM will be discussed. Next, we discuss a new polymer - Hydroxyethyl Cellulose (HEC)- which is nominated as an alternative to overcome HPAM limitations. Finally, we discuss HEC's drawback, that is its relatively low viscosifying ability compared to HPAM. We propose to do hydrophobic modification on HEC -adding hydrophobic groups to the polymer chain-backbone in a way that these hydrophobic modifications increases the entanglmenet of the chains, and thus, increase the viscosity of the polymer-water solution.

1.1 Oil Recovery

Oil recovery refers to the process of extracting the oil from its natural reservoir beneath the earth surface. Usually, oil recovery is divided into three main stages, depending on their time of implementation during the life of an oil field: primary recovery, secondary recovery, and enhanced oil recovery.

1.1.1 Primary and Secondary Oil recovery methods

Primary and secondary recovery methods are closely related to each other in terms of the main force driving the oil out of the reservoir, that is pressure. Primary recovery depends on the difference of pressure between the reservoir and the surface to extract the oil. Using pumps at the extraction well to draw the oil out is also considered as a primary recovery method. There are four main forces in the reservoir to exert pressure on the oil: Natural water drive, gas-cap drive, dissolved gas drive and gravity drainage.

Natural water drive can be explained in Fig 1-1. Because of the pressure drop when oil is produced, water inflow from the layers below the oil. This inflow exerts pressure on the oil, forcing it to flow to the extraction well. Usually, oil production is maintained at a certain rate to keep the ratio of (oil pressure drop) and (pressure due to water inflow) fairly constant. If the rate of extraction is high, water movement will not be able to keep up, and the reservoir pressure drops.

Gas-cap drive can be explained this way: usually oil reservoir takes a dome-like shape, where at the top of the dome natural gas accumulate while the oil resides at bottom layers -see Fig 1-1 -. When the pressure in the oil layers drops because of oil extraction, the gas at the top layer expands. This expansion forces the oil to go downward in the direction of the extraction well.

The dissolved gas drive – third drive force- works in the same way except that the gas now is initially dissolved in oil. As the pressure is dropping because of oil extraction, the gas eventually reaches a bubble point, at which gases that were trapped within the oil expands. When the dissolved gas expands, it exerts a force on the oil. Sometimes if the permeability in the reservoir is high, these dissolved gases travel upward to the gas cap area, which results in a secondary gas cap driving force.

Gravity drainage is the tendency of gas, oil and water to separate inside the reservoir due to their different densities. This separation enforces the other driving forces like natural water and gas-cap drives [3][4].

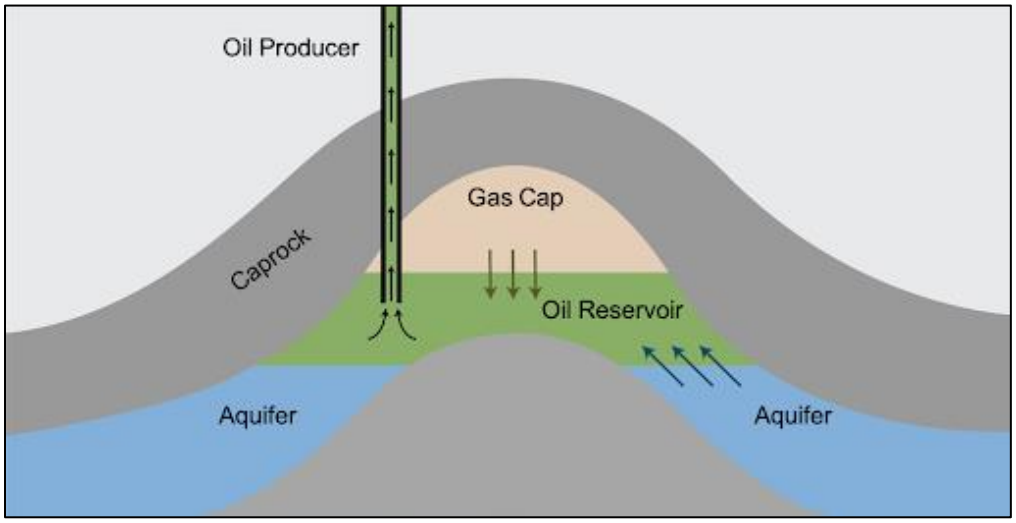

Figure 1-1 primary oil recovery driving forces (ref [3])

Secondary oil recovery methods are implemented after the production of oil drops to an unfavorable economic level. In this case, the key to maintain production is to maintain high pressure inside the reservoir. To do so, one or more of the primary drives is artificially enforced, such that either water is flooded to the reservoir to enhance the natural water drive, or gas is injected to enhance the gas-cap drive, or both. The end of the secondary oil recovery method is decided based on economic factors. On average, the recovery after primary and secondary oil recovery is in the range of 30-50%[5].

1.1.2 Enhanced Oil Recovery (EOR)

After primary and secondary recovery stages, it is not economically favorable to continue flooding water and gas to the reservoir for mechanical pressure extraction mechanism. One of two choices has to be chosen: abandon the well, or develop new techniques for oil extraction that are economically favorable. Since after the secondary stage, most of the oil remains in the reservoir, the first choice is not the best most of the time. The new techniques employed after the secondary recovery are referred to as tertiary recovery. Tertiary oil recovery -also called enhanced oil recovery- are techniques applied to further enhance the oil recovery rate. The distinguishing feature of EOR from primary and secondary methods is its tendency to alter the properties of oil such that it is easier to extract rather than exerting mechanical pressure as the main extracting mechanism. Nowadays, EOR can be classified into three main categories: gas injection, thermal injection and chemical injection. Each has its way to alter the properties of oil for easier extraction. Fig 1-2 shows several EOR projects still-in-operation globally from 2000 until 2017 [6]. The drastic jump of the number of EOR projects between 2000 and 2017 with almost 100 EOR projects difference shows the global interest in oil. This interest and

willingness to invest in recovering more oil emphasis that oil is still a significant energy source. In this section, an overview of gas and thermal injection is shown, while keeping the chemical injection at bay for the next section to be discussed in-depth.

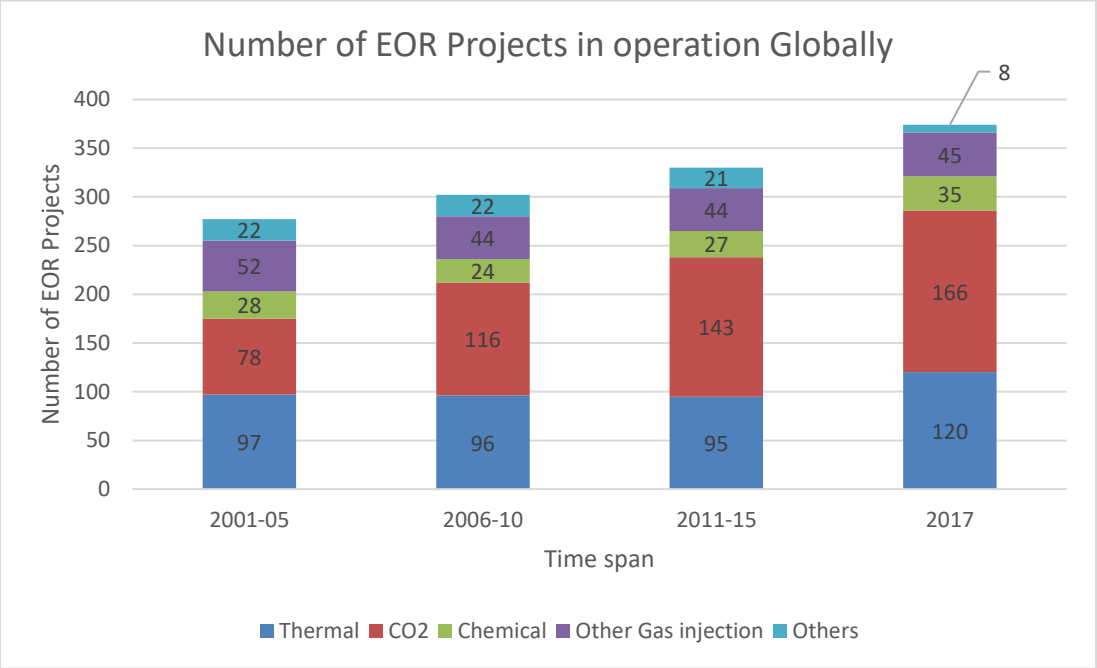

Figure 1-2 EOR project in operation globally by type (ref [6])

Gas injection works by injecting industrial gases like CO_2 or Nitrogen to the reservoir in order to mix with the oil and lower it is viscosity. This makes oil to flow easier to the extraction well. These gases also exert some pressure to help mechanically pushing the oil. Statistically speaking, CO_2 is more favored over other types of gases in gas injection, with 78% use of CO_2 in Gas injection EOR projects as of 2017 [6].

Now, CO_2 injection is divided into two types: miscible and immiscible CO_2 flooding, which one to use, it depends on the reservoir pressure. In miscible CO_2 flooding, CO_2 dissolves in the oil, forming a single phase, and the interfacial tension between oil and flooded water falls drastically, making the oil displacement process more effective. It is worth noting that CO_2 miscible flooding is considered the most effective among all EOR methods that were implemented in the USA since 2012 [7]. In immiscible CO_2 flooding, CO_2 and the oil don't form a single phase. However, CO_2 will dissolve in the oil causing the viscosity to reduce, which will improve oil displacement for recovery. Most of the time, the miscible flooding is favored over immiscible flooding. The latter is only used when the minimum miscibility pressure (MMP) – the pressure required to have a miscible solution- is too high for the miscible solution to form, that is, the reservoir pressure is lower than the MMP.

In thermal injection, various methods are used to heat the oil in the reservoir, which reduces its viscosity and increases its mobility for effective extraction. This technique is mostly used in reservoirs where the oil possesses high viscosity. The heating methods include flooding hot water, steam injection and fire flooding. In hot water flooding and

steam injection, the process is very similar to water flooding, even when steam is injected eventually it condenses to hot water. When steam is injected to the reservoir, it supplies a high amount of energy that heats the reservoir. This reduces oil viscosity, consequently the oil volume increases, making the recovery process more effective.

It is worth noting here that in recent years, the process of steam heating before flooding it to the reservoir has been done using solar power to reduce CO_2 emission. The biggest known project of this kind is the agreement between Oman and GlassPoint Solar in 2015 worth $600 million to build a solar field that will supply power to Amal oilfield for thermal injection. As of 2017, the first block of the project was completed, and the steam was successfully supplied to Amal oilfields [8]. The same solar company carried on a similar project in California to supply steam to South Belridge Oil Field in 2017. The project is targeting 12 million barrels of steam annually supplied to the oil filed, with an estimation of reducing carbon emission of 375,000 metric ton of CO_2 annually [9].

During the steam flooding there are three zones formed in the reservoir:

- Steam zone: which is located around the steam injection well, the temperature ranges from (200-400C°) depending on the flooded steam temperature. When this area get in contact with the oil, some oil evaporates than condensate, forming improved oil

- Hot condensate zone: in this area, steam starts to condensate to hot water and the formed hot water heats the oil in contact and pushes it toward the extraction well.

- Initial formation zone: the area that is not affected by heat, but is displaced mechanically due to steam injection toward the extraction well.

Fire flooding -or “in-situ” combustion flooding- is a method of thermal injection in which fire is ignited in the reservoir as the heat source. This is done by injecting a gas containing oxygen -such as air- to the reservoir and a special igniter at the bottom of injection well starts the fire. Note that without the oxygen the oil won’t burn, so the proportion of oxygen supplied to the reservoir will decide how big the ignition will be, and consequently, how much oil will be burned. The burned oil will help to heat the reservoir. Thus the viscosity of the oil will be reduced that improve the mobility and hence the recovery.

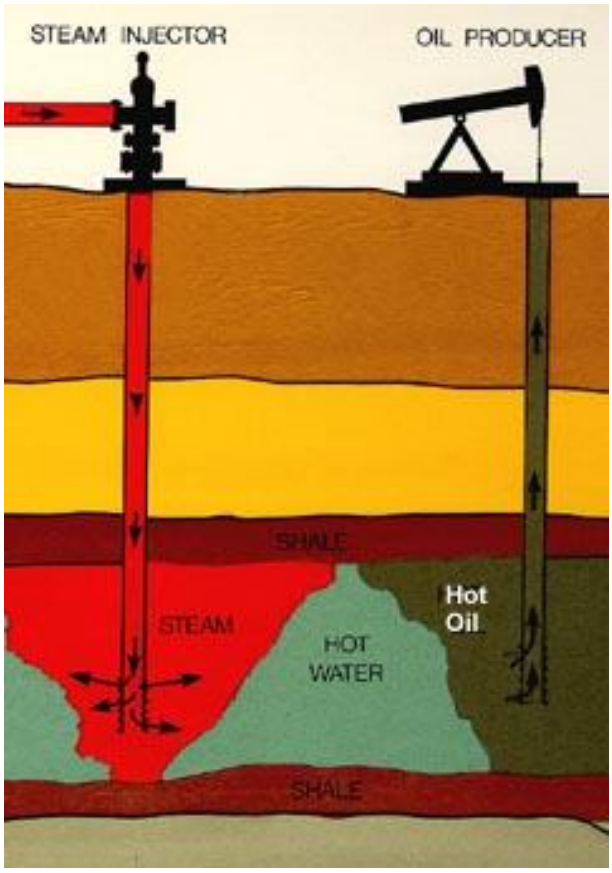

Figure 1-3 Thermal injection illustration

1.1 Chemical EOR

Chemical Enhanced oil recovery (cEOR) is a tertiary oil recovery technique that employee polymer and/or other chemicals to enhance the oil extraction. The previously mentioned Figure 1-2 shows that as of 2017, almost 9% of global EOR projects are concerned with cEOR. Other studies found a value of 11% of the global EOR projects to be chemical [10]. This shows that cEOR is not as popular as gas or thermal EOR techniques. However, this trend is changing over the last decade with the development of new cEOR techniques and chemicals such as Alkaline-Surfactant-Polymer (ASP) flooding [11–14], Surfactant polymer flooding [15] and Alkaline-Co-solvent-Polymer (ACP) flooding [16][17].

The extraction of oil using cEOR is based on two principles: the first is to increase water viscosity, and the second is to reduce the interfacial tension between water and oil. To assess why these two principles are important, it is best to see what is the situation with pure water flooding. Equation (1.1) describes the Mobility ratio M, where k_{rw} and k_{ro} are the permeabilities of water and oil, μ_w and μ_o are the viscosities of water and oil, respectively. When flooding pure water, the viscosity of water is relatively low and the permeability is high, thus, the Mobility ratio (M) will be greater than one M > 1. This results in water penetrating through oil layers in fingering pattern (Fig 1-4).

$$M = \frac{Mobility\ of\ Water}{Mobility\ of\ Oil} = \frac{krw/\mu w}{kro/\mu o} = \frac{(krw)\ (\mu o)}{(kro)\ (\mu w)} \tag{1.1}$$

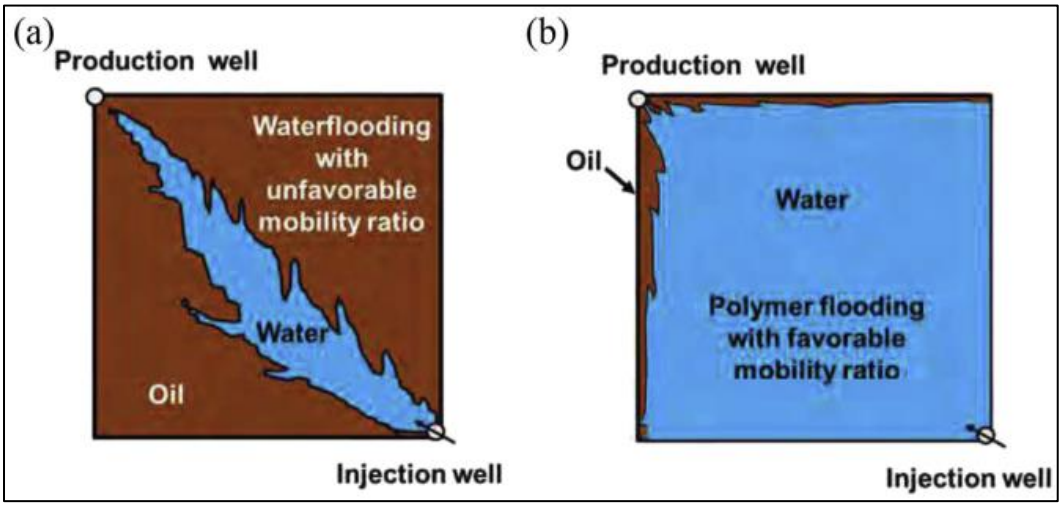

Figure 1-4 (a) unfavorable water flooding with M > 1 (water-fingring). (b) favorable water flooding with M ≤ 1, ref [14]

By definition for $M < 1$ – the mobility of water is less than or equal to the mobility of residual oil-, the flooded water flow in a piston-like behavior, which increases the oil sweeping efficiency [10][14]. From equation (1.1) to decrease the mobility ratio, we should either make the oil less viscous -gas and thermal EOR-, or increase the viscosity of flooded water. This is the reason for adding polymer in cEOR fromulations.

For the second principle, it is well known that water and oil are immiscible. As a result they don't mix, and this prevent them from displacing one another effectively. The same immiscibility nature of water and oil makes it hard for water only to clean oily hands. Speaking with more engineering terms, the high interfacial tension (IFT) between water and oil is the root cause of this immiscibility. If IFT is low enough, water and oil from a miscible mixture, and thus, enhance the oil recovery process.

Another issue concerning the natural high IFT is the capillary forces between oil and formation rock. Naturally, when pure water is flooded, these capillary forces results in a high residual oil saturation -oil is sticking to the formation rock-. These capillary forces can be represented with a capillary number in equation (1.2), where (v) is the brine velocity, (μ_w) is the water viscosity, (σ_{ow}) is the oil/water interfacial tension, and (θ) is the contact angle between the phase and the rock [14]. From the equation, it can be interpreted that the lower the IFT (σ_{ow}), the higher the capillary number, thus, higher viscous forces compared to capillary forces. As a result, more residual oil is recovered. Some polymers can naturally reduce the IFT at the water/oil interface. However, most of the time it is more convenient to use another chemical to be mixed with the flooded water along with the polymer. That chemical is called surfactant (Surface active agent).

$$Nc = \frac{viscous\ forces}{capilary\ forces} = \frac{(v)(\mu_w)}{(\sigma_{ow})(cos\theta)} \quad (1.2)$$

The role of surfactant is primarily to reduce the IFT at water/oil interface. Surfactants consist of two chemically distinct groups, a hydrophobic part that gets immersed in oil, and hydrophilic part -or polar part- that is immersed in water. Fig 1-5 shows an example of the conformation that surfactant takes at the water/oil interface. This arrangement significantly reduces the IFT at water/oil interface to form an "encapsulation" of oil inside the water to be flooded to the extraction well.

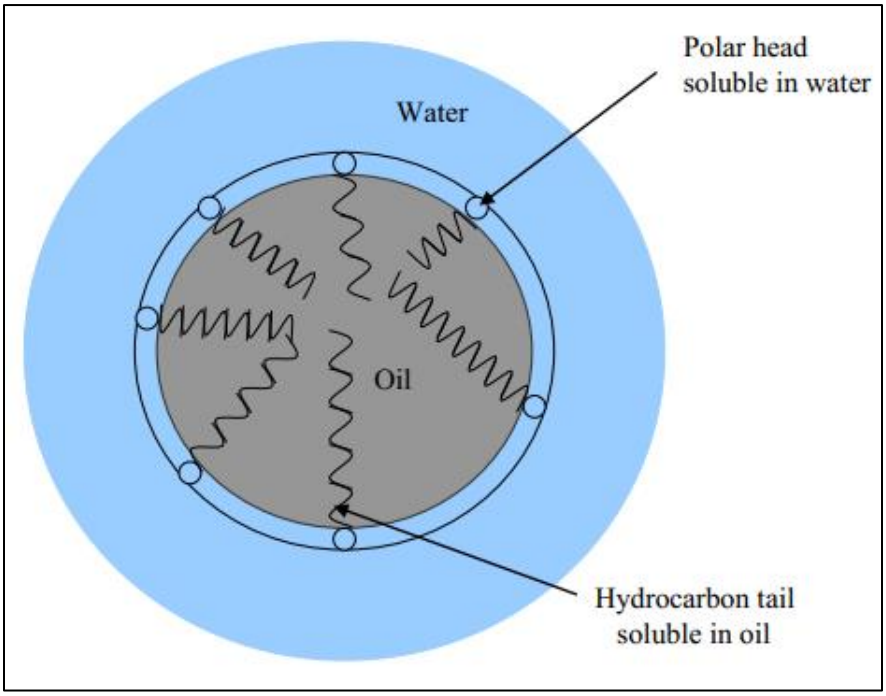

Figure 1-5 Arrangement of Surfactant to reduce IFT, ref [14]

Generally, polymers used in cEOR can be divided into two categories: bio-polymers and synthetic polymers. Bio-polymers are environmentally friendly, and are attractive as a cEOR option for their availability and insensitivity to the brine salinity. The limitation of this class in cEOR fromulations, is their susceptibility to degradation both chemically – acids in the reservoir- and biologically -bacterial attack. Currently, Xanthan gum is the most commonly used bio-polymer in EOR field. However, other Cellulose-derived polymers have been developed in recent years for cEOR application such as Hydroxyethyl Cellulose, and Hydroxypropyl Cellulose, and their hydrophobic modification.

The second type is the synthetic polymers such as acrylamide-based polymers. Currently, synthetic polymers are more dominantly used in the oilfield due to their chemical and biological stability compared to biopolymers, and their lower cost. The most used polymer currently is the partially hydrolyzed Polyacrylamide, HPAM for short. As it is the main polymer in the field, we should speak about it in more depth.

1.2 HPAM

Polyacrylamide (PAM) is a non-ionic polymer of which many synthetic polymers employed in cEOR are derived from. Hydrolyzed polyacrylamide (hydrolysis of PAM group into carboxylate) is considered currently as the most widely used polymer in cEOR applications. The structure of both PAM and HPAM can be seen in Fig 1-6, where (m) represents the degree of hydrolysis. The hydrolysis process takes place by converting of some of PAM group into acrylate group. The hydrolysis ratio determine the amount of acrylate to PAM along the polymer backbone. Both PAM and HPAM are used for cEOR applications with both having their limits. PAM has higher tendency to be absorbed by

formation rock, while HPAM is absorbed more frequently on calcite than PAM [18]. HPAM, however, has the electrostatic repulsion between negatively charged carboxylate groups the backbone, which results in an extended polymer conformation. This extended state increases the viscosity of the injected fluid much better than PAM polymer.

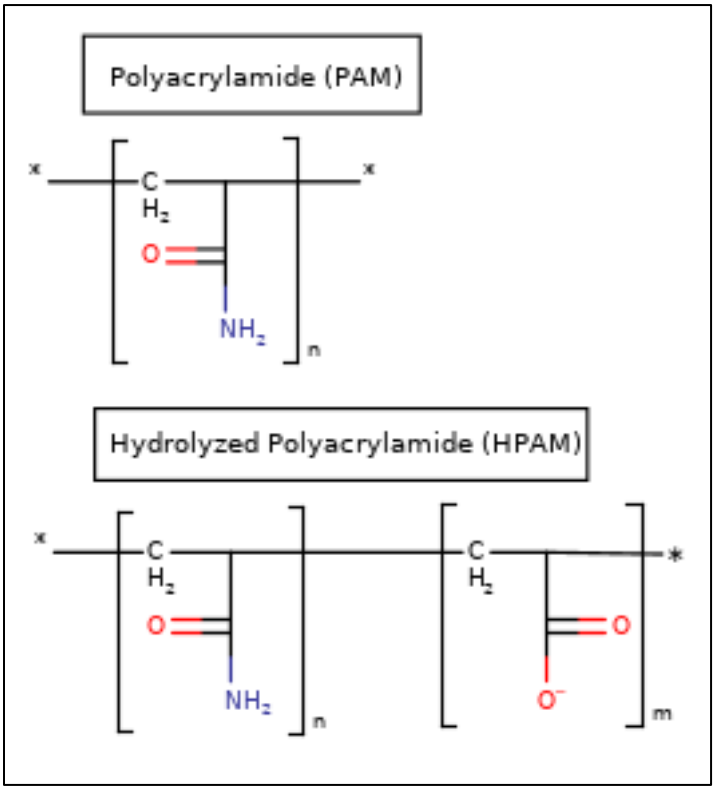

Figure 1-6 PAM and HPAM chemical structure

Usually, for EOR applications, the hydrolysis degree for HPAM is around 25%, although hydrolysis degrees in commercial products can range from 15% to 35% [19][20]. Previous studies [21][22] shows that with a higher degree of hydrolysis the solution viscosity is expected to be higher until around 30% to 40%, after this limit the viscosity starts to decrease. A follow-up study [18] showed that the reason for this reduction of viscosity after the 40% limit is due to the strong disturbing of the flexible chains of the polymer with a high number of carboxylate groups in the backbone. In addition, the high amount of negatively charged carboxylate groups results in a stronger interaction with cations that leads to polymer precipitation, or at least viscosity reduction [23–26]. There are many attractions to use HPAM in cEOR applications, that includes its chemical and biological stability, its high shear resistance and low capital cost, as well as being a soluble polymer and a good viscosifier.

Despite the benefit of using HPAM in EOR, as the oilfields become more mature and the development of these fields become deeper, harsh reservoir conditions limit HPAM from fulfilling its purpose as a viscosifier. As discussed previously, HPAM is negatively charged, and the high salinity of many reservoirs prevents the usage of HPAM under these conditions. At harsh reservoir conditions, HPAM interacts strongly with the brine cations, especially the divalent that enhance significantly the apolymer aggregation, which reduce the viscosity of the injected fluid.

In addition, recent studies showed that HPAM viscosity is molecular weight dependent. Several HPAM polymers of various molecular weights have been synthestized. [19][27] This results in a very high molecular weight polymer (>10,000 kDa), making HPAM vulnerable against shear degradation during flooding. The long HPAM chains are trimmed

to shorter ones, which reduces the molecular weight of the polymer. Consequently, HPAM losses its viscosifying source of power.

These limitations show that a modification or an alternative to HPAM is required if cEOR is to be employed in mature oil fields. Many studies modified HPAM in different ways to enhance its performance in cEOR. One of these modifications includes adding a hydrophobic group to establish an intermolecular association – Fig 1.7 – that significantly enhance the viscosity when the concentration of the polymer is high enough to establish this association [28][29]. The other modification incorporates a more stiff and rigid monomer to be synthesized with the acrylamide monomer, these stiff monomers possess higher resistance to cation shielding and can maintain better-extended conformation at high salinity [26][30].

Hydroxyethyl Cellulose (HEC) is a non-ionic bio-polymer, and its non-ionic nature is the key factor to solve the ionic sensitivity of HPAM. In addition to its non-ionic nature, HEC is considered an environmentally friendly alternative in cEOR application. When compared to HPAM, a study reported that HEC can be easily modified chemically for manufacturing different derivatives [31]. When compared to other bio-polymers, specifically Xanthan gum, HEC doesn't have injectivity issues. When producing Xanthan gum by the fermentation process, some cellular debris remains after the process. This cellular debris are considered a waste material, and causes injectivity issues and plug pore in low permeability formation zones.

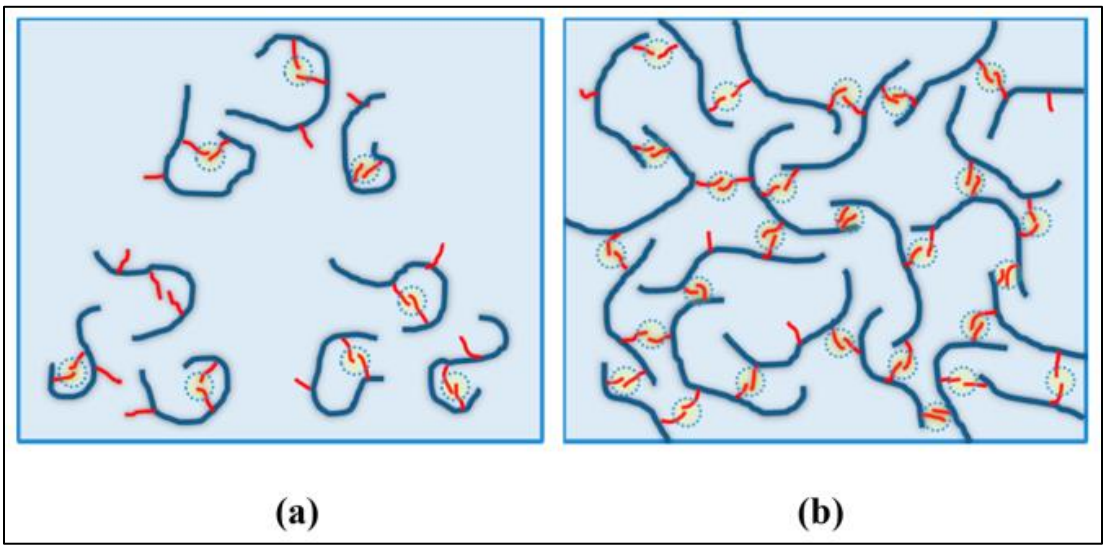

Figure 1-7 Shows two configurations for polymer soultions; a) at low concentration and b) at high concentration. The chains entaglment (associations) increased as the polymer concentration is increased. (ref [29])

1.3 Study Objectives

In this study, we are trying to understand and charachterize HEC as an alternative polymer to HPAM for cEOR applications. The main motivation behind our investigations is to solve the HPAM high sensitivity to the high salinity brines, for which HEC is very tolerant. We seek to study the applicability of HEC, and its hydrophobically modified version for EOR application. To achieve this, we employed MD simulation to investigate the behavior of cellulose, HEC and hydrophobically modified HEC under three different environments: freshwater, seawater, and reservoir or connate formation water. We also consider high temperature high salinity reservoir conditions. Our milestones are to achieve the following:

- Study the dynamics behavior of the chain backbone of Cellulose, HEC and HMHEC to examine the rigidity or the flexibility of the polymers under different environments.
- Conduct simulations on multi-chain systems of Cellulose, HEC and HMHEC to observe the aggregation behavior of these polymers under different environments, and probe the effect of concentration and environment on this behavior
- Investigate the interfacial properties of these polymer at water-oil system interface, more specifically the impact of these polymers on the IFT of water-oil under different environments.
- Examine the effect of adding a surfactant to the phase behavior of water/polymer solution.

Chapter 2

LITERATURE REVIEW

Hydroxyethyl cellulose is the candidate we are characterizing as an alternative for HPAM for cEOR applications . In this section, an overview of the past and current literature research with details about HEC is presented. In addition, we will discuss the results of these studies and what different problems or techniques they are trying to tackle. We will also review studies for other applications where the properties investigated can be used to further enhance the employment of HEC in cEOR. An overview of the HEC applications in literature weather in field, or lab-scale experiments will be presented.

2.1 On-field application

The Only implementation of HEC on-field to the best of the author's knowledge is the water-flooding HEC based in Romashkino field in Tartarstan, Russia [32]. In this oil field, over 180 well were flooded with 3500 tons of HEC over the course of 5 years (1992-1997) and the additional oil produced reached 1,000,000 tons, with an efficiency of almost 377.7 (tons of oil) / (ton of HEC flooded) at the time when the study was published. The amount of flooded HEC and the rate of injection to the well varied significantly depending on the well's formation structure. Also, the efficiency of recovery process varied drastically between different wells flooded, and the highest reported efficiency was 3,952 tons/ton, while the average as stated previously was 377.7 tons/ton the authors didn't explain the reason behind this trend . The Romashkino oil field is considered one of the largest in Russia with a net production since the oil extraction started has reached 2.5 billion ton, with the remaining reserved estimated to be 1.8 billion ton. The conditions of the reservoir

highly decided how the recovery process has to be carried out. The temperature of the reservoir was about 36°C, the oil viscosity was about 2-3 cp, and the salinity was 250 g/L TDS. The low temperature and high salinity of the reservoir makes HEC a better candidate over HPAM as it would precipitate due to high salinity. The study also pointed out something important about the storage and solubilisation of HEC. As with any polymer, it was supplied to the field in a powdery form, and stored in an inert nitrogen-rich atmosphere until it should be used. When it's time to use HEC, it could be solubilized using simple mixing tools, unlike polyacrylamide polymers that requires specialized protocols to be mixed properly [33]. It's worth noting that the relatively low oil viscosity in the reservoir is an indication that polymer flooding can be used in this field compared to other EOR methods like thermal which is favored for heavy oil reservoirs (>150 cp).

2.2 HEC-Experimental

Most experimental literature for HEC isn't concerned with HEC itself, rather, it's hydrophobic modifications. These studies use the behavior of HEC as a measure to show how good the modification is, in terms of rheological and viscosifying properties. Herein we discuss some of the research done on HEC and its modification that was done experimentally, from the discussed papers, one can grasp the current situation and the trend for studying HEC and its hydrophobic modification.

Bai et al. (2012)[34] studied the effect of hydrophobically modifying HEC with 14 aliphatic carbon chain in an amount varying from 0.2% – 2.0% on its viscosifying capacity and rheology for EOR application. The molecular weight was varied also -720k, 1000k, 1300k Dalton- to find the combination of hydrophobic modification amount and a molecular weight that shows the most promising results. Sand-pack core flooding test was

employed to study the oil recovery performance. Their results show that the higher the molecular weight, the better oil recovery performance. For the hydrophobic modification, it is observed that up to 1.0% hydrophobic amount in the chain showed good oil recovery, above this amount, showed significantly lower oil recovery. The best combination for oil recovery was 1300k molecular weight with 0.85% hydrophobic grafting ratio in the chain, while the worst was 720k and 1.4% respectively.

Bai et al. (2018)[29] synthesized hydrophobic HEC with 12 aliphatic carbon chain as the hydrophobic group. The first aim of this study is to investigate the effect of polymer concentration and temperature on viscosity. The second aim in their study is to test the oil recovery performance by sand-pack core experiment to optimize the injecting parameters -injecting rate, injection concentration-. Their results showed a proportional relation between the polymer concentration and the solution's viscosity. The hydrophobic modified HEC had higher viscosity compared to unmodified HEC with any polymer concentration. Their study also observed that once the concentration of HMHEC exceeds a certain amount referred to as the Critical Association Concentration (CAC), the hydrophobic polymer takes a supramolecular structure. This supramolecular structure increased the viscosity of HMHEC 10 times compared to HEC at the concentration 4,000 mg/L -635 cp and 61 cp- and 20 times at the concentration 10,000 mg/L -4,230 cp and 216 cp respectively-. The effect on the interfacial tension at the water/oil interface was also studied, they observed a reduction of IFT in the HMHEC above the CAC at 4,000mg/L – the value of IFT was 54-55 mN/meter- compared to HEC – 63 mN/meter. This reduction in IFT showed emulsification of oil and water in the single phase when the sand-pack core experiments were conducted for HMHEC.

Liu et al. (2017)[31] compared the oil displacement efficiency of HMHEC with HEC and HPAM in a core-flooding test, the experimental conditions pressure and temperature were to match the same conditions as the PuTao well in Daqing oil field in China to make the experiment as realistic as possible. The results showed that when the concentration of HMHEC was above 4,000mg/L, it outperforms the rheology properties of HEC and HPAM. Also, the oil recovered from core-flooding tests was 7-14% more oil recover compared to HEC and 67% better oil recovery compared to pure water flooding.

Another trend in the literature to further enhance the viscosifying ability of HEC, and thus, the oil recover performance, is to combine hydrophobic and hydrophilic modification in the same chain. Akiyama et al. (2007)[35] followed this procedure in their study to find the combination of hydrophobic/hydrophilic modification that shows the most promising results. The hydrophobic group was aliphatic carbon chain, and the hydrophilic was sodium sulfonate group. Their results show remarkably higher viscosities even to the values in Bai (2018). At the highest hydrophobic/hydrophilic ratio of 0.059 and the highest tested polymer concentration of 0.5wt% the viscosity of the solution was 33,900cp. Recall that Bai (2018) had a viscosity of 4,230 cp at 10,000 mg/L. This shows that this technique can achieve much higher viscosities compared to only hydrophobically modifying HEC. However, the molecular weight used in this study was ~$1.65*10^6$ Da, which is much higher than what Bai (2018) reported (370kDa).

Anna et al. (2008)[36] also followed a different approach to enhance the viscosity of HEC. In addition to the hydrophobic modification of HEC, they added a negatively charged group to the chain backbone. Their theory is that the negatively charged moieties should repel each other, resulting in a more extended chain compared to the non-ionic

chain. They compared their new charged to the same hydrophobically modified HEC but without the charged group to examine the effect of the negatively charged group on the viscosity. Their results concluded that, compared to non-ionic HMHEC, the charged HMHEC showed stronger viscosifying ability even at low concentrations. They observed at 0.5wt% (HMHEC-) had 10,000 times higher viscosity compared to HMHEC or HEC. Numerically speaking, (HMHEC-) at 0.5wt% had a viscosity of 100,000 cp while HMHEC non-ionic and HEC had viscosity around 10 cp each. The authors mentioned a similar limitation of this polymer to that of HPAM, which is the low salinity tolerance. The authors also state that below 1wt%, the uncharged HMHEC had viscosity lower than that of HEC, but above this concentration the supramolecular structure forms in HMHEC and enhance the viscosity significantly.

Zhao et al. (2005)[37] studied the interaction of two non-ionic surfactants -C12E5 (pentaethylene glycol monododecyl ether) and C12E6 (hexaethylene glycol monododecyl ether)- with HMHEC. Their goal was to investigate the correlation between the molecular interaction with the surfactant and the flow behavior. The results showed that the viscosity of the system HMHEC-surfactant increased with increasing the surfactant up to 0.01% of surfactant in the system. Above this concentration, the surfactant disturbs the supramolecular structure and cause the viscosity of the system to fall drastically.

Up to the author's knowledge, no study in the literature tackled studying HEC and its modification with computational simulation. Our study is the first computational study that targets investigating the behavior of HEC and HMHEC for EOR application. Computational simulation can give very fine details about which atoms are interacting with

which. This study gives insights and explanations about the physics of HEC and HMHEC to be used in EOR applications.

Chapter 3

COMPUTATIONAL METHOD

This section is dedicated to explaining the theoretical part of this study, and it is divided into three parts: the first will explain the theory used to carry out this study, which is the Molecular Dynamics (MD) Simulation. The second part will illustrate the properties we will look at in this study and why we chose them to describe the polymer behavior. The third part will give the general scheme of the computational details used in this study.

3.1 Molecular Dynamics Simulation

Molecular Dynamics is a simulation technique that studies the movement of atoms and molecules to extrapolate the macroscopic averaged properties from the microscopic behavior. The physics used in MD is the classical physics, namely Newton's second law of motions, where atoms move in the system under the influence of forces exerted on it. The Hamiltonian equations are the main equations used to calculate the energy of the system, the forces exerted on the atoms, and determine the direction of movement. These equations are a re-write of Newton's laws of motion such that it is more convenient to describe the system using MD simulations.

The position and momentum are the two primary data form MD simulation, based on which most of the properties are calculated. The position of each atom (r_i) and momentum (p_i) are calculated using the following equations:

$$\dot{\vec{r}}_i = \frac{\vec{p}}{m_i} \tag{3.1}$$

$$\dot{\vec{p}}_\iota = \vec{F} \tag{3.2}$$

Where $\dot{\vec{r}}_i$ is the first derivative of position, $\vec{p}$ is the momentum, m_i is the mass of atom (i), $\dot{\vec{p}}_i$ is the first derivative of momentum, $\vec{F}$ is the resultant force acting on atom (i). The force between two atoms is minus the gradient of the interatomic potential between these two atoms. The force used in equation 3.2 is the sum of the forces exerted on an atom by its neighbors and is calculated using the following equations:

$$\vec{F}_i = -\nabla \, \mathrm{V}(\mathrm{r}_i) \tag{3.3}$$

$$\vec{F} = \sum_{i=1}^{N-1} \vec{F}_i \tag{3.4}$$

Where N is the number of atoms. To exclude self-interaction N-1 is used. The interatomic potential V(r) can either be calculated using first-principle calculations or by fitting to the experimental data. The interatomic potential is a critical parameter since it describes the physics of the system, which has to be done accurately. If the potential doesn't represent the true nature of the relation between atoms, the forces calculated based on these potentials will be incorrect, and thus the positions and momentums of atoms, and the general behavior of the system will not represent a real system.

The total energy of the system is calculated using Eq. 3.5. The Hamiltonian (H) represents the total energy of the system, that is the sum of potential and kinetic energies:

$$H(\{r_i\},\{p_i\}) = V(\{r_i(t)\}) + \sum_{i=1}^{3N} \frac{p_i(t)^2}{2m_i} \tag{3.5}$$

Based on the introduction above, to begin an MD simulation, two things are needed: first is an initial configuration and velocities, second is the interatomic potential. The initial configuration depends on the system to be simulated and the goal the simulator has in mind to pursue. The velocities of the atoms could be defined to follows a Gaussian distribution that depends on the temperature of the system. As said previously, interatomic potential -also called Force Field (FF)- is a critical parameter, the simulator should always verify and convince the readers that the potential chosen simulate real systems behavior correctly. It is similar in experimental studies where the conditions of the experiment should be explained to the readers to convince them that the results are accurate. One way to verify the force-field in simulation is to re-generate experimental data using simulation with the chosen potential or the general trend of the experimental observations. There are many potentials available in the literature that can be used for aqueous systems, such as CHARMM, GLYCAM, GROMOS, OPLS-AA, etc... Each potential has its strengths in simulating certain types of systems, and limitations of not being able to do so with other systems. For example, the literature has comparisons between these potentials in simulating proteins or polysaccharides [38].

Fig 3-1 summarizes the steps of MD simulation. Starting with the initial configuration, we calculate the force on each atom using equations 3.3-3.4, then using equations of motion 3.1-3.2 we can find the new positions and velocities. The exact integration of the equations of motion in the computational world is done using algorithms, which are explained extensively elsewhere [33][34] and out of the scope of this brief explanation. The new positions and velocities are saved frequently during simulation, and will be the bases for finding the properties of the system. After finding the new positions and velocities, the

simulator can either stop the simulation or re-calculate the force using the same procedure and find the next position and velocity, until he is satisfied with the simulation length.

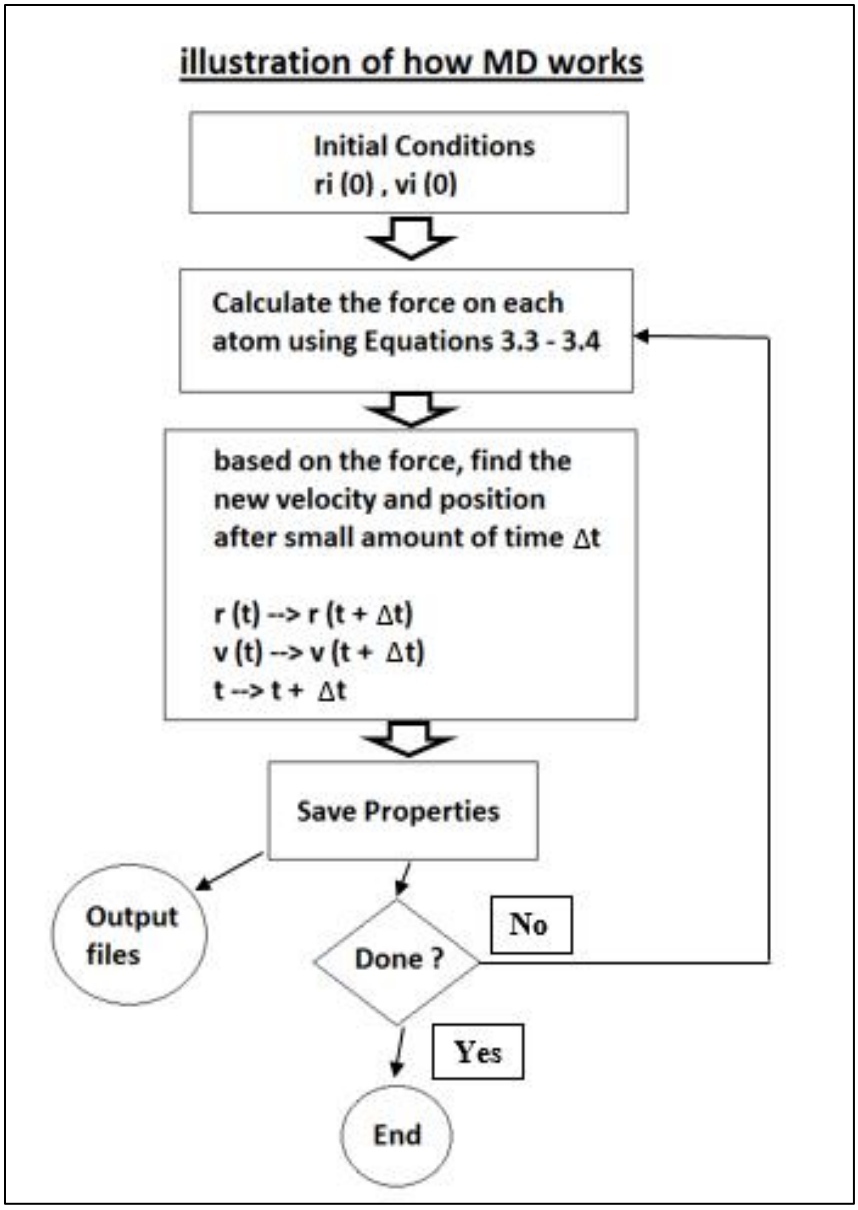

Figure 3-1 General scheme of MD simulation.

The next thing to explain is what kind of information the potential – the force field – contains exactly for aqueous systems. The explanation here will be concerned about the general picture, and not to discuss the very fine details. The type of interaction can be divided into two parts: bonded interactions, and non-bonded interactions. Both interactions are shown in equation 3.6:

$$V(r) = \sum_{bond-stretch} \frac{1}{2} k_r \left(r - r_{eq}\right)^2 + \sum_{bond-angle-bending} \frac{1}{2} k_\theta \left(\theta - \theta_{eq}\right)^2 + \sum_{bond-rotation} \frac{vn}{2} [1 + \cos(n\varphi - \gamma)] + \sum_{non-bonded} [\frac{A_{ij}}{r_{ij}^{12}} - \frac{B_{ij}}{r_{ij}^{6}} + \frac{q_i q_j}{\varepsilon_{ij} r_{ij}}] \quad (3.6)$$

The first three terms represent the bonded interaction, while the forth represent the non-bonded interaction. Fig 3-2 illustrates the bonded interaction meaning physically. The first two terms are simulated in spring-like behavior. The first term is the strength between two atoms with k_r as the spring constant and r_{eq} as the equilibrium position. The same can be said about the second term, which is the strength of the angle between three atoms. The third term represents the dihedral angle strength or the resistance of twisting the angle between four atoms. The fourth term is the non-bonded interaction term, and it represents the Van der Waals interaction $\boxed{\frac{A_{ij}}{r_{ij}^{12}} - \frac{B_{ij}}{r_{ij}^{6}}}$ and columbic interaction. $\boxed{\frac{q_i q_j}{\varepsilon_{ij} r_{ij}}}$

The purpose of the above illustration is to notify the reader about what forces and interactions are considered while doing MD. It should be notified that electrons aren't considered in classical MD simulations,. Another field of computational simulation is concerned with this kind of interaction, that can be found elsewhere [35][36].

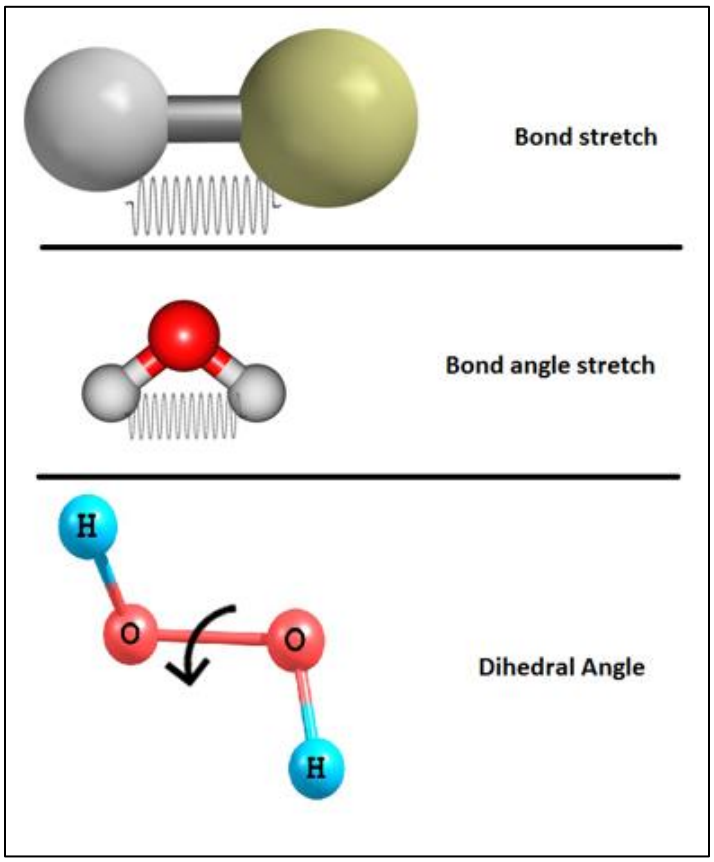

Figure 3-2 the bonded interaction in force field potential.

3.2 Investigated properties

In this section, we will present the properties, which we are interested in to examine the polymer phase behavior. The three main properties are: the dynamic properties, aggregation properties, and interfacial tension. The details are to be discussed next.

3.2.1 Dynamic Properties

The properties we looked at to analyze the dynamics of the polymer chains are 5 properties: Radius of gyration, end to end distance, dihedral angle distribution for side group, intra- and interchain hydrogen bonds.

The radius of gyration is the mean radial distance of all atoms in the polymer chain with respect to the chain's center of mass. The higher the radius of gyration means the chain takes a more extended state, while lower values mean the chain takes a more compact state.

The end-to-end distance is also used to look at the conformation of the polymer form a different angle. Fig 3-4 represent the end-to-end distance physically. The radius of gyration and the end-to-end distance are tracked as a function of time to observe how the polymer conformation is changing. For simulation with more than one chain, the average end-to-end distance is calculated.

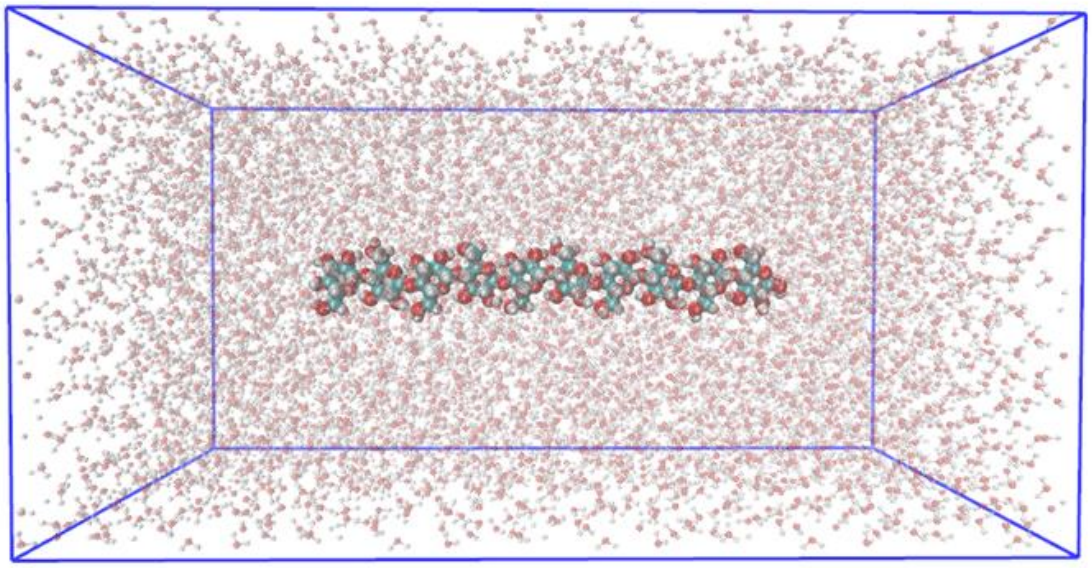

Figure 3-3 Cellulose solution (deionized water).

.

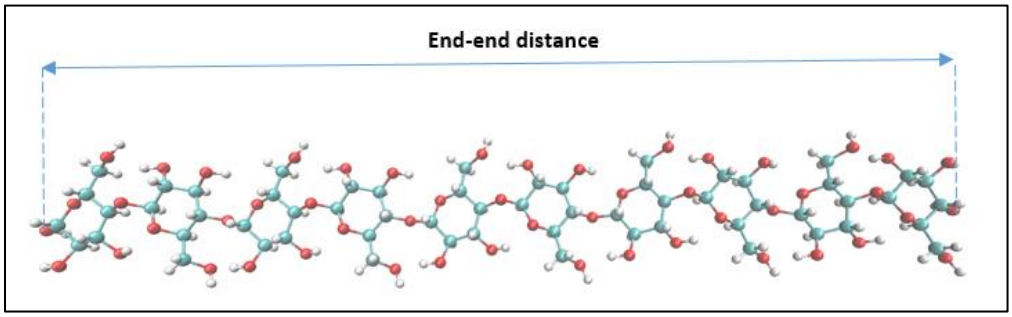

Figure 3-4 End to end distance definition of apolymer chain

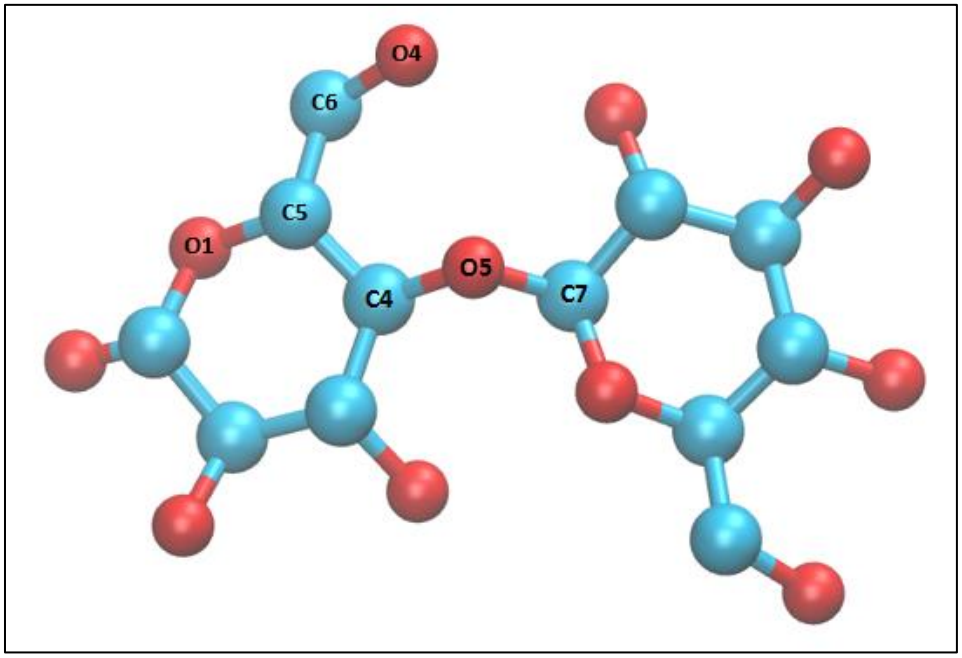

Figure 3-5 the building unit of cellulose.

Dihedral angles: The dihedral angles distribution of the side group (O1-C5-C6-O4) and the backbone (C5-C4-O5-C7) will be used in order to investigate the flexibility of the side and backbone chains [37][38].

The intra- and interchain hydrogen bonds: The density of hydrogen bonds around the polymer chains will give deeper insights on the molecular interactions that are connected to its flexibility, and its solubility. For these properties, we want to see the polymer behavior under different salinity conditions to observe how the salinity is affecting the polymer's rigidity and hydration.

3.2.2 Aggregation properties

We are also investigated the tendency of the polymer chains to aggregate because it is tightly linkted to its macrospcopic property such as viscosity. In these simulations, two properties are looked at: the number of clusters, and the average size of the cluster. The number of clusters shows how many bulk fragments of the polymer are presented in the system. For example, if a system has two chains sticking together while the other two are separated, the number of clusters here will be 3. If the other two are also sticking together, we would have 2 clusters, and so on.

The average cluster size indicates overall the average aggregate size that is formed along the MD trajectory.

3.2.3 Interfacial Tension (IFT)

The interfacial tension is discussed previously in this study in section 1.2. Usually, the lower the IFT at the oil/water interface, the better the oil recovery process. Herein we looked at the effect of adding polymer to the IFT between water and simulated oil. The model we used for oil represent light oil model make by Kunieda et al. [45], the composition of the oil model is shown in TABLE I. The model was modified proportionally if the system is big. An general overview of the IFT simulation system is represented in Fig 3-6. In studying the IFT, we monitor it in different conditions of salinity as well.

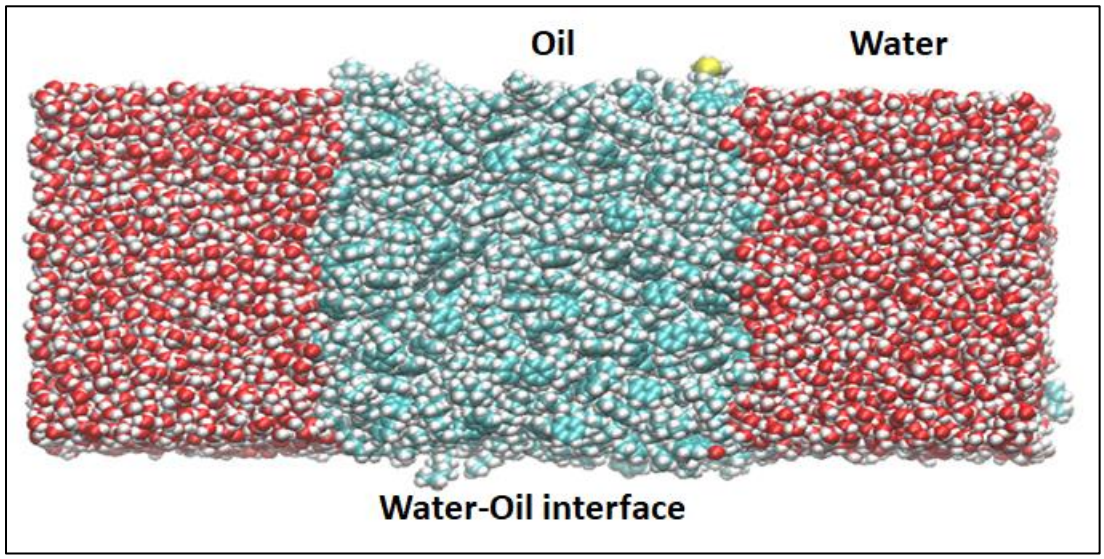

Figure 3-6 IFT system model overview

TABLE 3-1 Composition of Oil model	
Component	**Number of molecules**
Hexane	288
Heptane	264
Octane	312
Nonane	360
Cyclic Hexane	192
Cyclic Heptane	312
toluene	312
Benzene	120

3.3 Computational Details

The general scheme for conducting the simulation -after having the configuration and the potential ready- consists of 4 steps:

- Energy minimization
- Equilibration (NVT + NPT)
- Production MD (NVE)
- Analysis

Each step will be briefly explained in this section.

3.3.1 Energy minimization

The purpose of energy minimization is to relax the initial structure to minimize the forces induced by atoms on each other by finding a structure that is energetically favorable. This can be done by using different algorithms such as the steepest descent method or the conjugant gradient method [42]. Both methods aim to reduce the residual forces by moving the atoms in small steps to new positions with less total residual forces in the system. Bassically a sort of optimization of the system coordinates using its energy as a fitting score.

3.3.2 Equilibration (NVT + NPT)

The purpose of equilibration is to stabilize the system at a certain temperature and pressure. NVT means simulation at a constant number of atoms N, constant volume V and constant temperature T, which is called canonical thermodynamics ensemble. For NPT the pressure is constant and the volume can vary (isothermal-isobaric ensemble). These two-equilibration simulations are carried in the same order to equilibrate the system at a certain

temperature and pressure, respectively. In this step, velocities corresponding to the desired temperature are assigned to atoms in the system such that the velocity distribution follows a Maxwell-Boltzmann distribution. After stabilizing the system at the desired temperature, the system should be stabilized at a specific pressure.

3.3.3 Production MD

All restrictions on atoms movement are removed and the system is left to behave in accordance to the potential and forces between atoms. The length of production simulation is considerably longer than equilibration simulations most of the time. The exact length of production MD depends on the nature of the system and the property of interest.

3.3.4 Analysis

We have done structural and thermodynamics analysis of the simulated polymer solutions. The properies of interest are mentioned earlier. We have used the available analysis tools in GROMACS package.

Chapter 4

Result & Discussion (Paper Manuscript)

Abstract

Hydroxyethyl cellulose (HEC) is a non-ionic, environmentally friendly polymer that is used for oil recovery applications. We seek to investigate the properties and behaviour of the polymer (HEC) for Enhanced Oil Recovery applications (EOR). Molecular dynamics (MD) simulation is used to investigate the phase behavior HEC and its interfacial properties under different salinity and temperature conditions. Three polymer concentration solutions were used in order to find the optimal one for better performance. We studied the dynamic behavior, aggregation behavior, viscosifying ability, interfacial tension effect and surfactant "Sulfonate" interaction with cellulose and HEC. We have also benchmarked HEC against Cellulose taken as reference case. The outcome of our simulation is the link between the atomic structure and the macroscopic properties of the polymer in order to tune these properties for better EOR performance.

Keywords

Enhanced Oil recovery (EOR) - Hydroxyethyl cellulose (HEC)

Molecular dynamics (MD) – GROMACS – Chemical EOR

4.1 Introduction

Depending on the oil reservoir specific conditions, primary oil recovery can produce about 15% on average of the residual oil. To improve this recovery, maintaining the pressure of the oil reservoir is the key factor. Secondary oil recovery, also known as improved oil recovery, done by injecting water or gas to the reservoir, can increase the recovery factor by up to 35% [14][40]. Tertiary recovery, also known as enhanced oil recovery (EOR), done by injecting industrial fluids such as CO_2, nitrogen, water-polymer solution, etc. can increase the recovery factor up to 70%.

Because of its much higher recovery factor, EOR is an important research field to find the best methods for implementation and investigate solutions for problems that arise in this field. EOR is divided into subcategories and each subcategory include different methods. One used EOR subcategory is the Chemical Enhanced Oil Recovery (cEOR). It uses a water-polymer mixture and/or other chemicals to be flooded into the oil reservoir through an injection well to push the oil to the extraction well. The main difference between this flooding and water flooding in the secondary stage, is that in EOR, the key factor is altering the properties of the oil to make it easier to extract. The purpose function for which we add polymers to the injected fluid is to increase the water phase viscosity in order to decrease the mobility ratio and hence improves the sweep efficiecncy. When polymers are the only chemicals flooded with water, the process is called “polymer flooding”. If the solution is combined with a surfactant, it is called “polymer-surfactant flooding”. Sometimes, an inorganic base such as NaOH is also used to produce additional in-situ petroleum surfactants. Surfactants are added to the injected fluid to reduce the interfacial

tension at the oil-water interface and help to mobilize more oil. The alkali base addition goal is to reduce the possibility of the surfactant being absorbed by a rock. [41–43].

Polymers are the main components of the injected fluid of cEOR formulations. Recently, the partially Hydrolyzed Polyacrylamide (HPAM) polymer was investigated for cEOR application. HPAM has some drawbacks that inhibit it from fulfilling its target function at harsh reservoir condition (high temperature, pressure, and salinity). One of the main drawbacks of HPAM is its sensitivity to divalent ions which were reported in some studies [44–46].

Here in this paper, we are studying biopolymer which is another type of polymers that are much less sensitive to harsh reservoir conditions. More specifically, we are focusing on Hydroxyethyl Cellulose (HEC) as a possible alternative of HPAM. It is a non-ionic polymer, and its non-ionic nature is the key to eliminate the possibility of aggregation due to the ionic interaction with ions in the brine solution. In addition, for solubilisation, HEC is easy to hydrate and doesn't require any specialized equipment for dissolution, which reduces the cost and complexity of the EOR process [47–49].

HEC was used in 1992 in Romashkino field in Tatarstan, Russia. The reservoir temperature and salinity were 38 C° and 250 g/Liter, respectively. More than 3500 tons of HEC was flooded in 180 wells, which lead to an increase in incremental oil production by approximately 1,000,000 tons from 1992 until 2013 [52][32].

HEC, however, has an important drawback, that is the viscosifying ability of HEC is not high compared to HPAM. Thus, the water-polymer mixture will not extract the oil as effective [34]. One way to overcome this is by adding hydrophobic side-groups to the

backbone chain of HEC in a process known as Hydrophobic modification. This addition results in a group of polymers called hydrophobically modified HEC (HMHEC). These extended HEC chains significantly increase the viscosity of water, and thus, solve the low viscosifying ability issue. Some studies suggest using hydrophilic and hydrophobic groups simultaneously to get a synergistic effect[31][50][51].

In this study, we seek to investigate HEC and HMHEC for EOR applications. The aim of our study is to characterize different biopolymers that share the same backbone skeleton in order to draw a conclusion on the link between the atomic structure and the macroscopic properties. We used molecular dynamics simulation (MD) to study the chain dynamics, aggregation behaviour, interfacial interaction with oil, and phase behavior in the presence of surfactant. Since the major drawback of HPAM is its sensitivity in high-salinity condition, we conducted chain dynamic simulations under three different environment conditions (fresh water: 300 K, 1 bar, no ions) (sea water: 300K, 1 bar, seawater salinity as in Table 4.1) (formation water: 373K, 300 bar, formation salinity as in Table 4.1). In the aggregation simulations, we used a fixed chain length of 10 units of D-glucose rings with different environments and concentrations to observe the effect of both the environment and concentration on the aggregation behavior. Finally, we investigated the interfacial interaction in water with oil, and the interaction with surfactant at different salinity conditions. This study will give us deeper insights into the physics of this polymer for better implication in EOR.

TABLE 4-1 Ionic compositions of formation brine and Arabian Gulf seawater.		
Ions	**Formation water ions concentration (ppm)**	**Seawater ions concentration (ppm)**
Na^+	59,491	18,300
Ca^{2+}	19,040	650
Mg^{2+}	2,439	2,110
SO_4^{2-}	350	4,290
^-Cl	132,060	32,200
HCO_3^-	354	120
TDS	213,734	57,670

4.2 Computational Details

MD simulations were carried out using GROMACS 2018.1[56] program with (OPLS-AA) force-field [53–55] and (SPC/E) extended charge water model [60]. The Force-Field was verified by reproducing the density of glucose – the building unit of cellulose- at different wt% shown in Fig 4-1(a) and the viscosity Fig 4.1 (b). References for experimental data are density[61], viscosity [62].

Simulated systems were first energy-minimized using the steepest descendent method to a convergent of maximum force of 100 kJ mol^{-1} nm^{-1}. The particle mesh Ewald (PME) algorithm [63] was applied to treat the electrostatic interactions with a cutoff of 12 Å. The same algorithm was used for van der Waals (VDW) and short-range electrostatic interactions treatment. All bonds were constrained by (LINCS) algorithm [64]. The system was coupled to a thermal bath by a Berendsen thermostat [65] with a time constant of 0.1 ps for equilibration and 0.5 ps for production. The pressure was controlled with a Parrinello-Rahman barostat [66] with a time constants of 2 and 5 ps for equilibration and

production, respectively. A time step of 2 fs was set for all simulations except viscosity calculation where one fs was used, and the coordinates were saved at ten ps time intervals except for viscosity calculation where it was saved every one ps. Outputs were analyzed using GROMACS analyzing-tools. For all the systems, the Leap-Frog integrator was used.

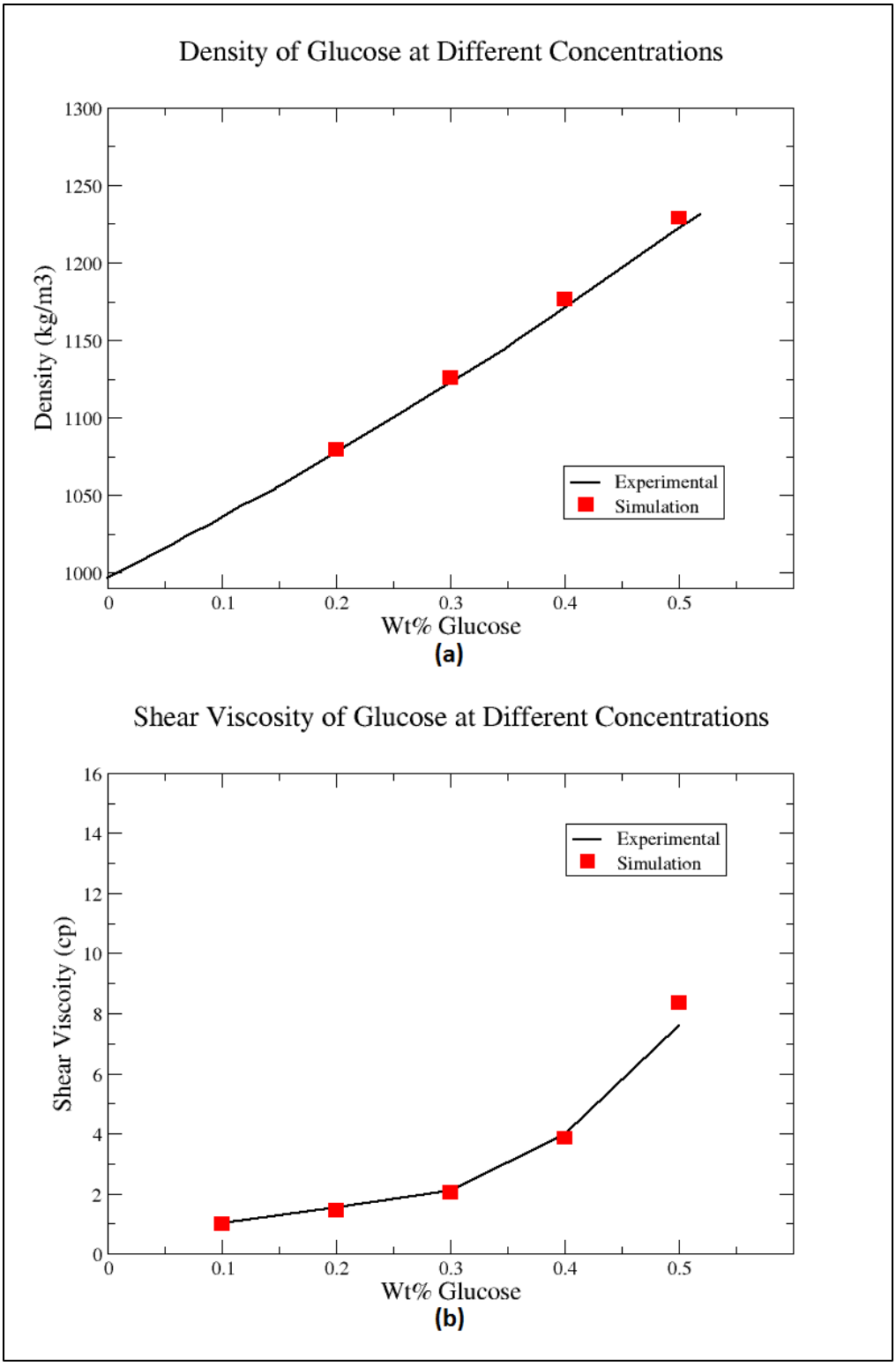

Figure 4-1 Compare experimental data of (a) density and (b) shear viscosity with simulation result.

4.2.1 Chain Dynamics

The simulation time for 30 units chain of HEC and HMHEC was 250 ns -and further extended this time for cellulose system to 500 ns to achieve a stable state. The simulations were done under 3 environment conditions: fresh water (300 K, 1 atm and no salinity), sea water (300 K, 1 atm and sea water salinity) and formation water (373 K, 300 atm and formation salinity). In all systems, the chain composed 1% of the system's weight.

4.2.2 Aggregation

The chain length in this section is fixed to be ten units long for cellulose and HEC, and 30 units long for HMHEC. We used 30 units for HMHEC to have a hydrophobic content that is comparable with the literature. The cellulose systems are composed of cellulose chains to have 1% weight of the system. We simulated this specific wt% under three environments: fresh water, sea water and formation water condition. The compositions of salts in seawater and formation condition are shown in Table II. The simulation box was cubic with a dimension of 10 nm. Each system was simulated for 500 ns. The same procedure was repeated for 2% and 3% weight of cellulose, so in total, we have nine systems for cellulose. The aggregation analysis was conducted for HEC at 1 and 3%, and for the hydrophobic modified HEC at 1% only. HEC and HMHEC are compared with cellulose at the same concentration.

4.2.3 Viscosity calculation

For the viscosity calculation, we tried several methods to accomplish that: 1) the Green-Kubo method, 2) Diffusion coefficient method. Both methods were carried out using Gromacs analysis tools. For the first method, we generated 20 different initial conformations from the aggregation simulations at different times. Then we conducted

short simulations of 2 ns on each simulation. We took the average of these 20 results as the final average viscosity. This method was the one used for the viscosity verification used in the previous section for the Glucose system. In the second method, we used a direct relation between the diffusion coefficient and the viscosity shown in equation 4.1 [67]. We had to use this method after the first one didn't yield reasonable results. The diffusion coefficient was calculated using Gromacs tools (gmx msd), and then plugged-in equation 4.1 to give the viscosity.

$$D\eta = \frac{k_B T}{6\pi r_H} \tag{4.1}$$

Where D is the diffusion coefficient, η is the viscosity, k_B is the Boltzmann constant, T is the temperature, and r_H is the hydrodynamic radius.

4.2.4 Interfacial tension with oil

We conducted MD simulation of oil-water system to investigate the interfacial tension (IFT) between the water-polymer system and light oil. The model used For the oil model, we followed the model proposed by Kunieda et al.[45] that is composed of the molecules shown previously in section (3.2.3). The same water-polymer system used in the aggregation simulation was feed-in here . IFT is done for systems of light oil with water at three salinity conditions (fresh, sea and formation). The length of each simulation was 100 ns. The IFT values were averaged every ten ns to "wash-out" statistical fluctuations. The concentration of polymer in the water-polymer system was 1% for both cellulose and HEC.

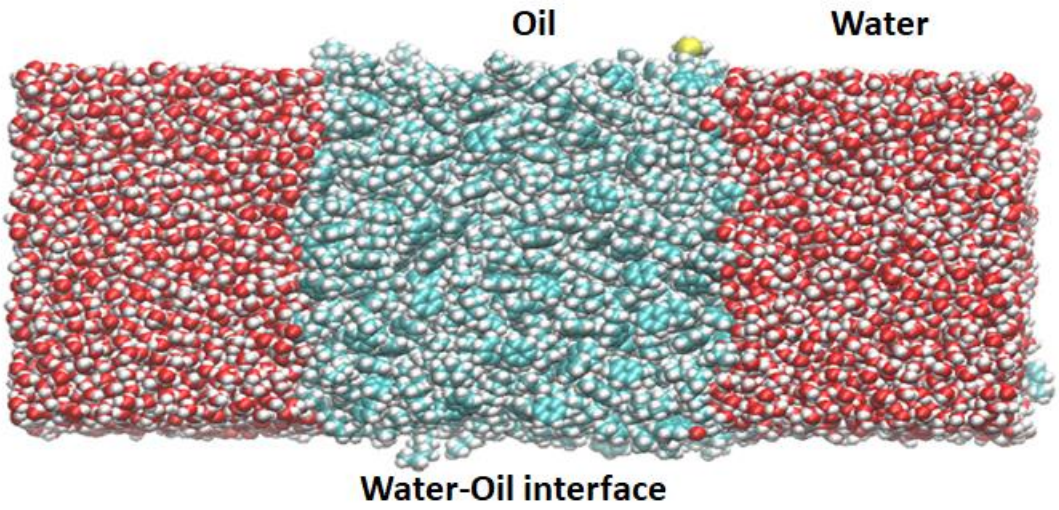

Figure 4-2 show the water-oil interface model

4.2.5 Phase behavior of polymer+surfactant solutions

To study the polymer+surfactant phase behavior, we have generated a solution of 1%wt of the polymer and sodium dodecyl sulfate (SDS). The model and force-field of SDS were taken from the recent study by Abdel-Azeim [68]. The simulations were conducted for 300 ns in NPT ensemble. This systems also are simulated at different salinity conditions. The same procedure was repeated for the HEC system.

4.3 Results and discussion

4.3.1 Chain Dynamics

We have perform benchmark simulations in order to select the polymer chain length that describe the polymer properties and at the same time efficient computationally. We have conducted a simulation run of 100 ns on three chain lengths, namely: 10-mer, 30-mer and 50-mer lengths. We analyzed the radius of gyration, side and backbone dihedral angles, and the hydrogen bonds for each chain length.

The results are shown in Figures 4-(3,4,5) below. Indeed, the behaviors of 30 and 50 units are conveged to a quite similar behavior, especially for angles distributions. For the H-bonds analysis, the figure shows the number of H-bonds between cellulose and water molecules per repeating unit of cellulose. There is a slight reduction in the number of H-bonds with the 10 units compared to the 30 and 50 units, while the 30 and 50 are fairly close to each other. For the angle distribution, it is observed that 30 and 50 units' behaviors are almost identical compared to the 10 units, which slightly deviates from the other two in the angle distribution. The 10 units chain is drastically different in the dihedral angle distribution for both the backbone ether connection and the side-group dihedral. From these results, we decided to continue the dynamics simulation and analysis with the 30 units-long chains of the polymer.

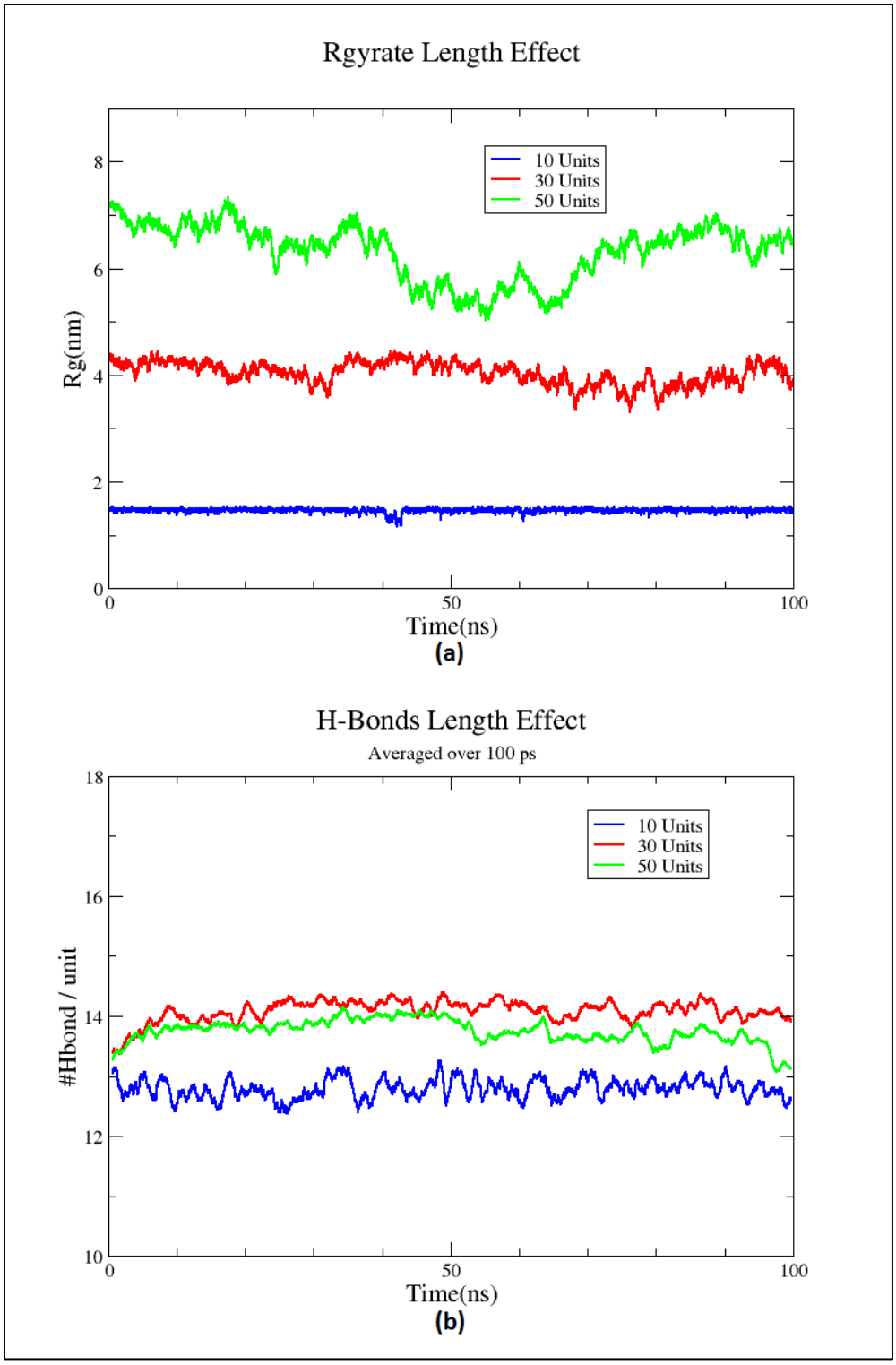

Figure 4-3 comparing the Length effect on (a) Radius of gyration, (b) Interchain Hydrogen bonds

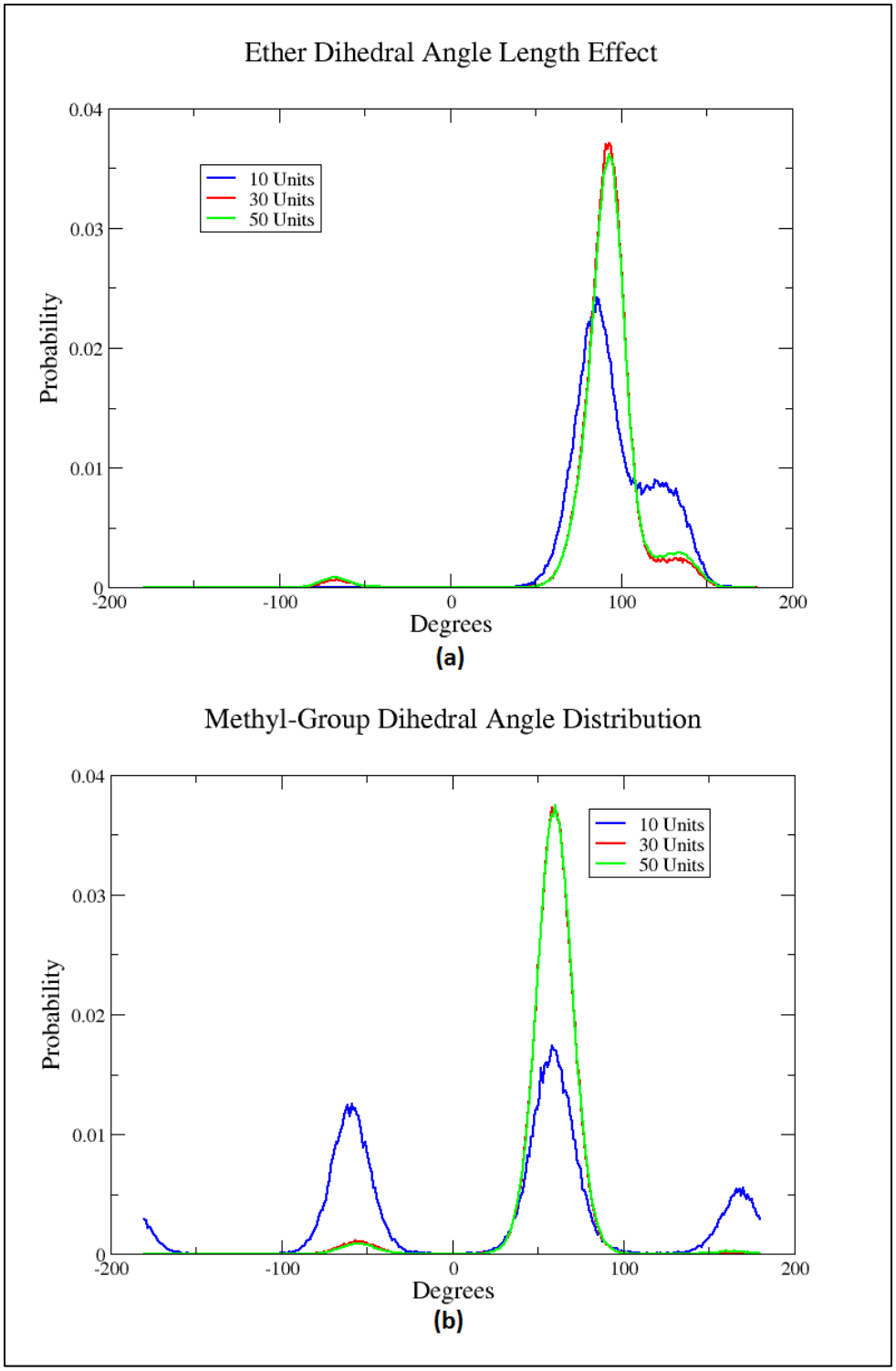

Figure 4-4 Comparing the Length effect on: (a) Ether-connection Dihedral angle distribution, (b) Side-group Dihedral angel distribution

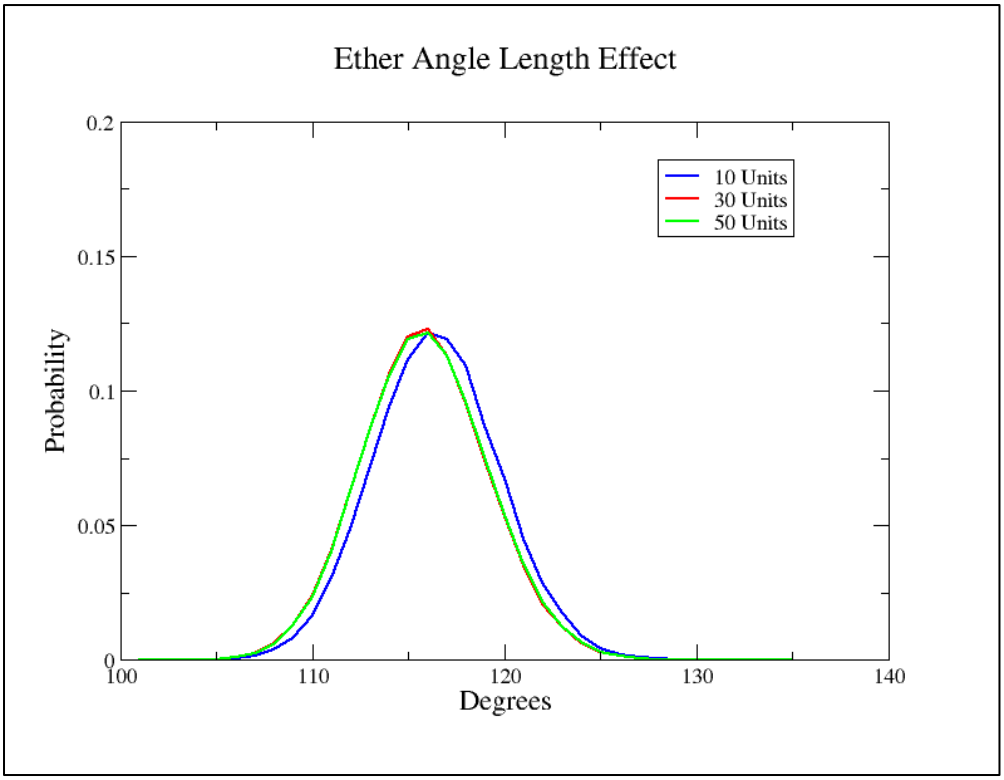

Figure 4-5 Comparing the Length effect on the Ether-connection angel distribution

To study the dynamics of cellulose, HEC, and HMHEC, we conducted three simulations with 30 units-long chains of cellulose under three different salinity conditions as described in the computational details. The purpose of simulating under different salinity conditions is to inspect the behavior of cellulose chain under these salinity conditions to help us better evaluate HEC, and HMHEC as an adequate alternative for HPAM at high salinity. We ran each simulation for 250 ns for both HEC and HMHEC, and 500 ns for cellulose. We targeted few properties to evaluate the dynamics of the chain, namely: radius of gyration, end-to-end chain distance, (polymer-polymer) and (polymer-water) hydrogen bonding, radial distribution function (RDF), and the side & backbone dihedral angles distribution for cellulose and ethyl group for HEC and HMHEC .

Side Group Dihedral-Angle Distribution

The rotameric conformation is a critical parameter which describes the structural organization of the cellulose crystal. To achieve this, the dihedral angle with the hydroxymethyl group was analyzed. There are three known conformation for this dihedral angle: gauche-gauche (gg) at -60°; gauche-trans (gt) at +60°; and trans-gauche (tg) at 180°. The distribution of the side group dihedral angle is shown in Fig 4-(6,7). To describe flexibility of cellulose, it is known that for crystalline cellulose, (tg) is the dominant conformation, while for the aqueous solutions, the gg conformation dominates. That is why tg usually describe crystal-like cellulose state, while gg describes amorphous-like cellulose state. The gt conformation becomes most populated in the presence of other solvents, like ionic liquids.

It is observed that for cellulose, the distribution isn't affected at all by the environment, for the three salinity cases, they all have the same dominant conformation of

gt +60°. When compared with HEC, It is observed that switching from methyl to ethyl group drastically changes the conformation. For HEC, more rigid polymer conformation occurs with tg 180° as the most prominent distribution. We can also observe for HEC that the formation water environment influences the distribution with an increase in gt +60° and reduction of both tg and gg conformations. An almost identical behavior to HEC is observed for HMMHC, which suggest a negligible effect of hydrophobic modification of the rigidity of the HEC.

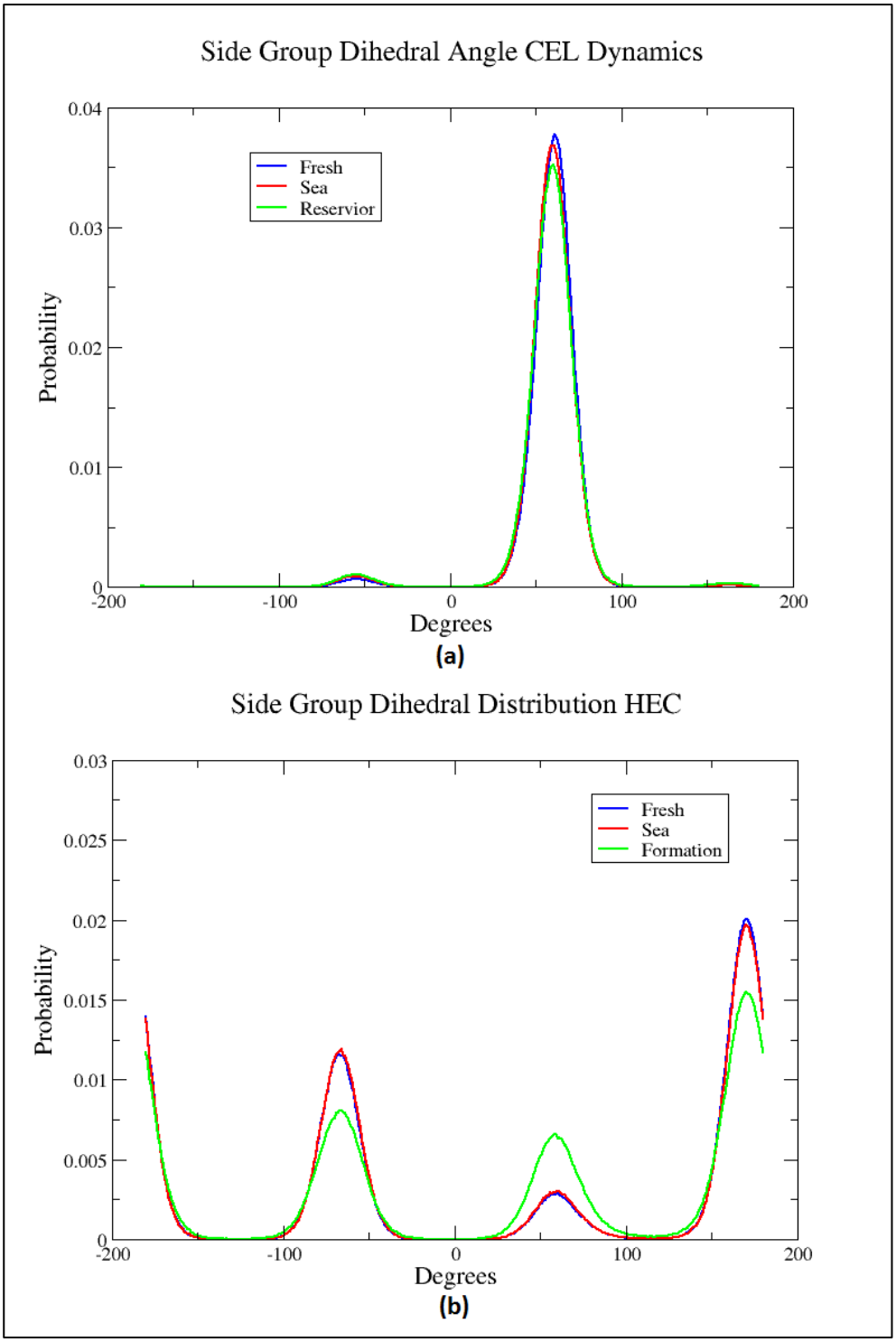

Figure 4-6 Side group dihedral angle distribution for: (a) Cellulose, (b) HEC

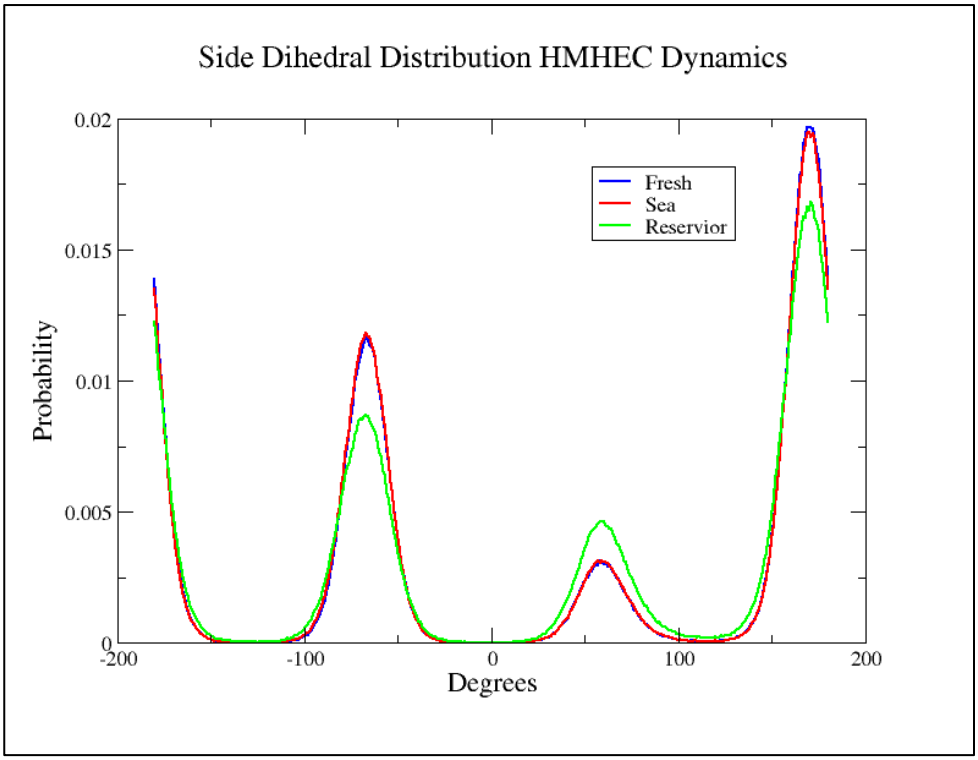

Figure 4-7 Side group dihedral angle distribution for Hydrophobic modified HEC

Radius of Gyration and End-end distance

The radius of gyration and end to end distance, are two parameters related to one another in describing the conformation of the polymer (coiled, extended or compact). If the polymer is tending to have a more compact form, we expect these parameters to decline with time. Also, if the salinity is causing the polymer to become more compact, these two parameters should have lower values when compared to no salinity condition (fresh water). In Figs 4-(8,9,10), we can see the radius of gyration and end to end distance of cellulose, HEC, and HMHEC as a function of time.

For cellulose, the polymer is more stable at fresh water and reservoir conditions compared to seawater throughout the simulation. When comparing cellulose and HEC, cellulose is more stable especially for fresh and reservoir conditions. The trend for HEC at different salinities is similar irrespective of the environment, which shows a sign that this non-ionic polymer can be a good candidate as an alternative for HPAM at high salinity. The hydrophobically modified polymer is affected at reservoir condition and shows a very compact form, less than one-third of its extend state, before extending again. This is expected since the concentration of water decreased.

The takeaway message here is that cellulose as the backbone of HEC appears to be very stable and rigid even at high salinity, HEC appears more salinity resistive compared to cellulose because of the indifferent behavior with respect to salinity, and HMHEC takes a very compact form at reservoir condition before extending again.

Figures 4-(11-14) show the structure for HMHEC at 100 ns (compact) and 150 ns (a little extended). The reason behind the very compact conformation of HMHEC at

reservoir condition is that the polymer intertwined with itself forming high intra-chain H-bonds. This intertwined structure eventully breaks, and the polymer is extending again to lengths similar to fresh and seawater's polymers lengths. For EOR application, HEC will be favored for the salinity indifferent behavior.

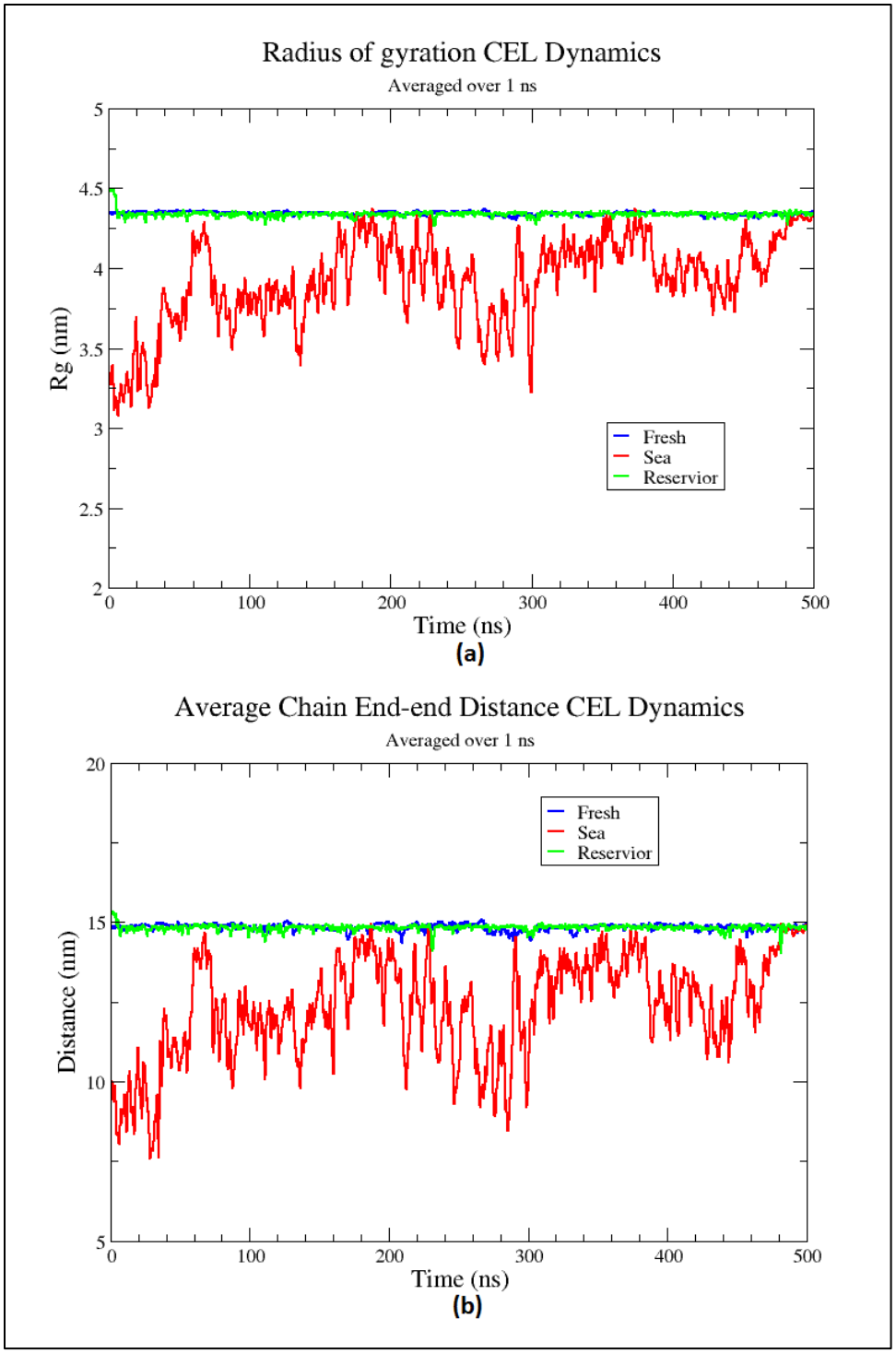

Figure 4-8 (a) Radius of gyration, (b) End-end distance, for cellulose dynamics system

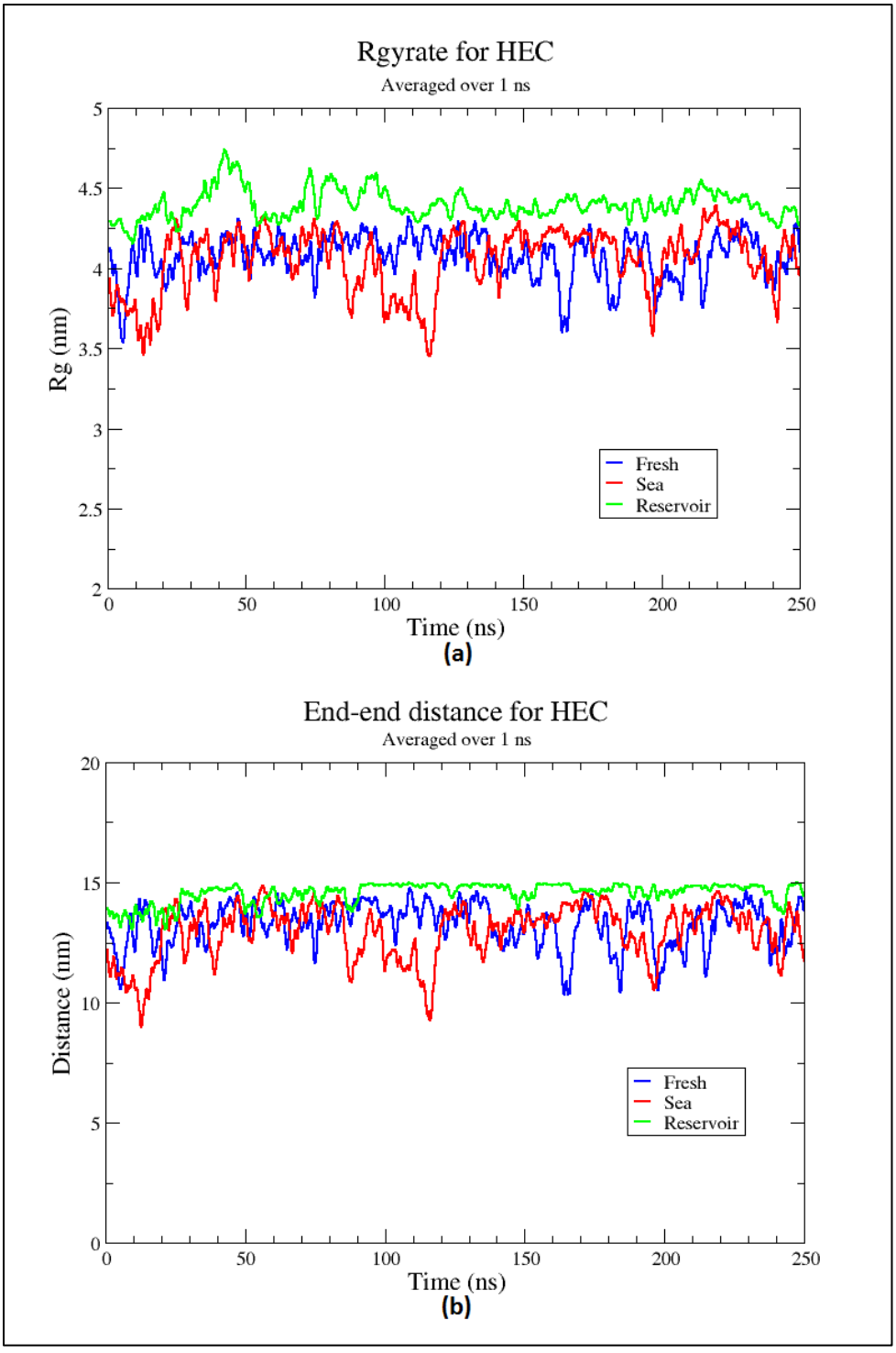

Figure 4-9 (a) Radius of gyration, (b) End-end distance, for HEC dynamics system

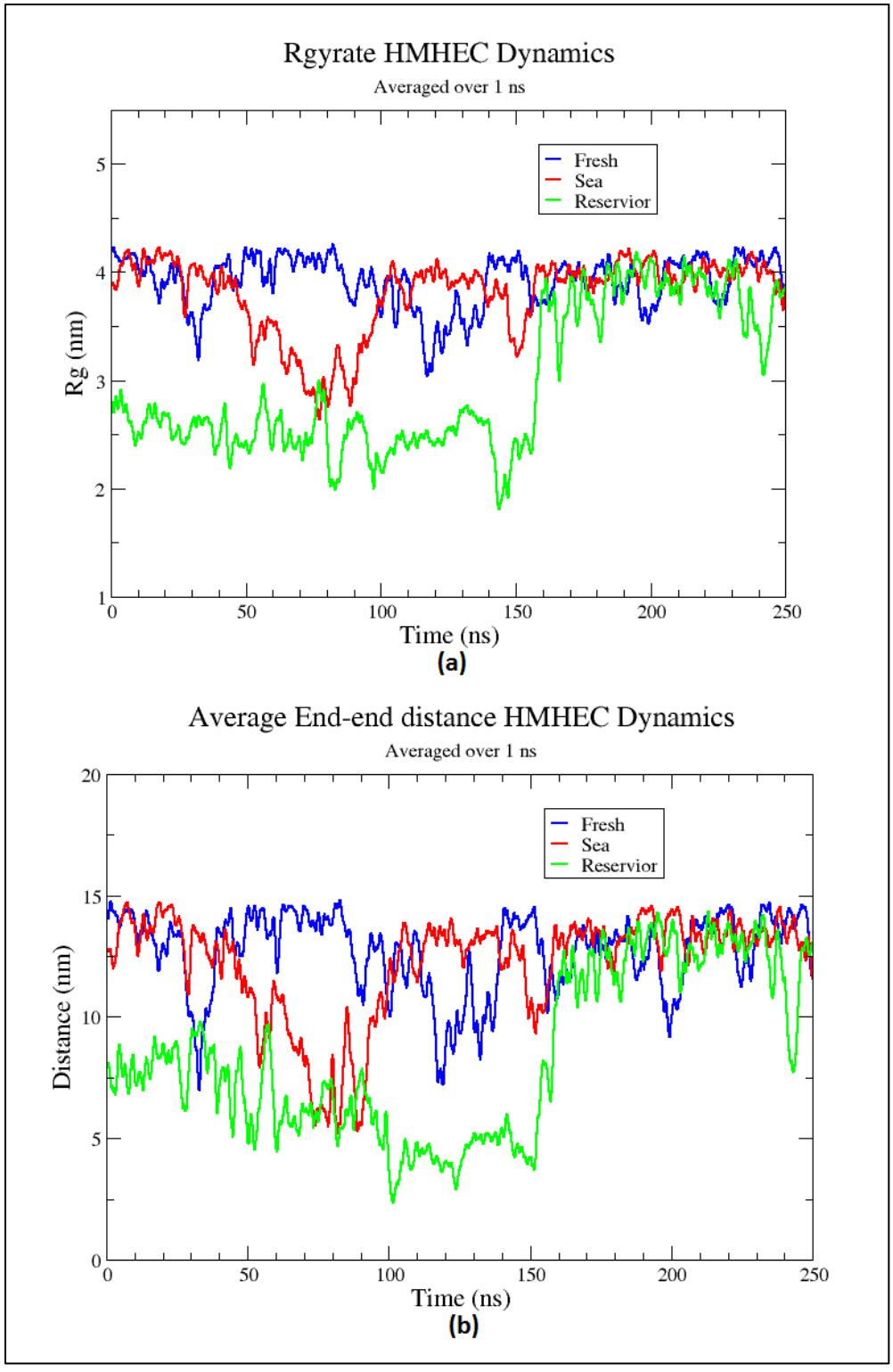

Figure 4-10 (a) Radius of gyration, (b) End-end distance, for HMHEC dynamics system

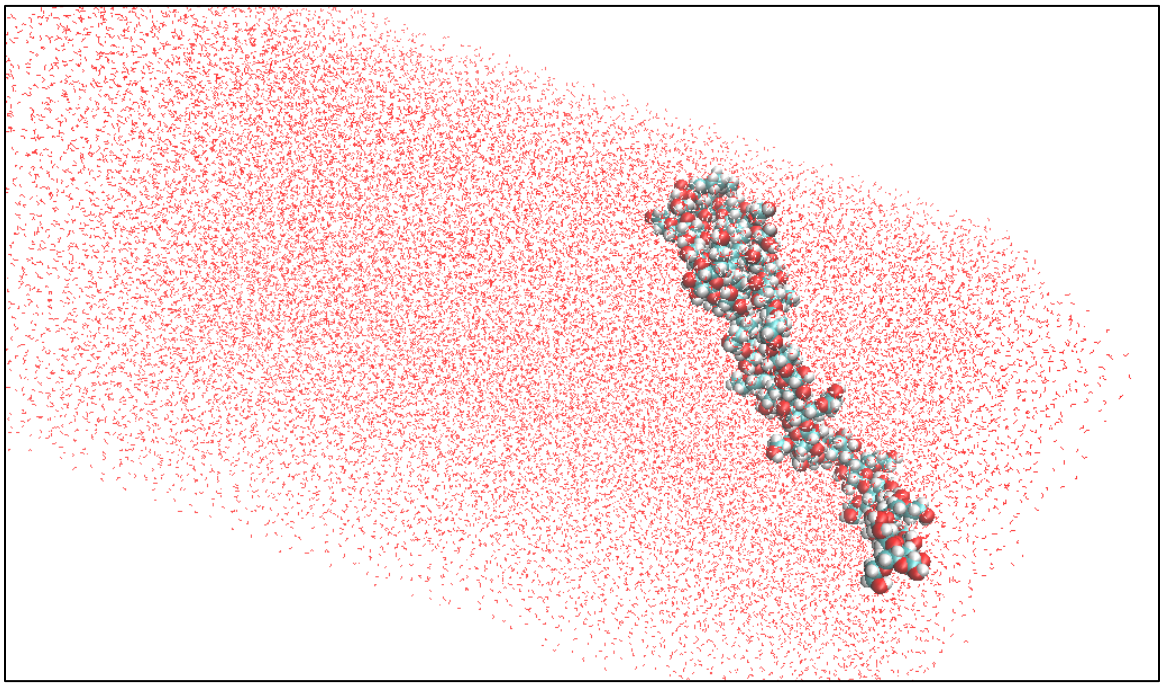

Figure 4-11 HMHEC structure at 100 ns (lowest end-end distance)

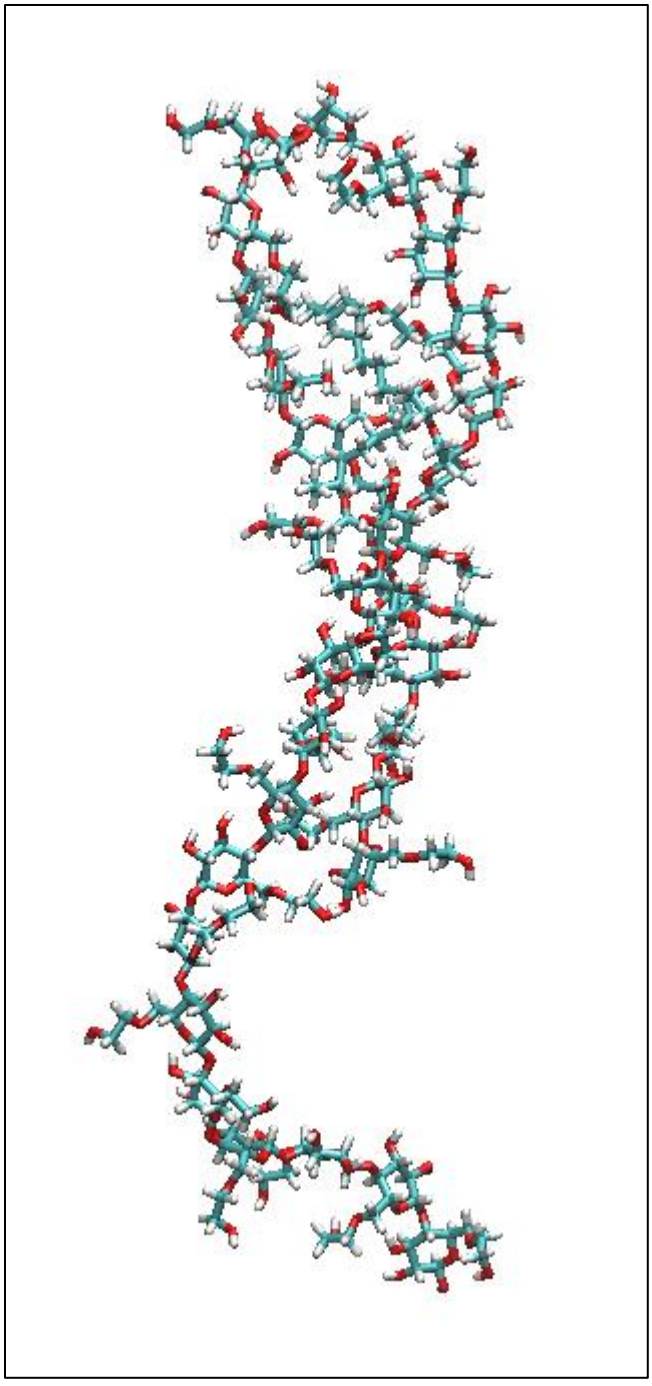

Figure 4-12 HMHEC structure at 100 ns without water molecules

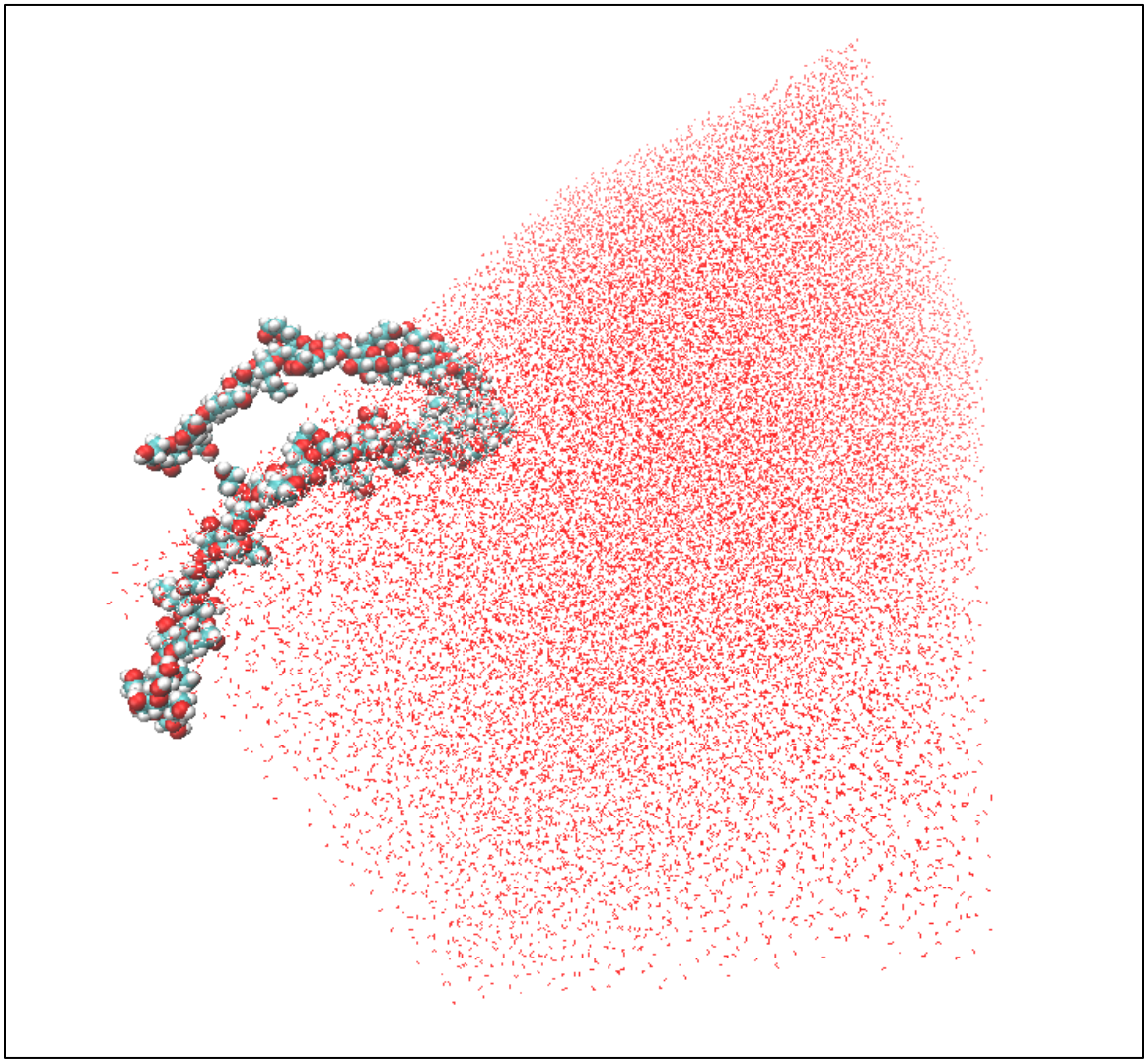

Figure 4-13 HMHEC structure at 150 ns

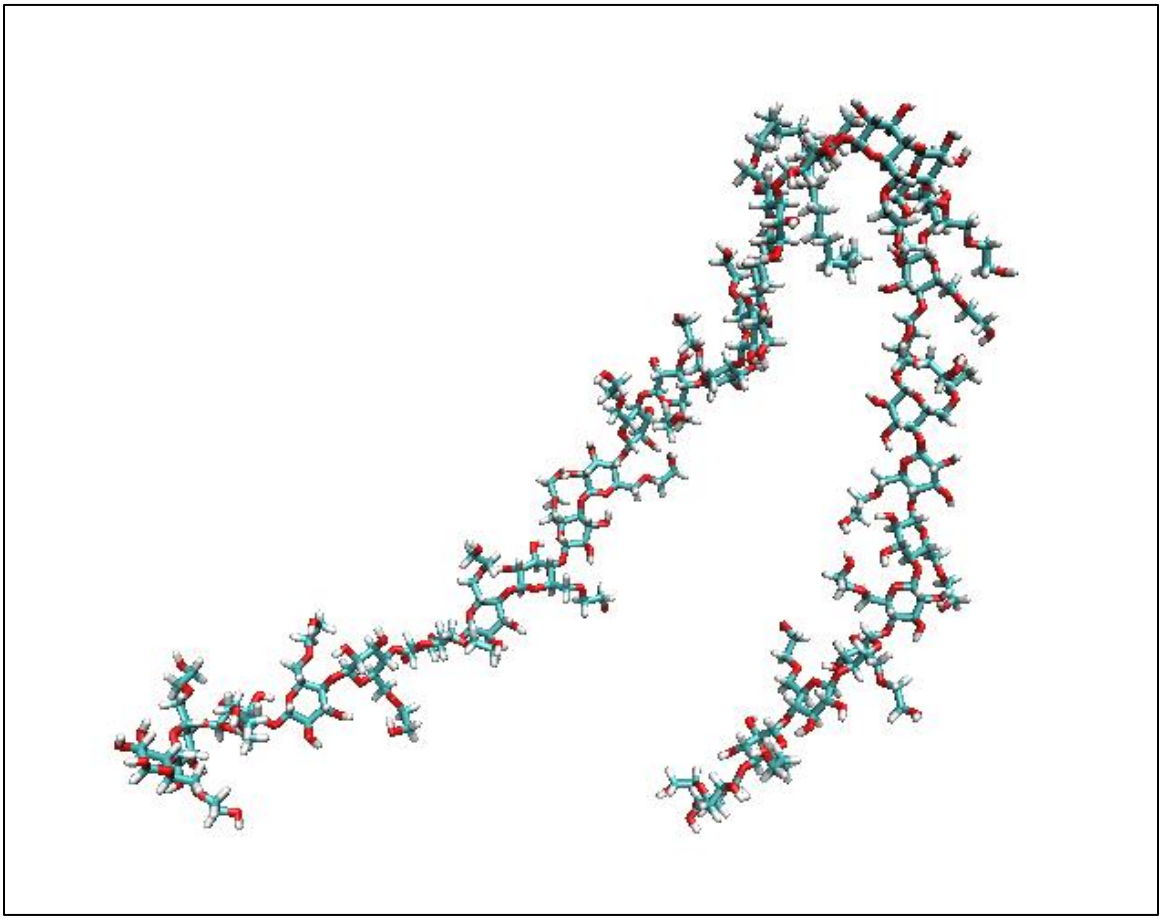

Figure 4-14 HMHEC structure at 150 ns without water molecules

Hydrogen Bonds

Inter- and Intra-chain hydrogen bonds are two parameters used to describe the stability of compact or extended states. Figs 4-(15,16,17) shows the hydrogen bonds for both inter-chain and intra-chain bonding for cellulose, HEC, and HMHEC.

For cellulose, Fig 4-15, the fresh water and reservoir connate water H-bonds are stable with no significate transition anywhere during the simulation. For seawater condition however, there is a visible transition at around 380 ns of increasing intra-chain H-bonds and decreasing inter-chain bonds. This transition means that the polymer is froming H-bonds withen the polymer itself, and reduce the interaction with water molecules. If we correlate this transition with radius of gyration and end-end distance (Fig 4-8) we observe that at the same time of H-bonds transition toward intra-chain bonds, polymer's end-end distance is increasing until it reaches similar values to fresh water and reservoir connate water. From these data we can observe the CEL rigidity represented in an extended chain that favours forming intra-chain bonds at different salinity conditions.

For HEC, Fig 4-16, for all three salinity conditions the number of H-bonds appears to be stable (no drastic transition) during simulation time. The reservoir connate water form more intra-chain H-bonds compared with fresh and seawater, at the expense of less inter-chain H-bonds. This means that the polymer at reservoir condition prefers forming higher intra-chain H-bonds, and thus, less interaction with water molecules compared to the other two environments. The effect of this on the rigidity of the chain can be correlated when comparing the end-end distance for HEC at different salinities from previous section (Fig 4-9). HEC at reservoir condition has extended chain with few flucutations – thus higher

rigidity – compared with the other two environments because of the higher intra-chain H-bonds.

For HMHEC, Fig 4-17, a reversed phenomena to CEL and HEC. A small increase intre-chain H-bonds at the expense of intra-chain can be observed for reservoir condition around 130~150 ns. When correlated with radius of gyration and end-end distance for HMHEC (Fig 4-10), we observe an extension in the polymer chain around the same time. This increase in inter-chain H-bonds is due to this extension of the polymer allowing more interaction and H-bonds forming with water molecules. HMHEC appears to be less rigid compared with CEL and HEC especially in reservoir connate water because of this contration it had.

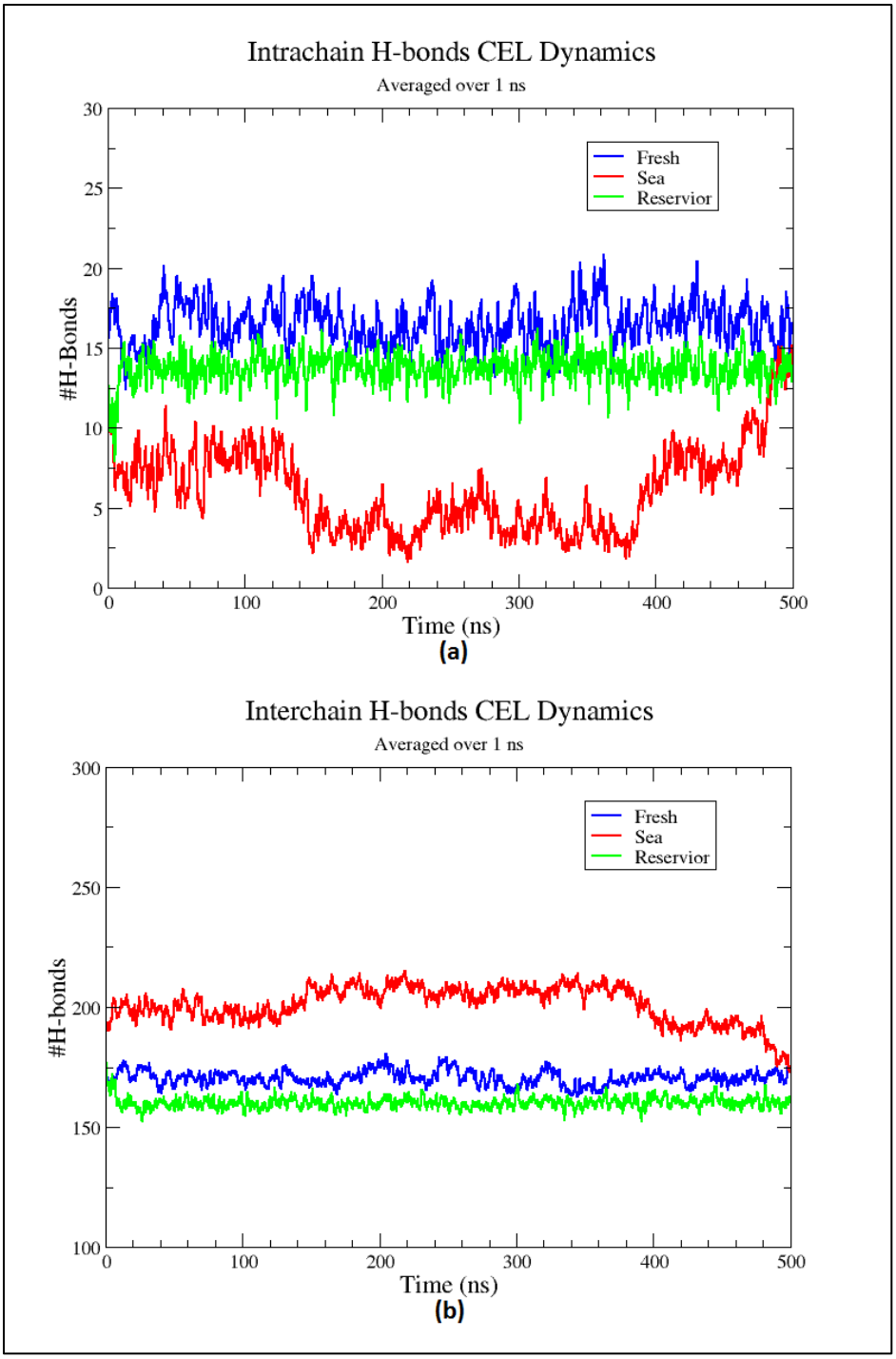

Figure 4-15 (a)Intrachain, and (b) Interchain Hydrogen bonds for cellulose dynamics system.

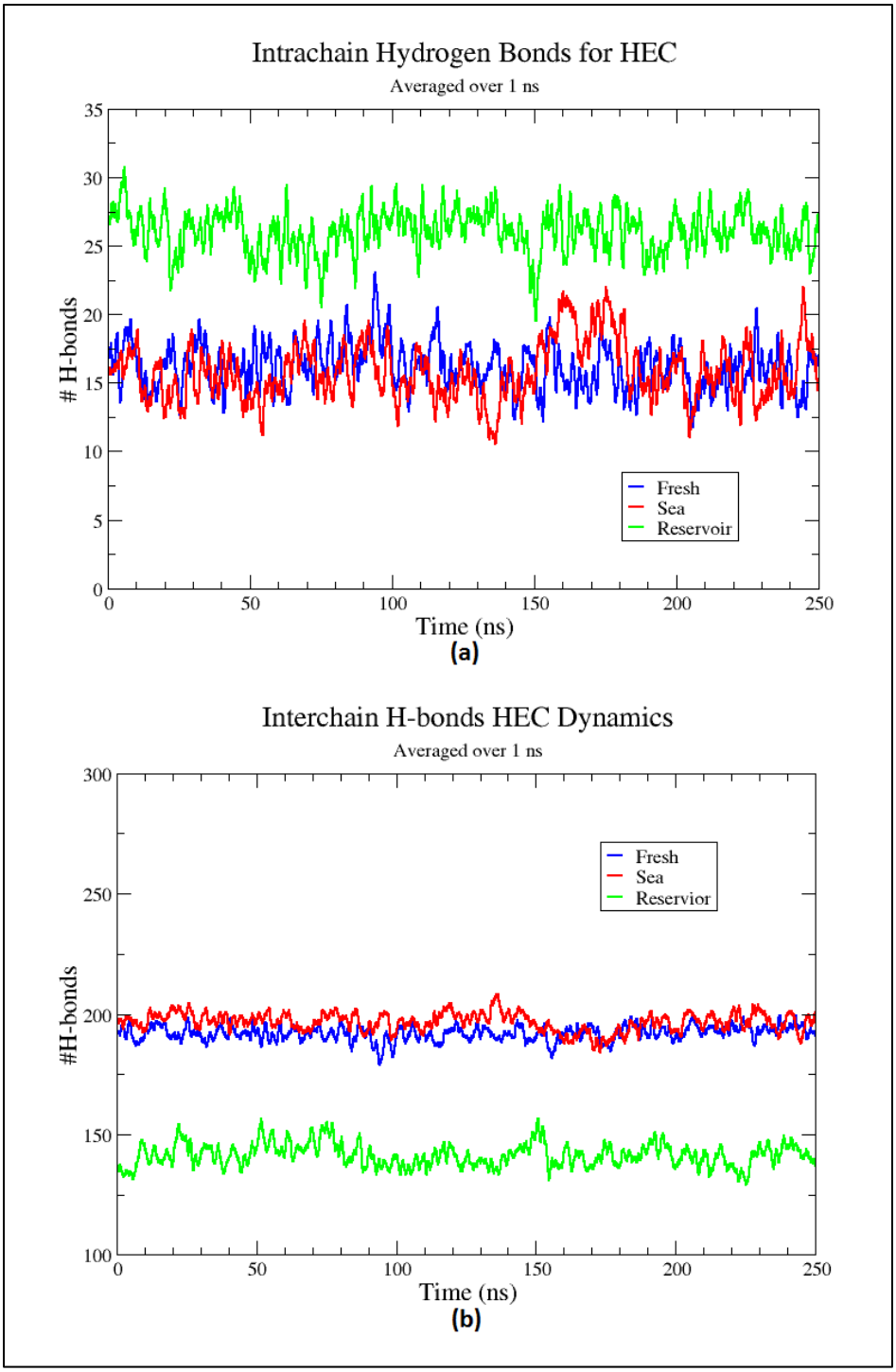

Figure 4-16 (a)Intrachain, and (b) Interchain Hydrogen bonds for HEC dynamics system.

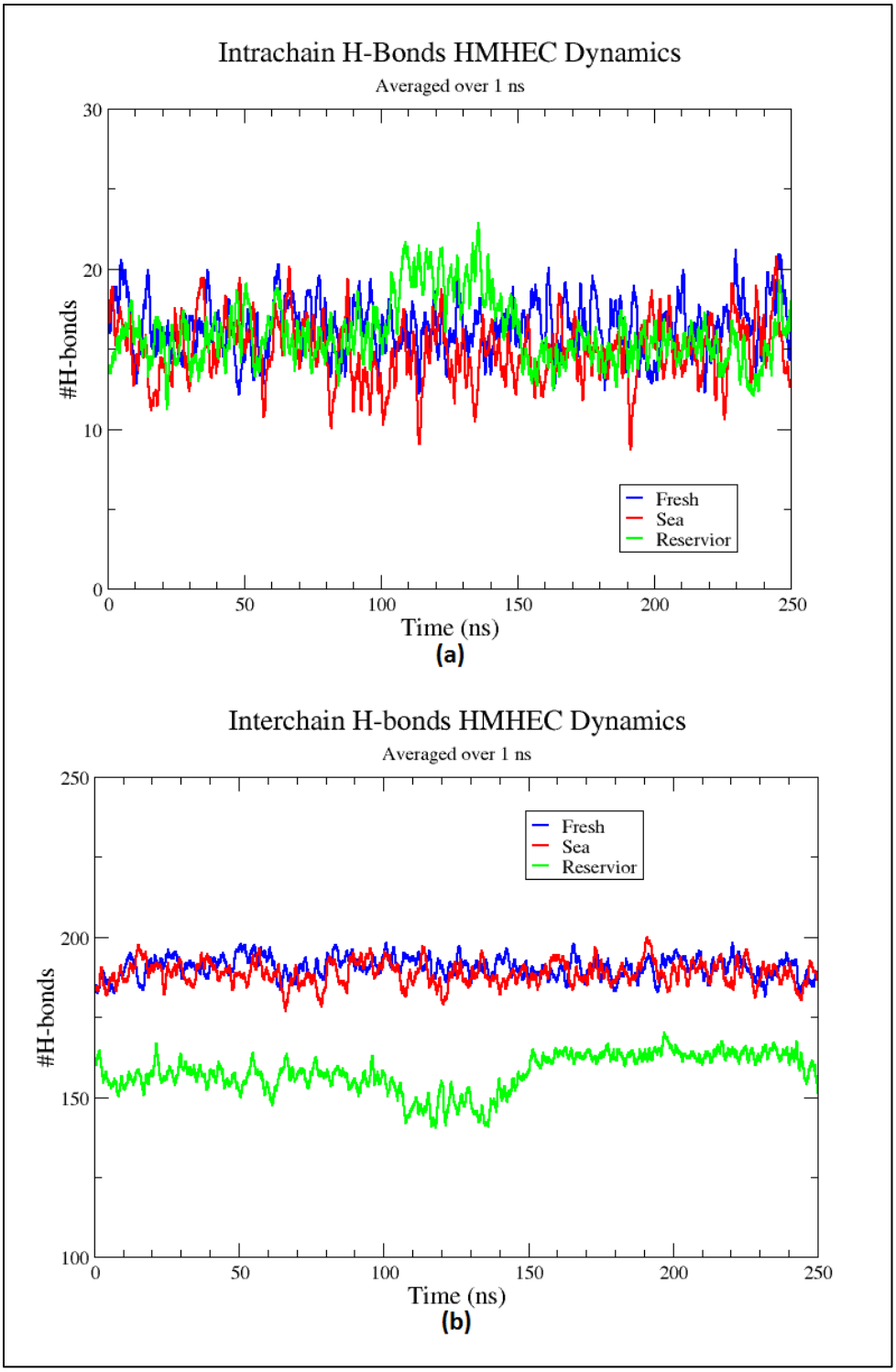

Figure 4-17 (a)Intrachain, and (b) Interchain Hydrogen bonds for HMHEC dynamics system

Radial Distribution function (RDF)

Radial distribution function (RDF) is an interesting tool to examine the internal packing of the material and its molecular interactions, especially we can confront the calculated RDF with the experimental counterpart obtained from neutron scattering [69]. This helps to illustrate whether the interaction between different molecules is likely to hapean or not. RDF can be correlated with other properties like the radius of gyration to explain why the polymer is extended or compact.

RDF for cellulose, HEC and HMHEC at sea and formation water conditions is shown in Figs 4-(18,19,20), respectively. The interaction was taken with reference to the oxygen atom in the polymer. There is limited interactions between cellulose with Na+ and water in both sea and reservoir condition, while the other two polymers show negligible interactions. This indicates that there is almost no interaction between the polymer and the solvent or with different ions. These results further strengthen the position of this non-ionic polymer as a good alternative of HPAM at high salinity since no interaction with ions is pronounced.

From the above analysis, we can conclude that cellulose and HEC have rigid chains since the chains lengths' remains close to the fully extended length of 15 nm most of the simulation time. We also conclude that the rigidity of these two polymers is negligibly affected by the environment since the chains are extended at different environments. The increase of H-bonds happens simultaneously as the chain length becomes very stable. This suggests that the reason for this stability in chain length is duo to the increase in the number of H-bonds, and limited interactions with ions. For HMHEC, the results for freshwater and seawater lead to a similar conclusion to the previous two polymers. For reservoir condition,

there is a drastic fall in the chain length that last for some time before extending again. This transition suggests that HMHEC takes some time to become stable at reservoir condition.

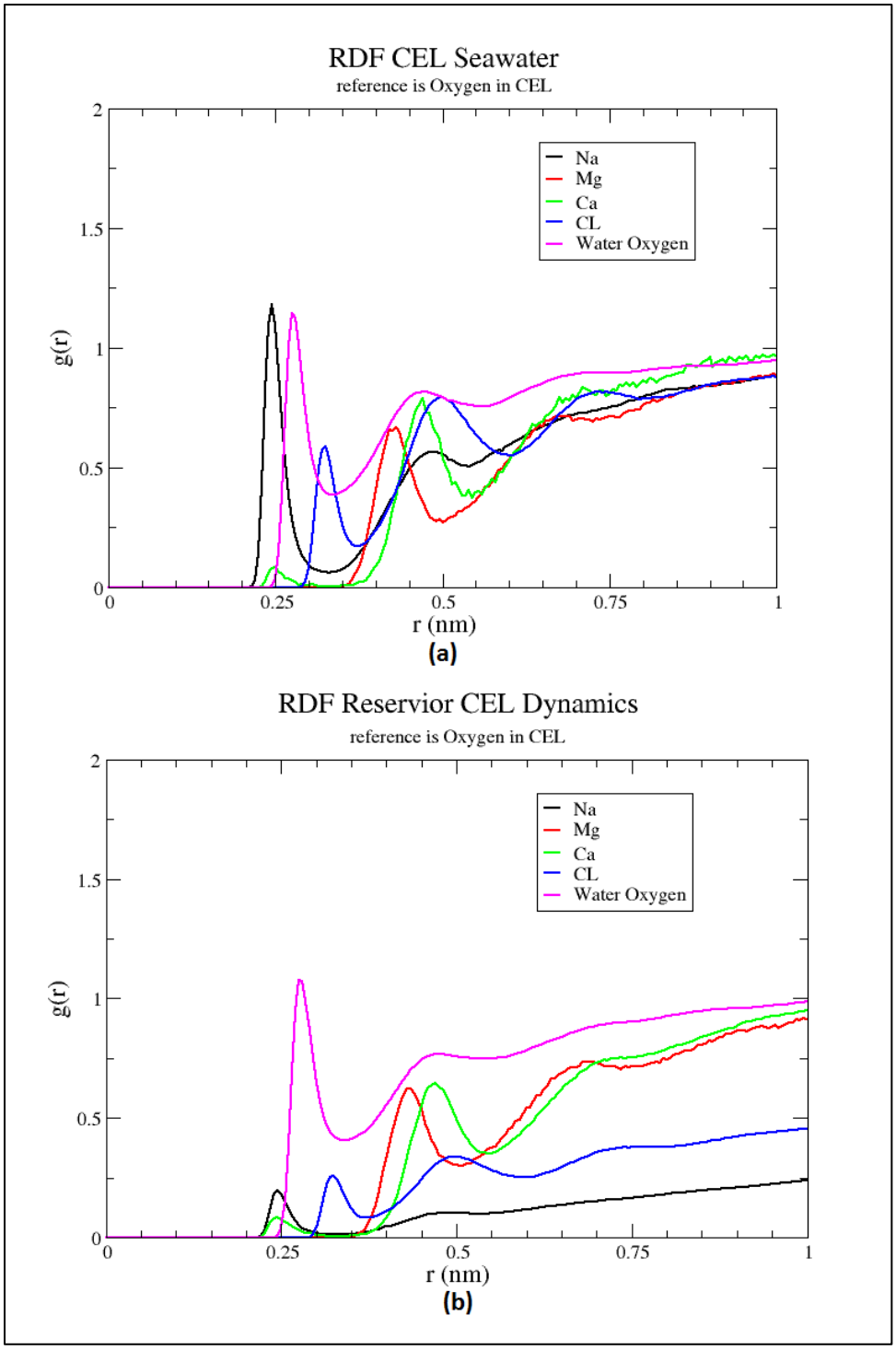

Figure 4-18 RDF analysis for Cellulose Dynamics system at: (a) Seawater, (b) Reservoir condition.

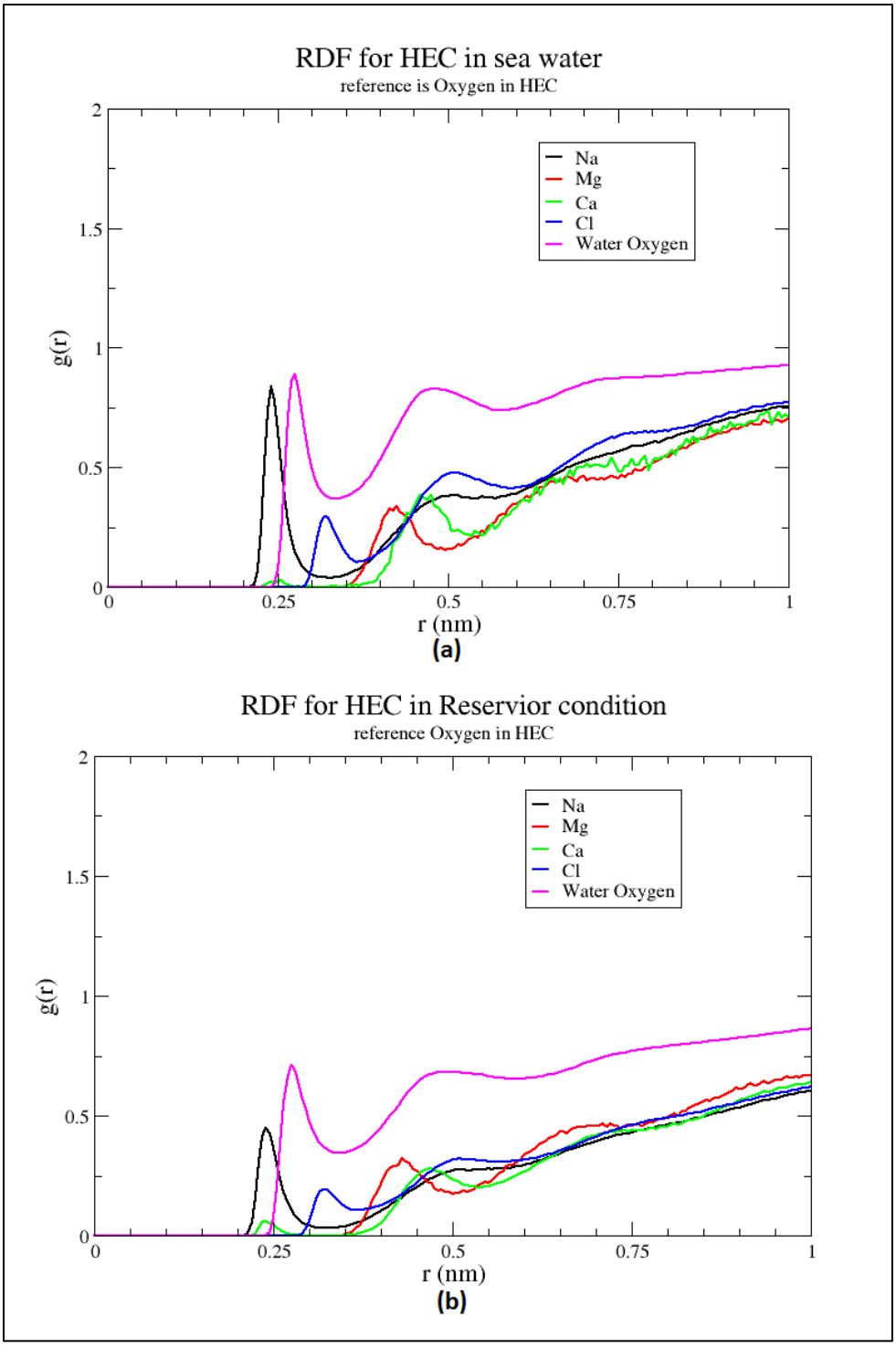

Figure 4-19 RDF analysis for HEC Dynamics system at: (a) Seawater, (b) Reservoir condition

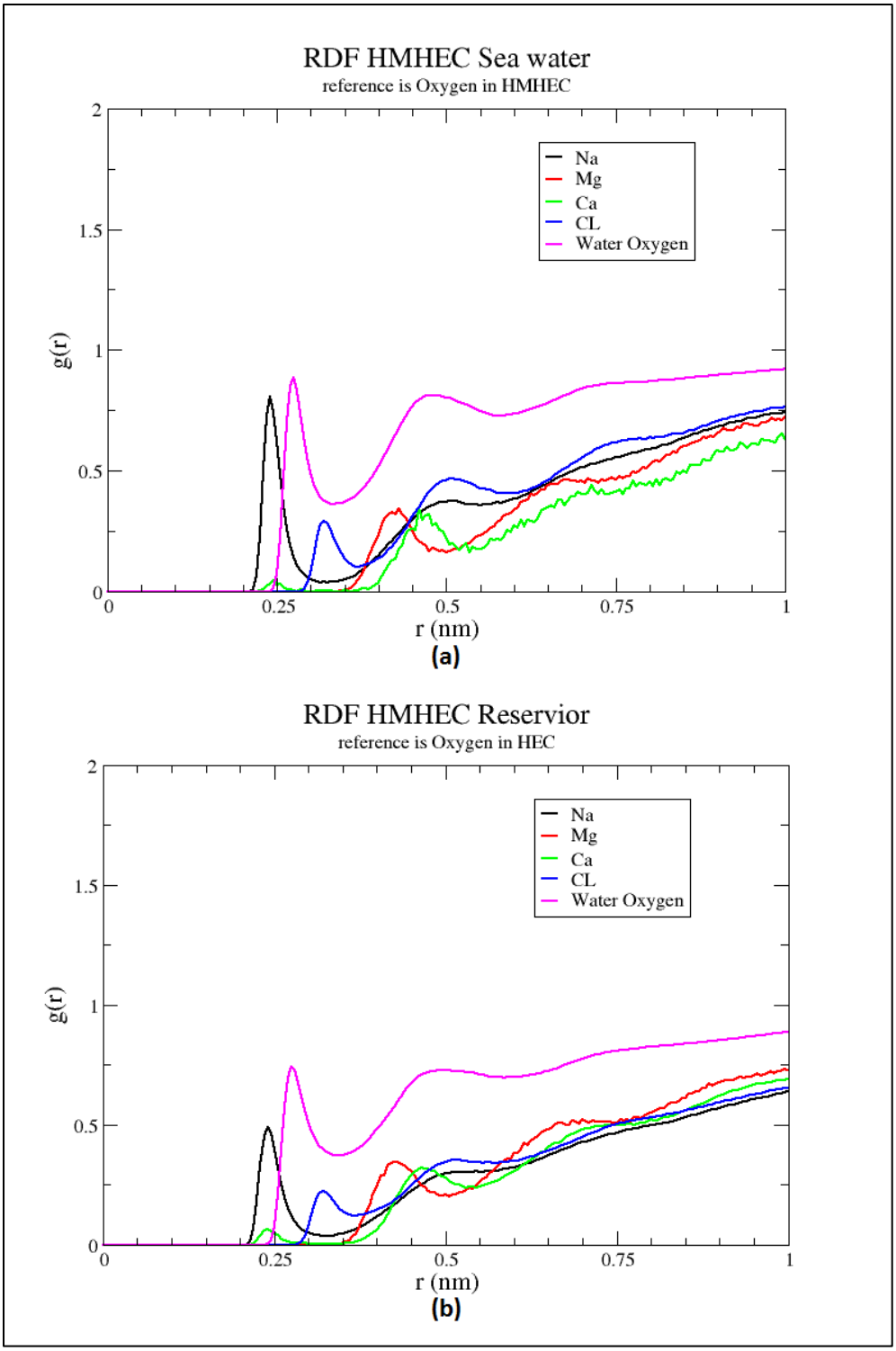

Figure 4-20 RDF analysis for HMHEC Dynamics system at: (a) Seawater, (b) Reservoir condition

4.3.2 Aggregation

For the aggregation analysis, we are interested in answering three questions: 1- does these polymers' aggregation behavior change with different salinity condition? 2- If these polymers aggregate, at what concentration? 3- what is the effect of the hydroxyethyl and hybdrophobically modified side-chain of HEC group on the aggregation behavior?

To answer the first question, we did simulations at identical cellulose concentrations and different salinities.Then we observed the number of clusters forming in the systems as a function of time. For the second question, we increased the concentration of cellulose in all three salinity conditions. This will show if these polymers aggregate with increasing the concentration, and further confirm if the aggregation behavior is changing for different salinities as we increase the concentration. For the third question, we simulated HEC at 1% and 3% concentration and compared it with cellulose, then we simulated HMHEC at 1% to compare with the former two.

Cellulose Aggregation

The aggregation behavior for cellulose at different concentrations and environments can be seen in Fig 4-21 (a) at 1% concentration with four chains in the system and is not pronounced. As per the number of clusters, most of the time there are 4 clusters, which indicated that the 4 chains are completely separated. We can conclude that at 1%, there is no aggregation irrespective of the salinity, which is a good thing for viscosity enhancement.

The 2% aggregation behavior in Fig 4-21 (b) shows aggressive aggregation behavior for cellulose at the formation water. With eight chains and alternation between 1 and 2 cluster numbers, this means there are two groups with an average of 4 chains sticking

together in each group, with these two groups occasionally sticking to each other forming one cluster of 8 chains. This indicated an unfavorable behavior for the viscosity enhancement. For the fresh and sea water conditions, there is no significant aggregation behavior, instead cellulose appears to be well dispersed in water.

The 3% aggregation behavior in Fig 4-22 shows that there is also aggregation behavior for the reservoir (formation water & high temperature) condition as compared to the fresh and sea conditions. However, the aggregation for the reservoir condition at 3% appears to be less aggressive compared to the 2% behavior. With 12 chains at 3%, on average there appears to be more aggregation behavior in sea and fresh water conditions when compared with 1 an 2% at other concentrations.

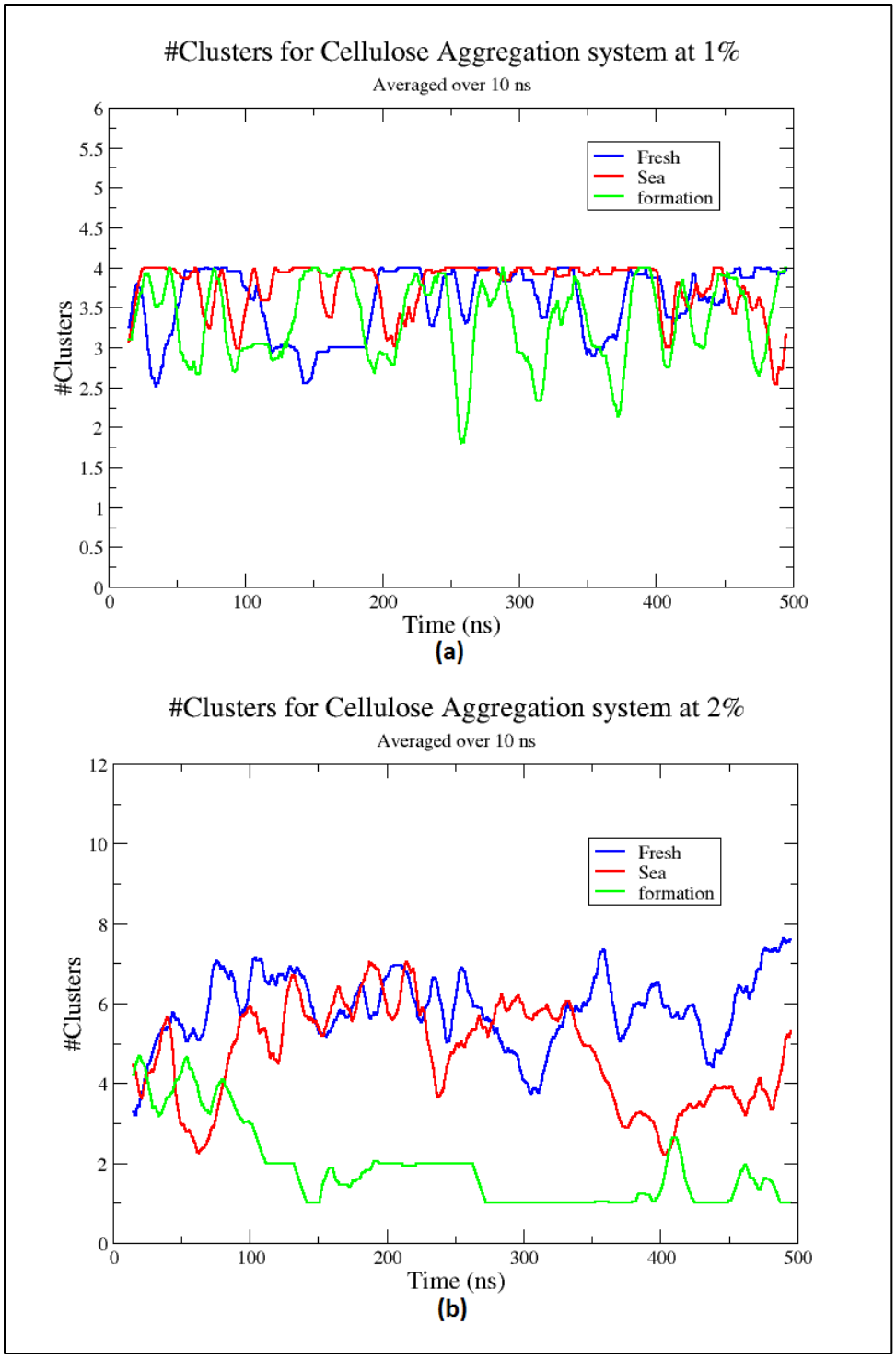

Figure 4-21 Aggregation Analysis for Cellulose at: (a) 1%wt, (b) 2%wt

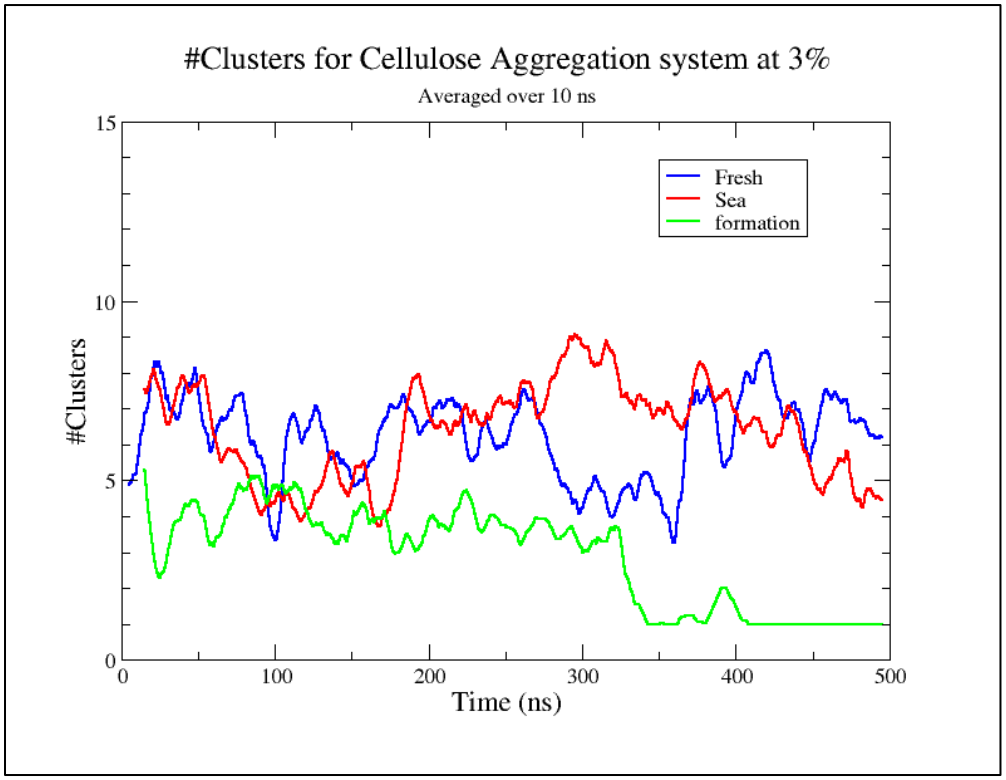

Figure 4-22 Aggregation Analysis for Cellulose at 3%wt

HEC and HMHEC Aggregation

Figs 4-(23,24) shows the aggregation behavior of HEC and HMHEC, respectively. A significant aggregation is observed at the reservoir (formation water & high temperature) condition compared to the other two conditions. This is not what we expected since HEC is a non-ionic polymer, so no significant effect of salinity on the aggregation is the expected result, the same is observed for HMHEC. The fact that only one cluster is present in the system most of the time means all chains in the system are sticking together, which means the viscosifying ability of this polymer won't be as effective as dispersed chains at that concentration. Also, the fact that at the same concentration, no aggregation is observed for the other two environments implies that this trend is because of the salinity, not the concentration. The RDF analysis shown in the dynamics section also implies no interaction with the ions in all three polymers. The reason for this behavior can be explained in terms of solubility of the polymer chains; as the salinity increased, water molecules became much less the the required amount to dissolve the polymer chains. Therefore, polymer chains are favorable to recompensate the interaction with water by the interaction between themselves.

From the above analysis, by comparing the freshwater behavior for cellulose and HEC, as the concentration increases from 1% to 3% there is a high tendency for the polymer to form clusters. By observing the environment effect on the three polymers, the reservoir condition with its high salinity encourages the polymer to aggregate. In the absence of electrostatic interaction between the polymer and salts in the solution, H-bonds and VDW interaction within the polymer chains appear to dominate in reservoir condition. In fresh and seawater, there are more water molecules to interact with and to form H-bonds with

compared to reservoir condition. This abundance of water molecules enhances the hydration of the polymer chains, thus forming H-bonds with water molecules, and inhibits the aggregation of the polymer chains.

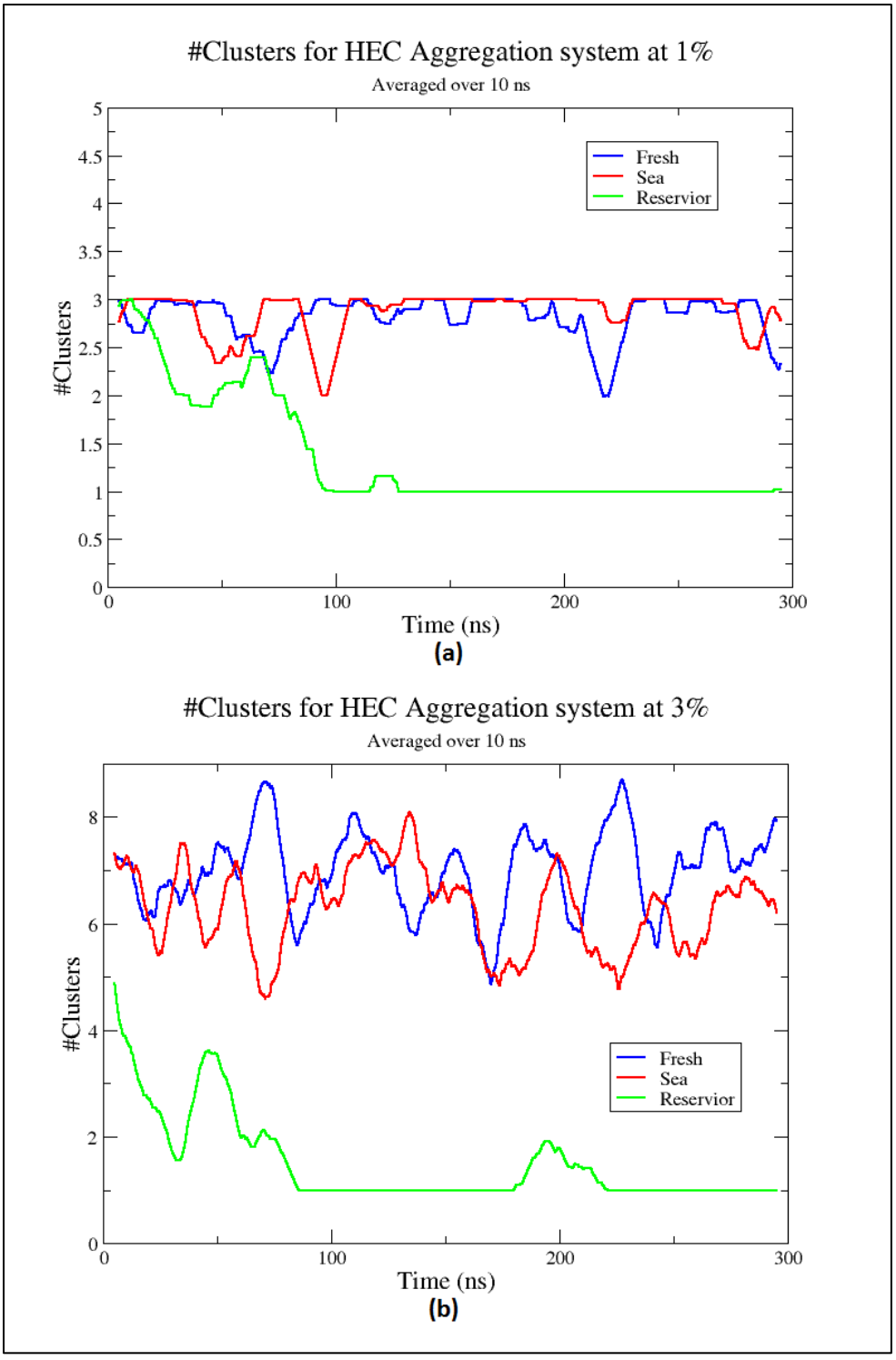

Figure 4-23 Aggregation Analysis for HEC at: (a) 1%wt, (b) 3%wt

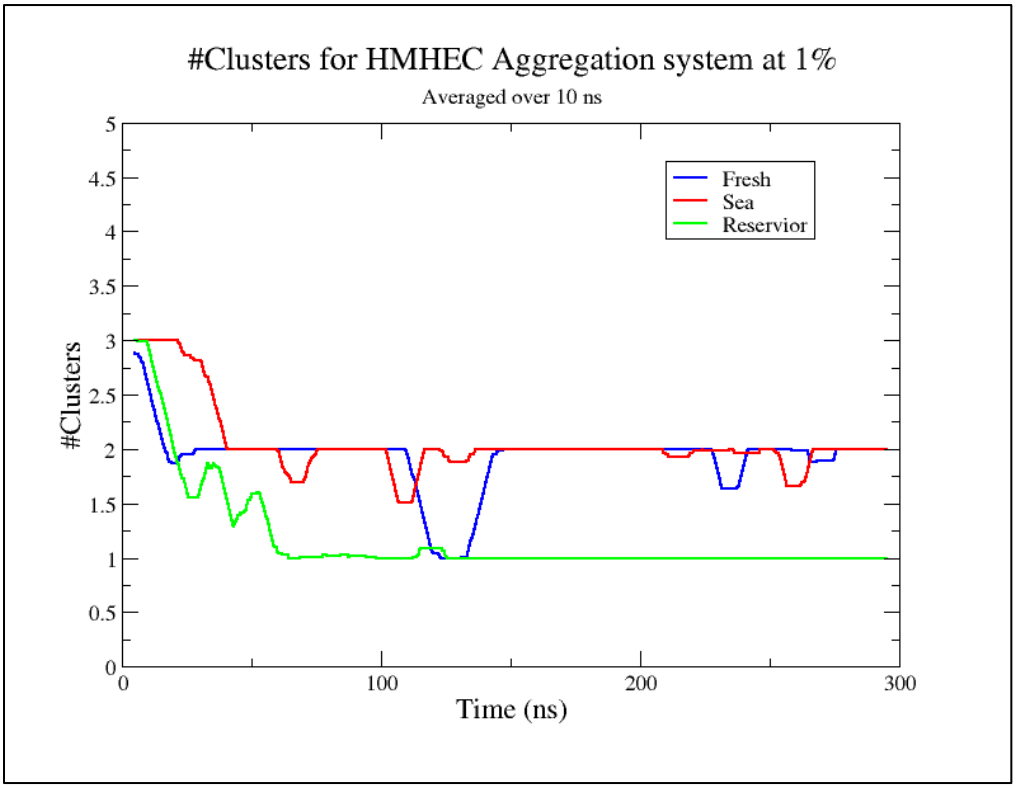

Figure 4-24 Aggregation Analysis for HMHEC at 1%wt

4.3.3 Viscosity Calculation

We tried two methods to calculate the viscosity: 1) The Green-Kubo method (GK), 2) the Diffusion Coefficient method. Both methods were done on 1% polymer concentration system. For the GK method, the results are shown in Table III. pure water viscosity is almost 0.85 cp. The below results show that some of our systems have viscosities lower than the water viscosity. We expected when adding a polymer to water an increase the viscosity, or at worst, give the same viscosity as pure water. The reduced viscosity signifies that the polymer chain might have disturbed the water structure leading to a decrease in the viscosity. At the dilute polymer concentration, Green-Kubo seems to be not suitable to calculate the viscosity of the polymer solutions. Especially, GK requires long simulations to reach steady state conditions, and this approach if time decomposition method is not accurate enough to overcome this issue [70]. Therefore, we tried using Stockes-Enstein equation, which indirectly calculate the viscosity via the calculation of diffusion cooeficient.

TABLE 4-2 Results of GK method to calculate the viscosity (cp) for 1% conc.

Environment	Cellulose	HEC	HMHEC
Fresh	0.72	0.73	0.88
Sea	1.09	0.91	0.47
Reservoir	0.65	1.66	0.64

In Stockes-Enstein method, we calculated the diffusion coefficient from the simulation, and then substitute it in equation (4.1) to find the viscosity. This analysis was conducted on aggregation systems (multiple 10-units long chains) and on dynamics

systems (single 30-units long chain). The results are shown in Table IV. Results for both system types don't agree with the experimental data of almost 200 cp at 1% HEC in fresh water [29].

TABLE 4-3 Results of Diffusion Coefficient method to calculate the viscosity (cp) for 1% conc.

Polymer		Fresh	Sea	Reservoir
Cellulose	**Single chain**	0.22	0.63	0.23
	Multi-chain	4.08	1.62	1.34
HEC	**Single chain**	0.21	0.52	0.24
	Multi-chain	2.17	2.00	1.85
HMHEC	**Single chain**	1.04	0.67	0.62
	Multi-chain	2.58	1.76	1.65

The difference between the results of the aggregation systems and the dynamics systems suggest that there is a significant finite-size artefact that affects the viscosity. These results from the two methods suggest using coarse grain simulation to find the viscosity of the systems. This investigation is outside the scope of this study, and will not be tackled further. However, its worth noting that the viscosity as we go from fresh to reservoir for HEC is negldibly different. There is a small difference in HMHEC of almost 1 cp and a larger difference in cellulose of 3 cp. This strengthen the trend observed so far for HEC's indifferent behavior with different salinity conditions.

4.3.4 Interfacial properties with oil.

An example of the IFT simulations if the oil-water system is shown in Fig 4-25. It is well known that a lower interfacial tension (IFT) at the oil-water interface helps emulsify them, and thus, enhance oil extraction efficiency. We aim to see the effect of cellulose and HEC on the IFT of water-oil system at different salinity conditions. Fig 4-26 shows the IFT values and trends averaged every 10ns for different salinities, and one curve without polymer.

Quantitively speaking, the sea water condition has the highest IFT values. Fresh and no-polymer conditions show similar values and trends. The difference between the values of IFT is negligible, which indicates that cellulose and HEC have minor effects on the IFT trend. This is in agreement with the experimental observation that the polymer is water-phase component and it has not interfacial activity. Therefore, polymer are added to cEOR formulations in order to control the mobility ratio rather than the IFT of water-oil system.

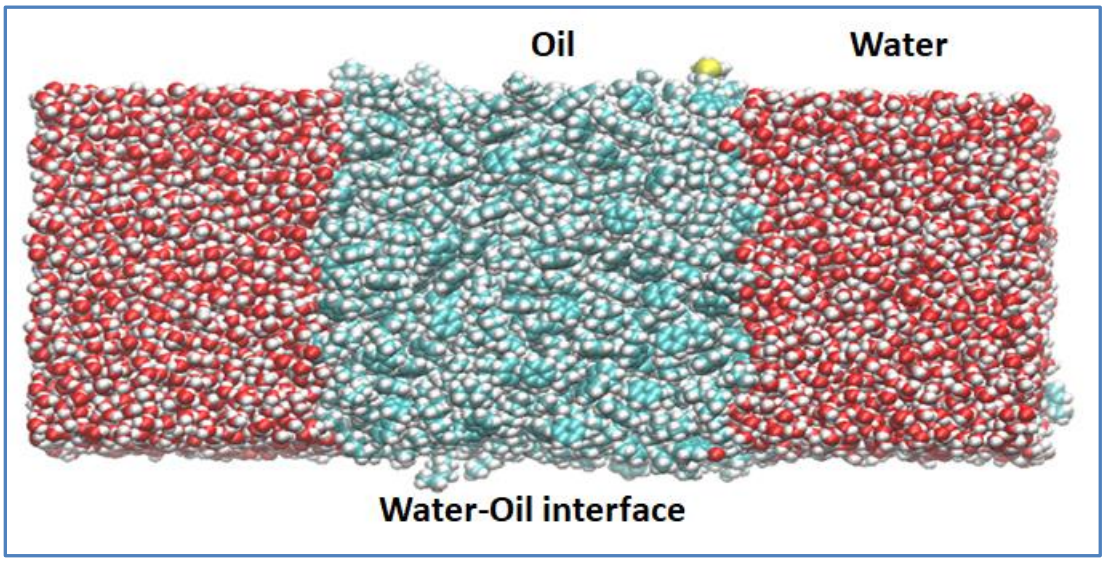

Figure 4-25: Shows an example system of IFT calculation of water-oil system.

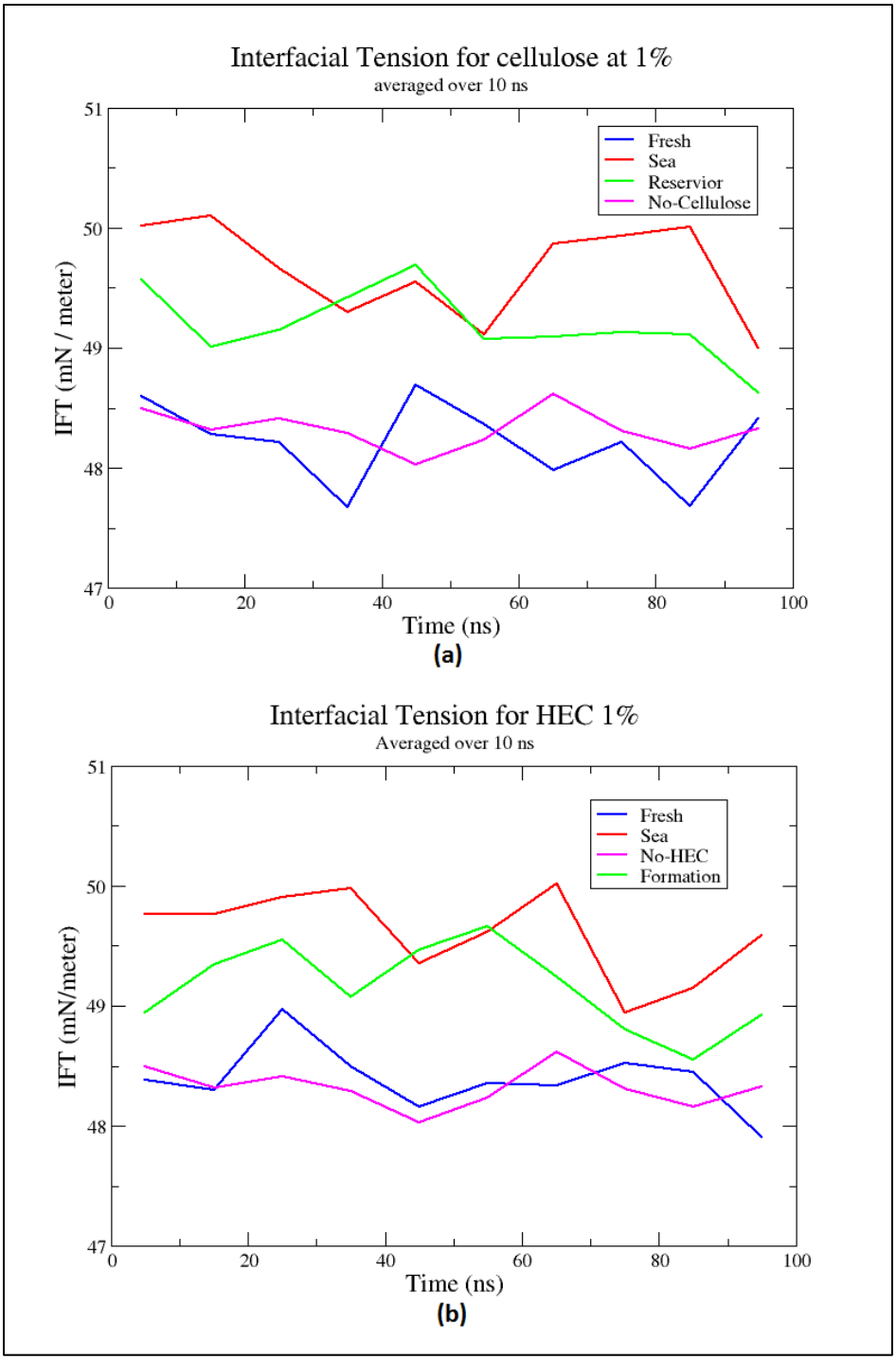

Figure 4-26 Interfacial Tension at different environments for: (a) Cellulose, (b) HEC

4.3.5 Interaction with surfactant

We have performed simulations in which we have studied the behavior of polymer+surfactant in order to examine the effect of the polymer and surfactant on each other. Surfactants are chemical compounds that consist of hydrophobic and hydrophilic parts such that the first is immersed in oil and the later in water. With this "bridge" at the interface, the interfacial tension between oil and water reduces significantly. An example of surfactants are the every day's washing hand soap. The reason why soap can help clean our oily hands is because it contains a surfactant that reduces IFT at the oil-water interface and helps to solubilize the dirties (hydrophobic in nature) in water. Thus, it becomes easier to remove sticky oil from our hands. The same situation in oil industry, we add surfactants to reduce IFT between oil-water and increase the mobility by forming emulsion solution and avoid water fingering.

The Surfactant used here is SDS (sodium deodecyl sulfate:SDS), and can be seen in Fig 4-27. We simulated four cellulose chains and three HEC chains in different systems with 24 SDS chains in each system corresponding to 1%wt for each chemical. The force field for SDS is taken from a recent study by Abdel-azeim [68].

First, we investigated the surfactant effect by comparing two systems at fresh water, without and with 1%wt of SDS. The results are shown in Figs 4-(28,29,30). The polymer side-chain dynamics is insensentive to SDS. The inter-chain H-bonds, by comparing with the fresh water conditions, also appear very close, with an average H-bond of 13 per mer of polymer chain. From these results, we conclude that the surfactant does not affect the dynamics of cellulose.

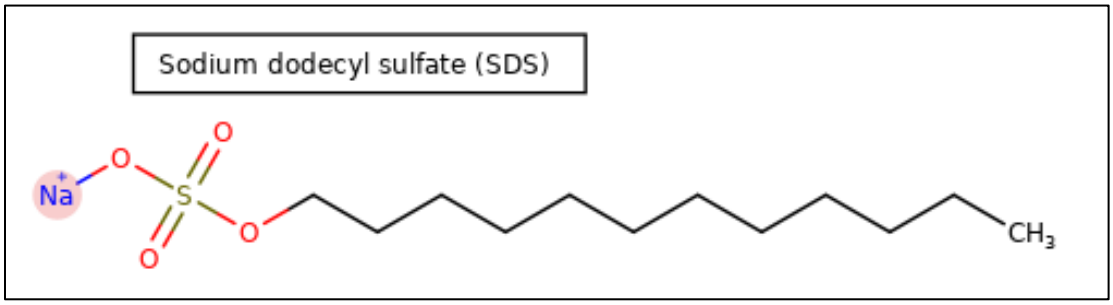

Figure 4-27 The chemical structure of the surfactant (SDS)

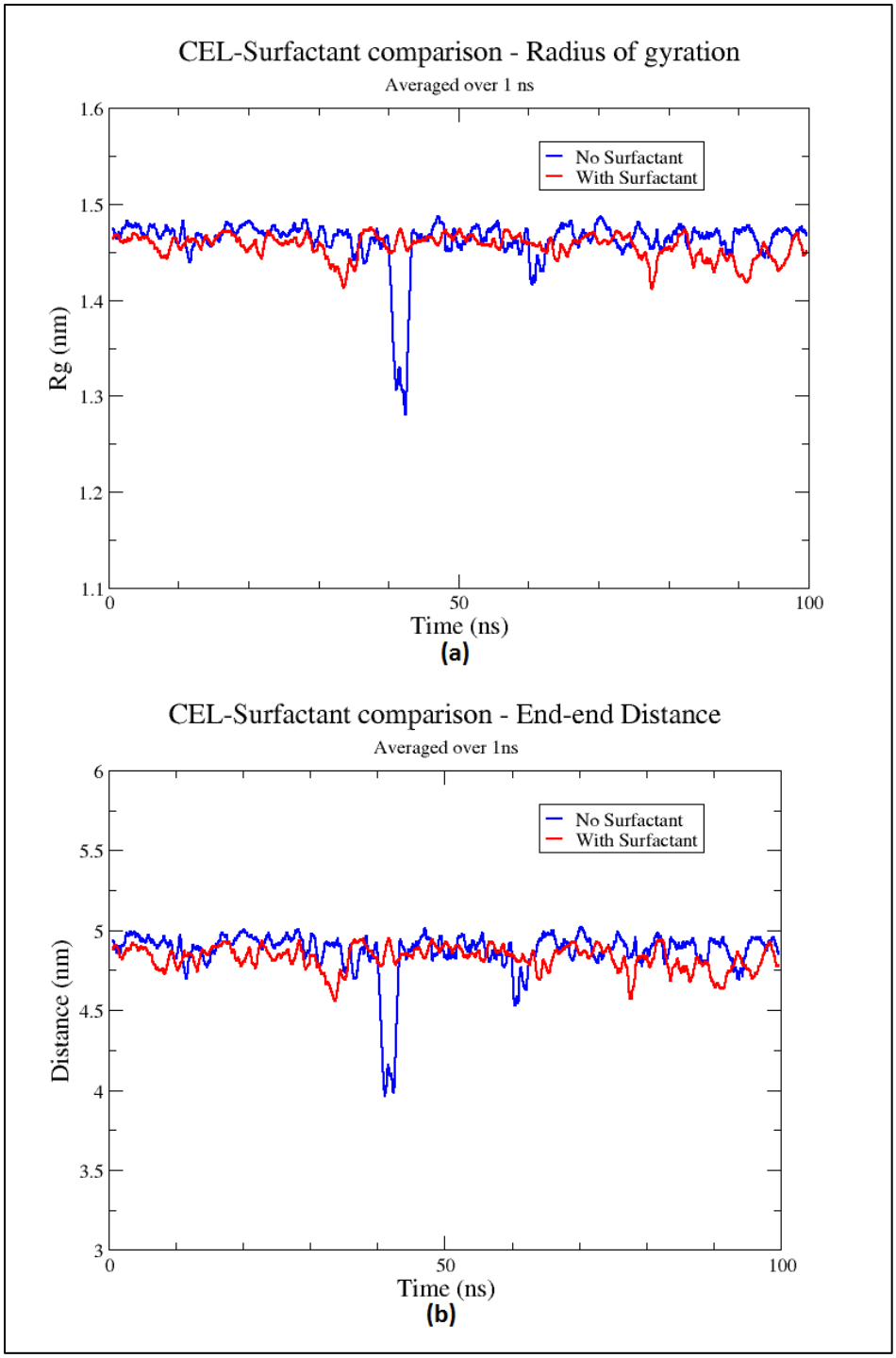

Figure 4-28 (a) Radius of gyration, (b) End-end distance, for comparison of Surfactant and No-Surfactant behavior

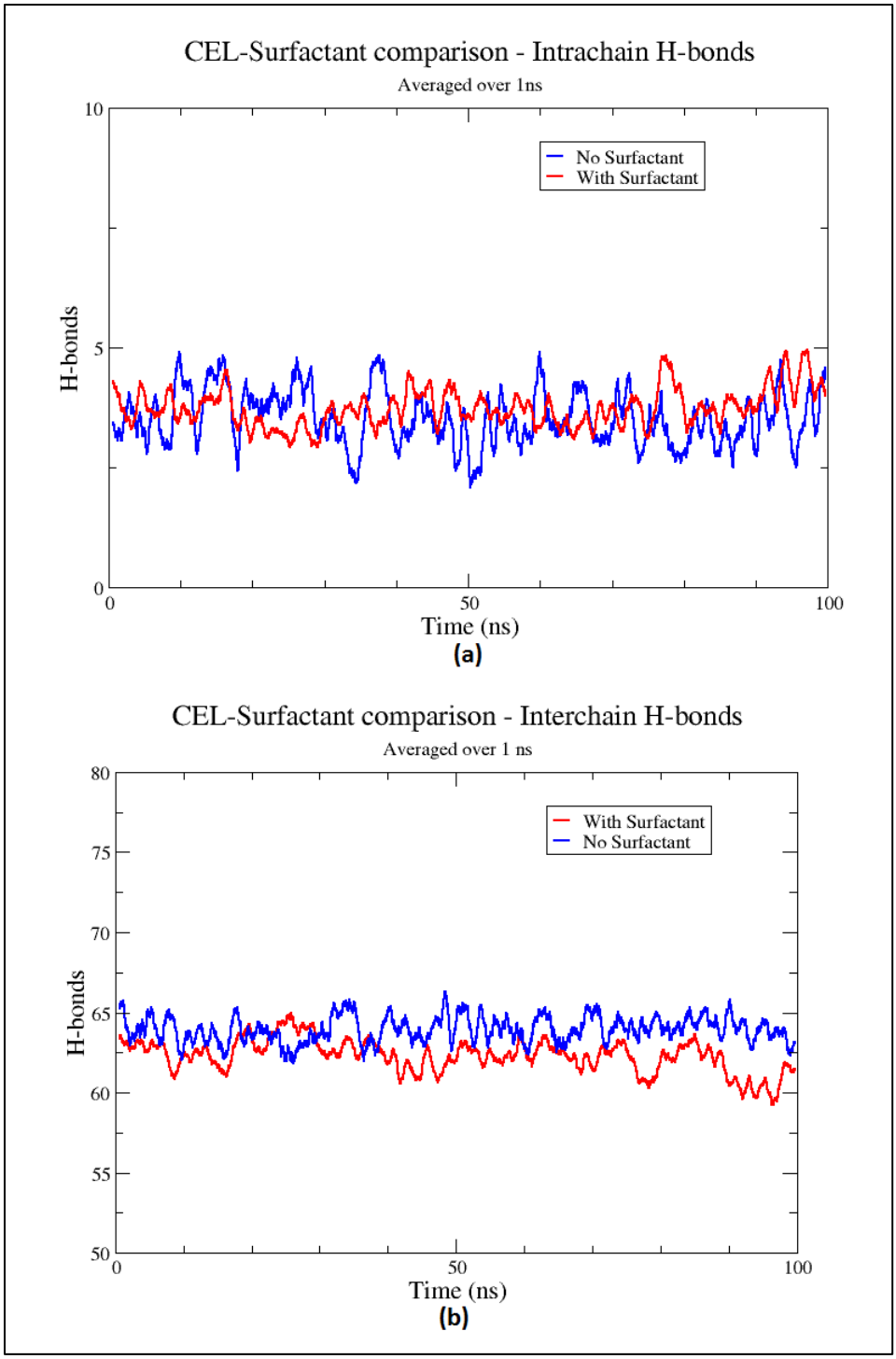

Figure 4-29 (a) Intra-chain H-bonds, (b) Inter-chain H-bonds, for comparison of Surfactant and No-Surfactant behavior

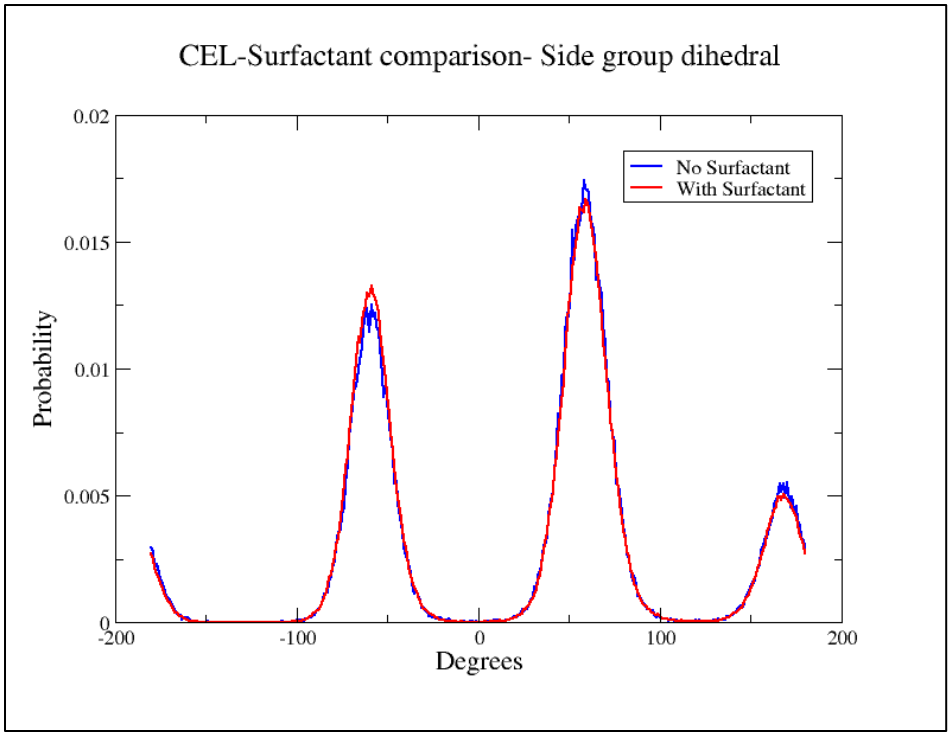

Figure 4-30 Side group Dihedral angle distribution for comparison of Surfactant and No-Surfactant behavior

Next, we compared the chain dynamics behavior of 1% wt of cellulose and HEC systems with 1% wt of SDS, each system at the three-different environmental conditions; fresh-water, sea-water and reservoir condition. The results are shown in Figs 4-(31-35).

The polymer chain dynmaics in case of CEL-SDS does not influenced by the presence of SDS at the three different surrounding conditions, as we can see in the trend of radius of gyration and end-to-end distance. The polymer hydration in the three different conditions, is similar to the polymer solutions, which dicussed earlier. In general, as the salinity increases the polymer hydration decreases. The interaction water-ions is much more stronger than the interaction water-polymer due to its non-ionic nature, which in turn minimize the polymer hydration. In agreement with the previous observation, the intra-chain supposed to increase and lead to more aggregation.

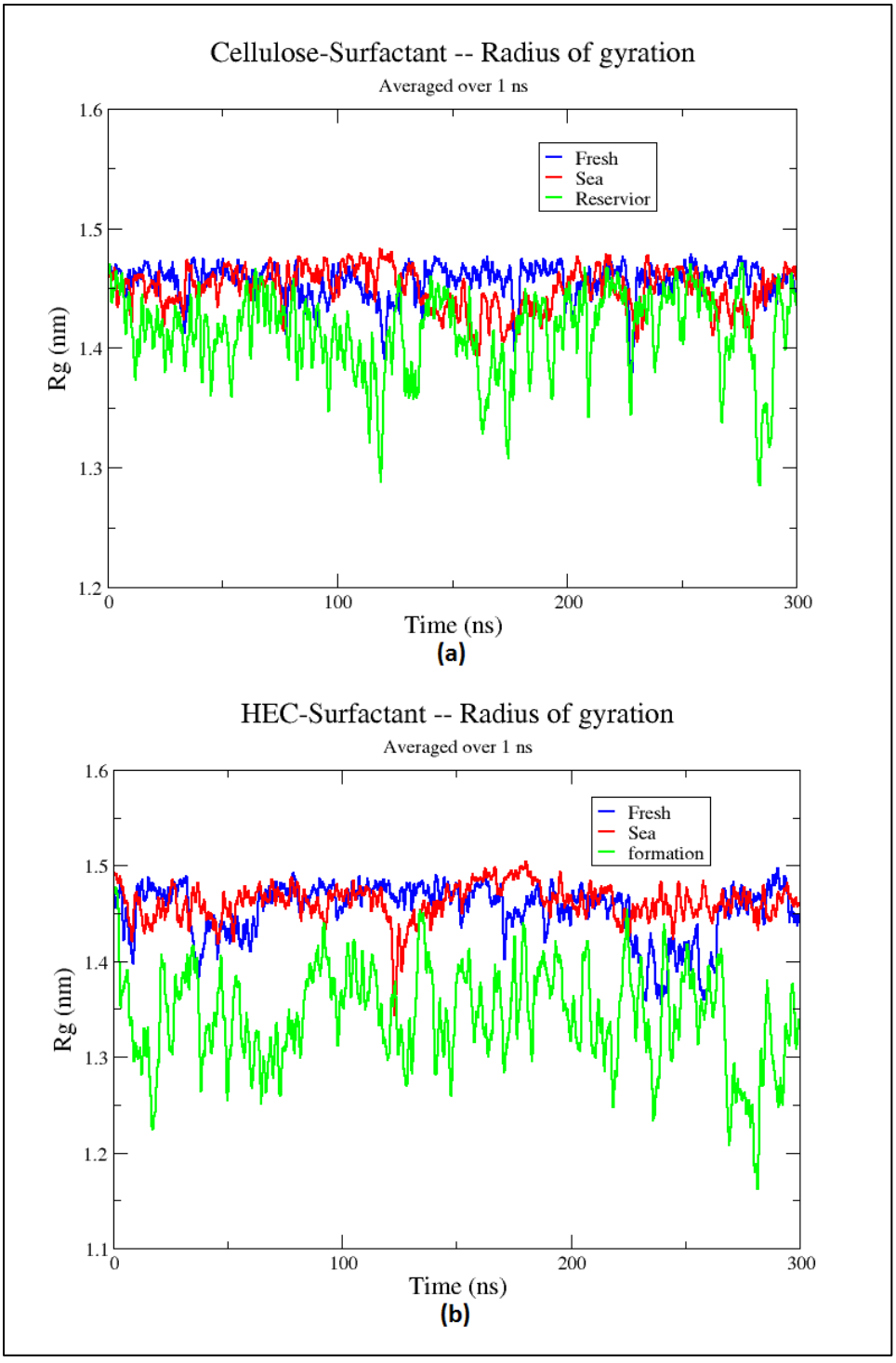

Figure 4-31 Radius of gyration for: (a) Cellulose, (b) HEC, with surfactant

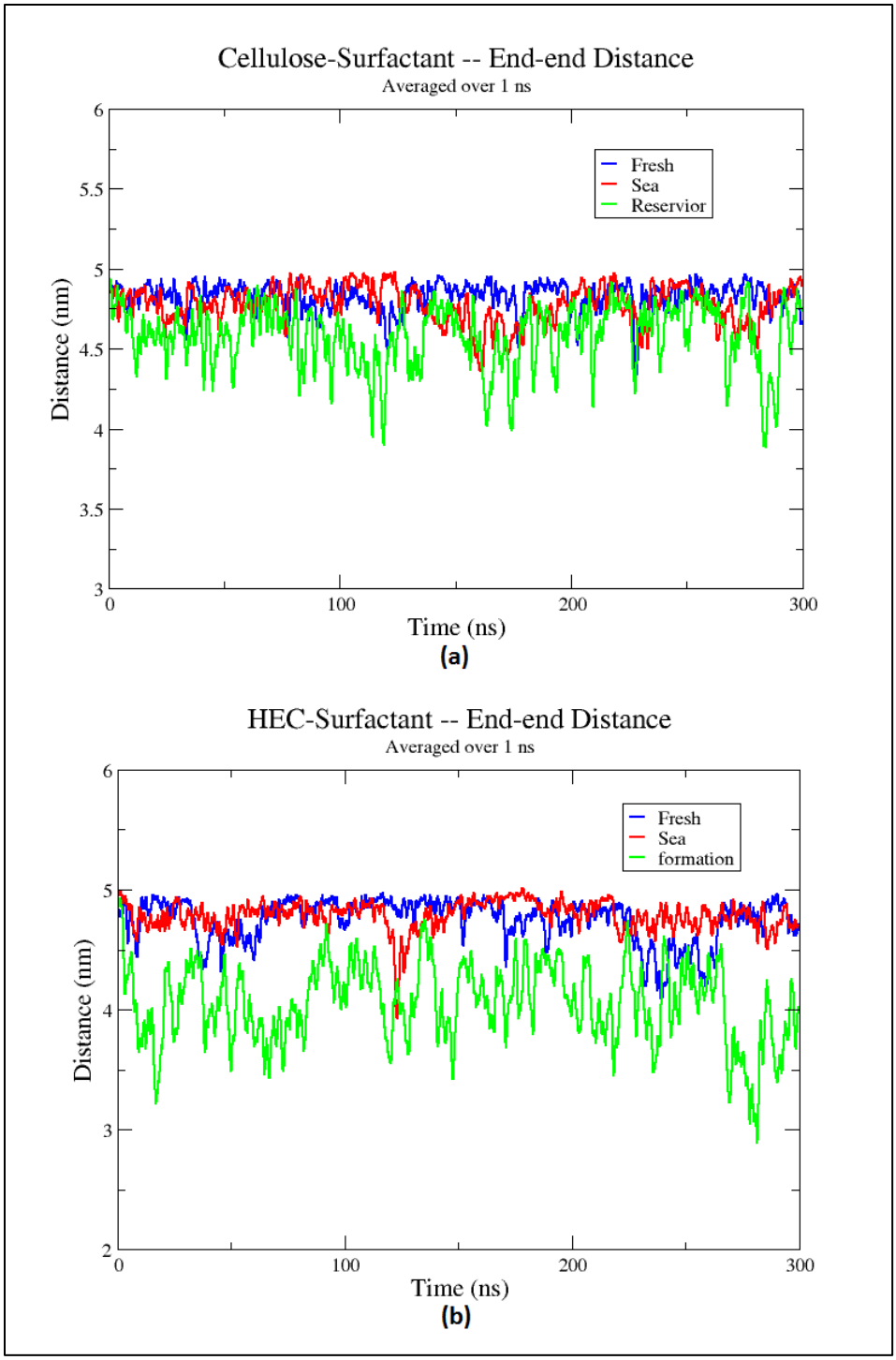

Figure 4-32 End-end Distance for: (a) Cellulose, (b) HEC, with surfactant

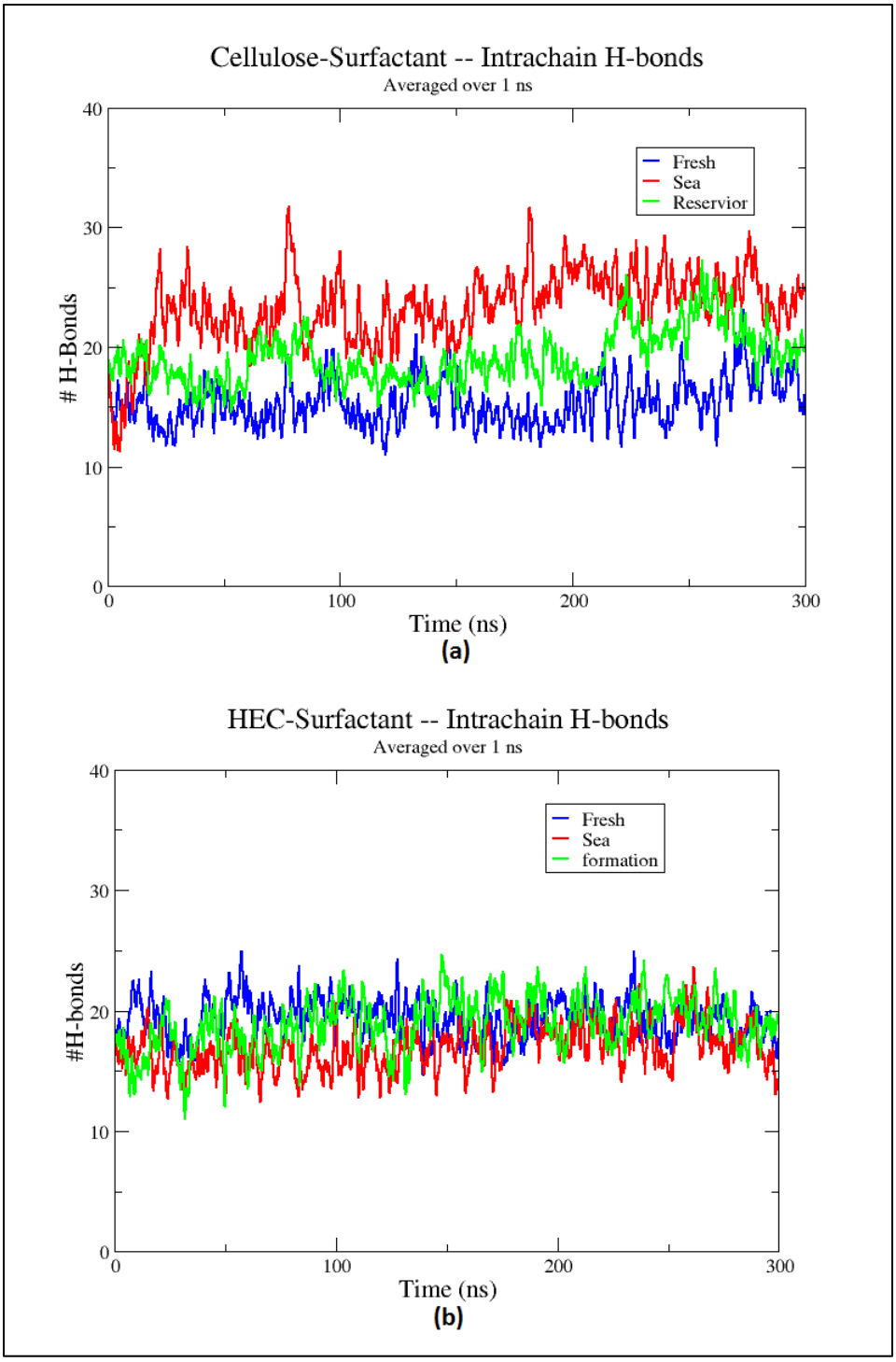

Figure 4-33 Intrachain H-bonds for: (a) Cellulose, (b) HEC, with surfactant

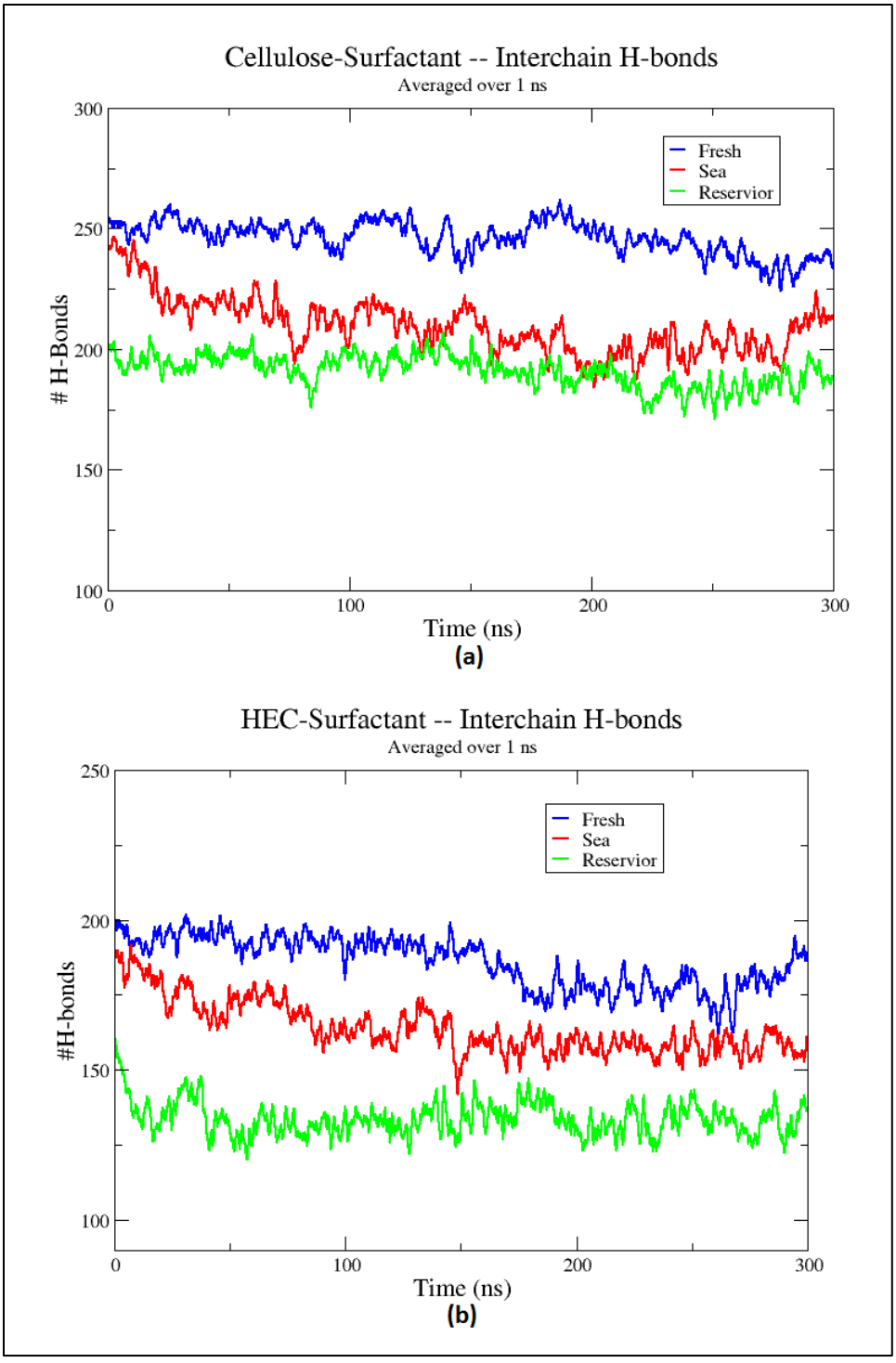

Figure 4-34 Interchain H-bonds for: (a) Cellulose, (b) HEC, with surfactant

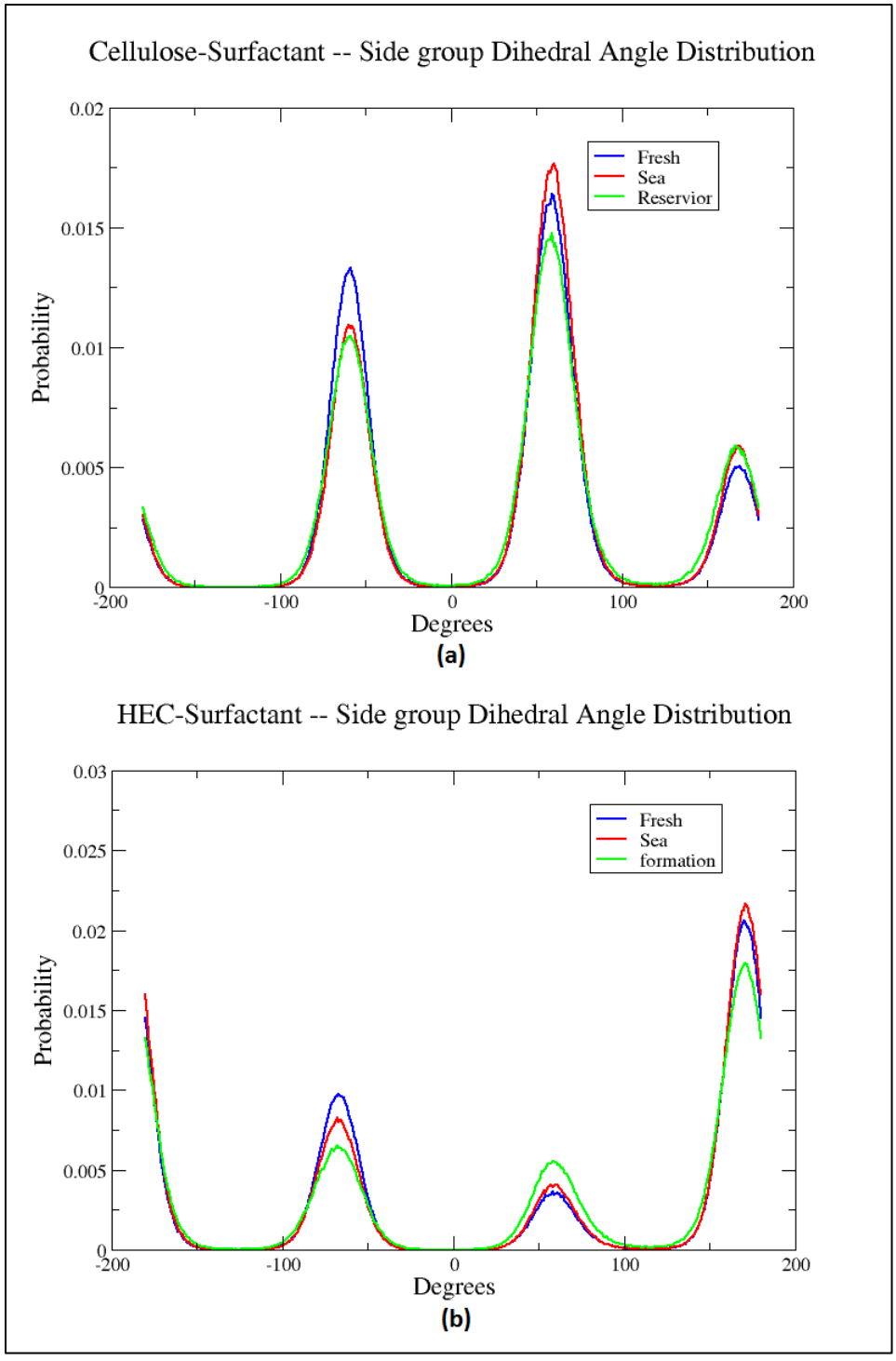

Figure 4-35 Side group Dihedral angle for: (a) Cellulose, (b) HEC, with surfactant

Simular results HEC are found to be quit close to those of CEL. Indeed, in Fig 4-31 the extended state in fresh and seawater is similar to that found in CEL. However, at reservoir condition, a more compact state is observed. This indicates that at reservoir condition, the ethyl group tends to make HEC more compact compared to CEL. However, the compactness isn't very big since the maximum compact state length is longer than half of the fully extended state shown in Fig 4-32. The Inter-chain H-bonds follow a logical order with freshwater condition having the highest number of bonds and reservoir condition the least. The intrachain again shows a strange behavior, the number of bonds here is almost the same irrespective of the environment. Comparing the number of Intrachain hydrogen bonds to cellulose shows almost the same number. For this analysis to be complete, we should check the RDF analysis in the next section to see if cellulose and HEC are forming bonds with the surfactant that affect the hydrogen bonding. The RDF analysis for cellulose and HEC is shown in Fig 4-(36,37).

The RDF analysis explains the behavior for Intrachain hydrogen bonds previously. The interaction with surfactant at sea and reservoir condition is almost the same in the case of cellulose. Now for HEC, the interaction at reservoir is significantly higher than seawater condition, leaving less space for the reservoir chain to form intrachain hydrogen bonds. Therefore, the intrachain hydrogen bonds are reduced in reservoir condition to be almost the same as sea and fresh water. If we compared cellulose and HEC interaction with a surfactant, HEC interacts with the surfactant more intensely compared with cellulose, this is due the longer ethyl group that give HEC more ability to interact and form bonds with SDS compared to cellulose. Herein, we observed a positive effect of SDS on HEC; the surfactant decrease the aggregation tendency of the polymer by forming H-bonds with the

polymer. It seems that the polymer and SDS have a protective effect on each other and avoid aggregation for both molecules.

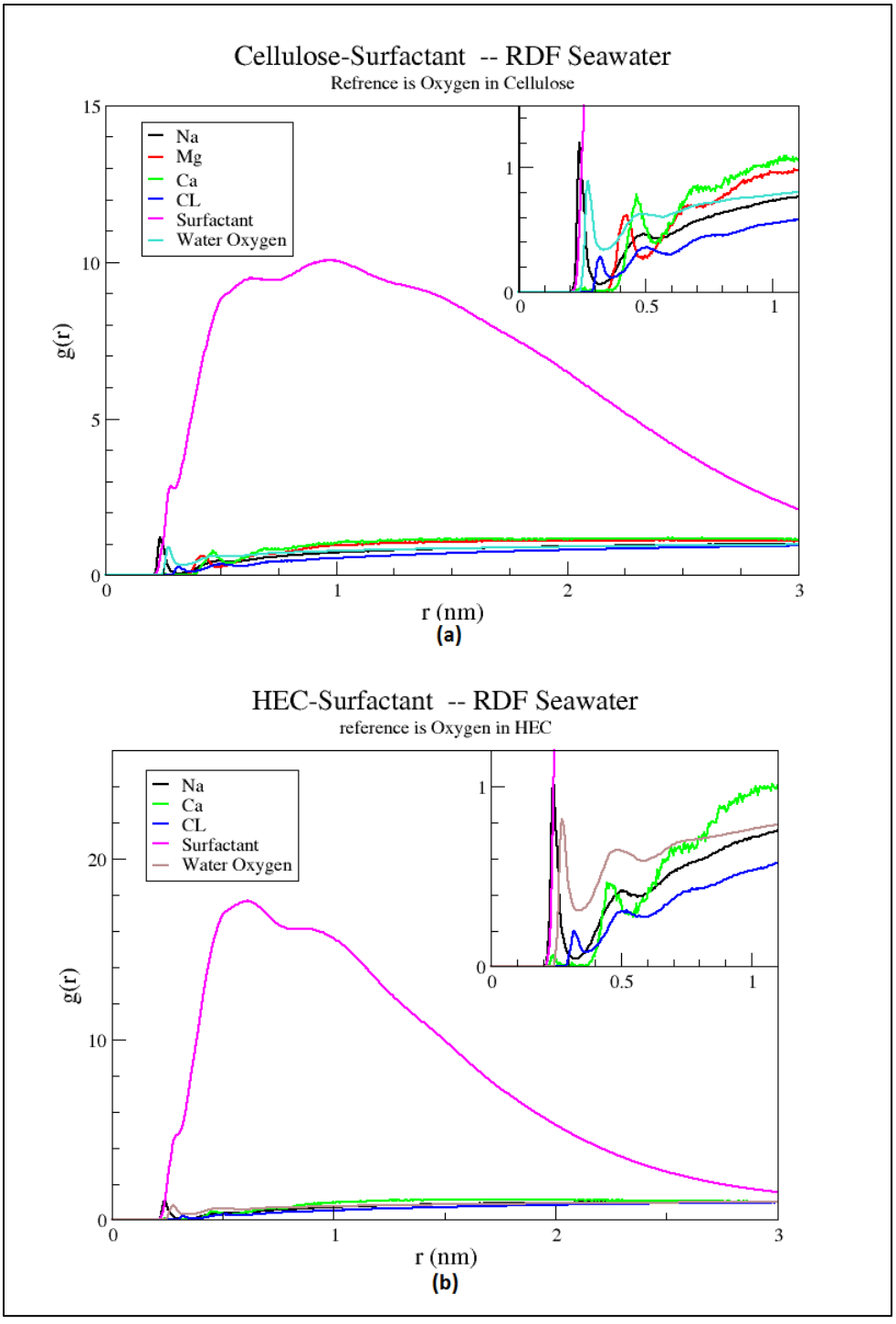

Figure 4-36 RDF analysis at Seawater condition for: (a) Cellulose, (b) HEC

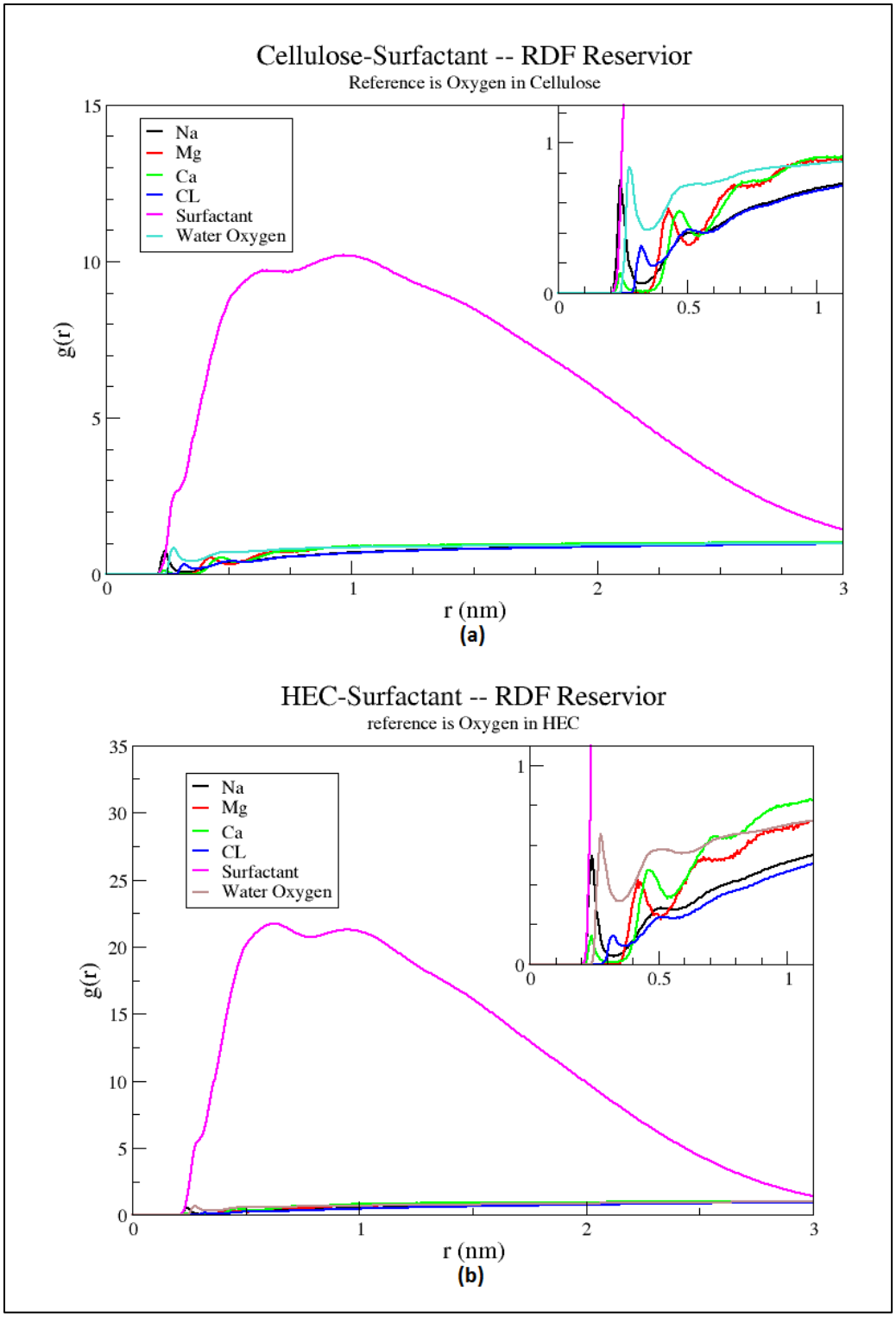

Figure 4-37 RDF analysis at Reservoir condition for: (a) Cellulose, (b) HEC

Since the interaction with the surfactant is stronger in HEC than in cellulose, does this cause HEC to aggregate? Also, one point wasn't explained by the RDF analysis, in the cellulose results, the seawater forms higher intrachain hydrogen bonds and has similar surfactant interaction when compared to the reservoir, why? We suspect that the reservoir condition either forms higher intrachain bonds, or have higher surfactant interaction to explain the "similar-to-seawater" intrachain hydrogen bonding behavior, but this is not what is happening. Next, we should look at the aggregation analysis in order to answer these two questions.

The aggregation behavior in the presence of surfactant is shown in Fig 4-38. To answer the first question above about HEC, seawater and reservoir condition indeed show aggregation behavior compared to freshwater. But comparing this to the cellulose behavior, the reservoir condition in cellulose doesn't show significant aggregation compared to HEC. For the second question, the cellulose seawater system shows indeed a very aggressive aggregation behavior. The four cellulose chains are sticking together most of the time resulting in the intrachain hydrogen bonds to be higher than comparatively dispersed reservoir chains.

Images of the systems (cellulose+SDS, HEC+SDS) in reservoir condition are shown in Figs 4-(39,40). The polymers don't interact with the ions by electrostatic forces since they are non-ionic, but they interact with the SDS by forming H-bonds and VDW forces. These interactions lead to the aggregation behavior of the polymer+SDS brine solutions. Such, nano-scale aggregation will help to protect the polymer and surfactant (anionic) somehow from the agrressive harsh conditions of oil reservoirs.

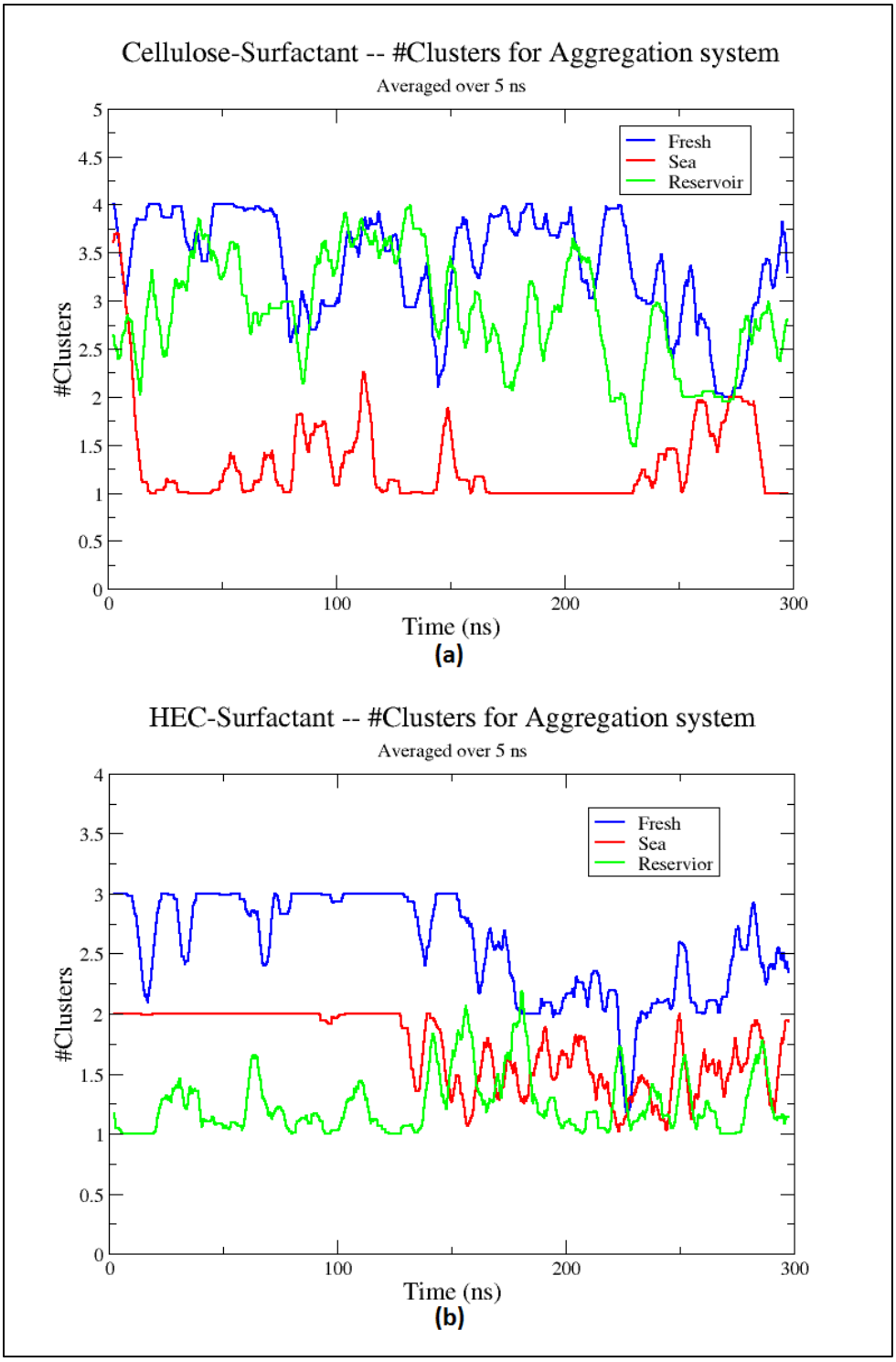

Figure 4-38 Aggregation Analysis in the presence of surfactant for: (a) Cellulose, (b) HEC

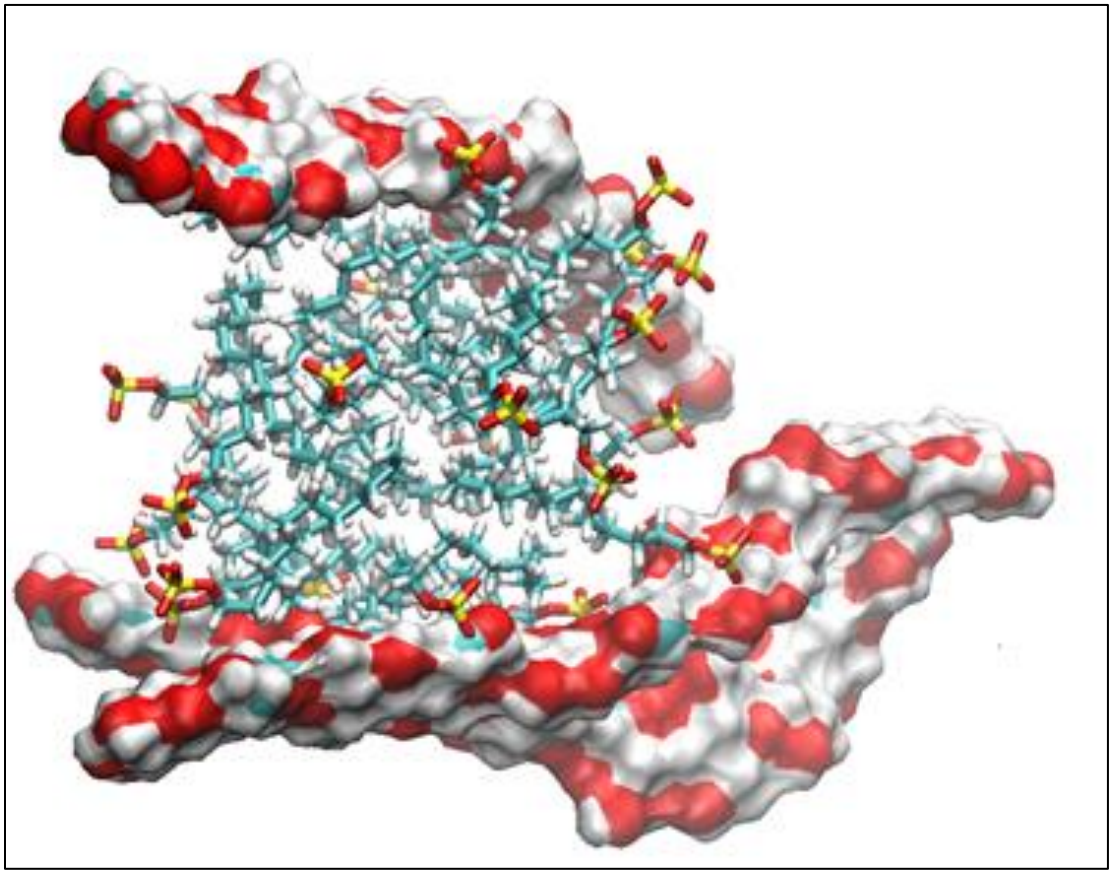

Figure 4-39 Cellulose + SDS system at Reservoir condition

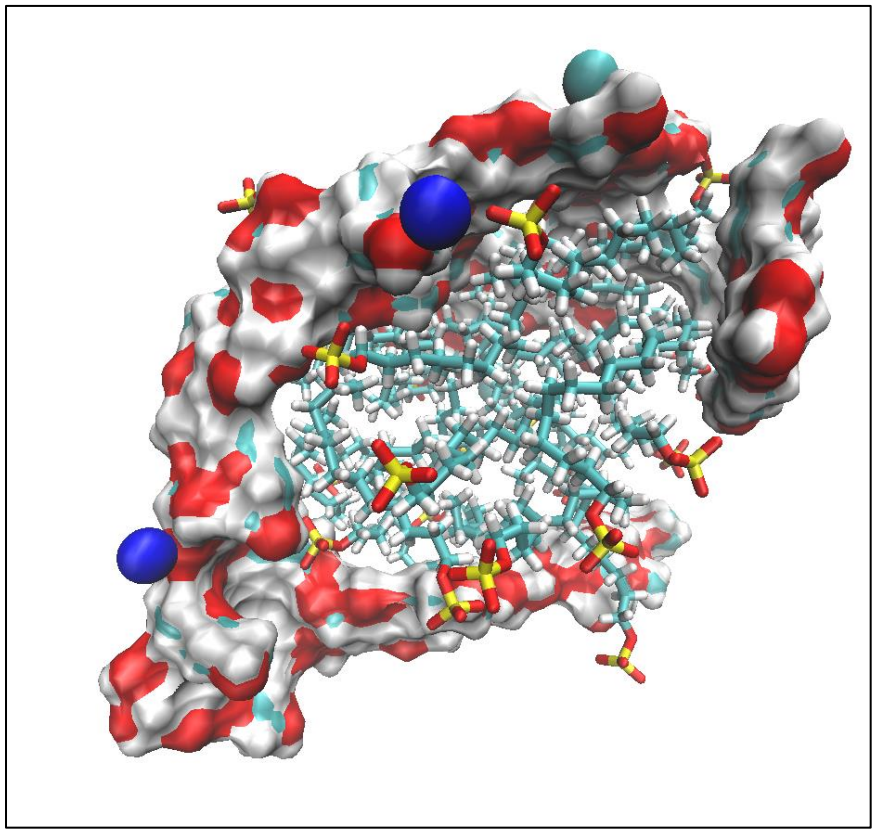

Figure 4-40 HEC + SDS system in Reservoir condition

4.4 Conclusion

We conducted MD simulation to investigate cellulose, HEC and HMHEC for EOR applications. We studied the polymer chain-dynamics, aggregation, interfacial properties and surfactant interaction at three different salinity conditions (freshwater, seawater and reservoir connate water). CEL and HEC were found to display a quite rigid backbone irrespective of the salinity conditions. This supports its application in cEOR activities as a good alternatives for HPAM at high salinity and temperature conditions. HMHEC however, was found to be somehow impacted by reservoir conditions, is displays compact conformations with less inter-Hbonds formed at these harsh environment.

Concerning the polymer aggregation, all considered polymers showed higher tendency to form nano-scale aggregates, which means that the application of these polymers should be at less than 1 wt. % concentration. Also, we have observed the formation of nano-scale composites between polymer and SDS, which acted as a protective parameter of both molecules against the reservoir harsh conditions of high salinity. The origin of the nano-scale composite of polymer+SDS is the HBons and VDW type of interactions.

With regard to the interfacial properties of the considered polymers; CEL and HEC showed a negligible effect on the IFT of oil-water system. However, these polymers can affect the diffusion of the surface active moelcules (surfactants) to the interface, which in turns impact oil-water IFT.

The analysis for CEl+SDS solutions showed that that the polymer chain dynamics was not affected by the presence of SDS. CEL and HEC tended to form nano-scale composites with SDS, which is a proptective parameter against the reservoir conditions. The main

driving forces of these composites are H-bonds and VDW type of interactions between the polymer and SDS.

Chapter 5 References

[1] " Statistical Review of World Energy Statistical Review of World" 2019.

[2] E. Information, "Annual Energy Outlook 2020," 2020.

[3] "Gas Cap Drive - GLOSSARY - Nafta Wiki." [Online]. Available: http://nafta.wiki/display/GLOSSARY/Gas+Cap+Drive. [Accessed: 04-Apr-2020].

[4] "Drive mechanisms and recovery - AAPG Wiki." [Online]. Available: https://wiki.aapg.org/Drive_mechanisms_and_recovery. [Accessed: 04-Apr-2020].

[5] E. Tzimas, A. Georgakaki, C. Garcia Cortes, and S. D. Peteves, "Enhanced oil recovery using carbon dioxide in the European energy system," 2005.

[6] "Number of EOR projects in operation globally, 1971-2017 – Charts – Data & Statistics - IEA." [Online]. Available: https://www.iea.org/data-and-statistics/charts/number-of-eor-projects-in-operation-globally-1971-2017. [Accessed: 04-Apr-2020].

[7] N. Zhang, M. Wei, and B. Bai, "Statistical and analytical review of worldwide CO2 immiscible field applications," *Fuel*, 2018.

[8] "Petroleum Development Oman and GlassPoint Announce Commencement of Steam Delivery From Miraah Solar Plant | Business Wire." [Online]. Available: https://www.businesswire.com/news/home/20171101005644/en/Petroleum-Development-Oman-GlassPoint-Announce-Commencement-Steam. [Accessed: 22-Mar-2020].

[9] "GlassPoint Brings Gigantic 850 MWth Solar EOR to California - Solarpaces." [Online]. Available: http://www.solarpaces.org/glasspoint-brings-gigantic-850-mwth-solar-eor-to-california/. [Accessed: 22-Mar-2020].

[10] A. Mohsenatabar Firozjaii and H. R. Saghafi, "Review on chemical enhanced oil recovery using polymer flooding: Fundamentals, experimental and numerical simulation," *Petroleum*, 2019.

[11] L. E. Zerpa, N. V. Queipo, S. Pintos, and J. L. Salager, "An optimization methodology of alkaline-surfactant-polymer flooding processes using field scale numerical simulation and multiple surrogates," *J. Pet. Sci. Eng.*, vol. 47, no. 3–4, pp. 197–208, 2005.

[12] W. Demin, Z. Zhenhua, C. Jiecheng, Y. Jingchun, G. Shutang, and L. Lin, "Pilot Tests of Alkaline/Surfactant/Polymer Flooding in Daqing Oil Field," *SPE Reserv. Eng. (Society Pet. Eng.*, vol. 12, no. 4, pp. 229–232, 1997.

[13] C. Dang, L. Nghiem, N. Nguyen, Z. Chen, C. Yang, and W. Bae, "A comprehensive evaluation of Alkaline surfactant polymer flooding and hybrid

process for enhanced oil recovery," *Proc. - SPE Annu. Tech. Conf. Exhib.*, 2017.

[14] A. A. Olajire, "Review of ASP EOR (alkaline surfactant polymer enhanced oil recovery) technology in the petroleum industry: Prospects and challenges," *Energy*, vol. 77, pp. 963–982, 2014.

[15] W. Hongyan, C. Xulong, Z. Jichao, and Z. Aimei, "Development and application of dilute surfactant-polymer flooding system for Shengli oilfield," *J. Pet. Sci. Eng.*, vol. 65, no. 1–2, pp. 45–50, 2009.

[16] R. Fortenberry *et al.*, "Use of cosolvents to improve alkaline/polymer flooding," *SPE J.*, vol. 20, no. 2, pp. 255–266, 2015.

[17] A. Aitkulov, H. Luo, J. Lu, and K. K. Mohanty, "Alkali-Cosolvent-Polymer Flooding for Viscous Oil Recovery: 2D Evaluation," *Energy and Fuels*, vol. 31, no. 7, pp. 7015–7025, 2017.

[18] J. Sheng, *Modern Chemical Enhanced Oil Recovery: Theory and Practice*. 2010.

[19] E. O. Recovery, P. Hall, T. C. Assumption, L. T. Equilibrium, and V. Flux, "Chapter 6 Conservation Equations for Multiphase- Multicomponent Flow Through Porous Media," *Media*, 1989.

[20] A. Borthakur, A. Sarmah, M. Rahman, and B. Subrahmanyam, "Dilute solution behaviour of partially hydrolysed polyacrylamide," *Indian J. Chem. Technol.*, 1996.

[21] M. E. Zeynali, A. Rabii, and H. Baharvand, "Synthesis of partially hydrolyzed polyacrylamide and investigation of solution properties (Viscosity Behaviour)," *Iran. Polym. J. (English Ed.*, 2004.

[22] S. K. Choi, M. M. Sharma, S. L. Bryant, and C. Huh, "pH-sensitive polymers for novel conformance control and polymerflood applications," in *Proceedings - SPE International Symposium on Oilfield Chemistry*, 2009.

[23] A. Zaitoun and B. Potie, "LIMITING CONDITIONS FOR THE USE OF HYDROLYZED POLYACRYLAMIDES IN BRINES CONTAINING DIVALENT IONS.," in *Society of Petroleum Engineers of AIME, (Paper) SPE*, 1983.

[24] H. Lu, Y. Feng, T. Zhang, and Z. Huang, "Retention behaviors of hydrophobically associating polyacrylamide prepared via inverse microemulsion polymerization through porous media," *J. Macromol. Sci. Part A Pure Appl. Chem.*, 2010.

[25] Y. Wu, K. S. Wang, Z. Hu, B. Bai, P. Shuler, and Y. Tang, "A new method for fast screening of long-term thermal stability of water soluble polymers for reservoir conformance control," in *Proceedings - SPE Annual Technical Conference and Exhibition*, 2009.

[26] A. Sabhapondit, A. Borthakur, and I. Haque, "Characterization of acrylamide

polymers for enhanced oil recovery," *J. Appl. Polym. Sci.*, 2003.

[27] J. Choi *et al.*, "Evaluation of highly stable ultrahigh-molecular-weight partially hydrolyzed polyacrylamide for enhanced oil recovery," *Macromol. Res.*, 2015.

[28] Z. L. Yang, B. Y. Gao, C. X. Li, Q. Y. Yue, and B. Liu, "Synthesis and characterization of hydrophobically associating cationic polyacrylamide," *Chem. Eng. J.*, 2010.

[29] Y. Bai, X. Shang, Z. Wang, and X. Zhao, "Experimental Study on Hydrophobically Associating Hydroxyethyl Cellulose Flooding System for Enhanced Oil Recovery," *Energy and Fuels*, vol. 32, no. 6, pp. 6713–6725, 2018.

[30] G. D. Khune, L. G. Donaruma, M. J. Hatch, N. H. Kilmer, J. S. Shepitka, and F. D. Martin, "Modified acrylamide polymers for enhanced oil recovery," *J. Appl. Polym. Sci.*, 1985.

[31] P. Liu, Z. Mu, C. Wang, and Y. Wang, "Experimental Study of Rheological Properties and Oil Displacement Efficiency in Oilfields for a Synthetic Hydrophobically Modified Polymer," *Sci. Rep.*, vol. 7, no. 1, pp. 1–11, 2017.

[32] A. Loppinet, S. Iakovlev, and P. Glenat, "Five years of injection of hydroxyethylcellulose: An ecological pure product for enhanced oil recovery in the field of Romashkino," *Offshore Eur. Conf. - Proc.*, pp. 39–43, 1997.

[33] Yukihiko Sekimoto and Okamoto Osamu, "United States Patent (19) Sekimoto et al. (54) EQUIPMENT FOR DISSOLVING POLYACRYLAMDE POWDER FOR," 25-Mar-1983.

[34] J. Bai, F. R. Wassmuth, R. W. Jost, and L. Zhao, "Hydrophobically-Modified Cellulosic Polymers for Heavy Oil Displacement in Saline Conditions," *SPE Heavy Oil Conf. - Canada 2012*, pp. 1–9, 2012.

[35] E. Akiyama, T. Yamamoto, Y. Yago, H. Hotta, T. Ihara, and T. Kitsuki, "Thickening properties and emulsification mechanisms of new derivatives of polysaccharide in aqueous solution. 2. The effect of the substitution ratio of hydrophobic/hydrophilic moieties," *J. Colloid Interface Sci.*, vol. 311, no. 2, pp. 438–446, 2007.

[36] A. L. Kjøniksen, N. Beheshti, H. K. Kotlar, K. Zhu, and B. Nyström, "Modified polysaccharides for use in enhanced oil recovery applications," *Eur. Polym. J.*, vol. 44, no. 4, pp. 959–967, 2008.

[37] G. Zhao, C. C. Khin, S. B. Chen, and B. H. Chen, "Nonionic surfactant and temperature effects on the viscosity of hydrophobically modified hydroxyethyl cellulose solutions," *J. Phys. Chem. B*, vol. 109, no. 29, pp. 14198–14204, 2005.

[38] E. Fadda and R. J. Woods, "Molecular simulations of carbohydrates and protein-carbohydrate interactions: Motivation, issues and prospects," *Drug Discovery Today*. 2010.

[39] D. Frenkel, B. Smit, J. Tobochnik, S. R. McKay, and W. Christian, "Understanding Molecular Simulation," *Comput. Phys.*, 1997.

[40] J. M. Haile, I. Johnston, A. J. Mallinckrodt, and S. McKay, "Molecular Dynamics Simulation: Elementary Methods," *Comput. Phys.*, 1993.

[41] D. S. Sholl and J. A. Steckel, *Density Functional Theory: A Practical Introduction*. 2009.

[42] F. Jensen, "Force Field Methods," in *Introduction to Computational Chemistry*, 1999.

[43] M. L. S. Batista, G. Pérez-Sánchez, J. R. B. Gomes, J. A. P. Coutinho, and E. J. Maginn, "Evaluation of the GROMOS 56ACARBO Force Field for the Calculation of Structural, Volumetric, and Dynamic Properties of Aqueous Glucose Systems," *J. Phys. Chem. B*, vol. 119, no. 49, pp. 15310–15319, 2015.

[44] R. J. Woods, "Predicting the Structures of Glycans, Glycoproteins, and Their Complexes," *Chem. Rev.*, vol. 118, no. 17, pp. 8005–8024, 2018.

[45] M. Kunieda, K. Nakaoka, Y. Liang, and C. R. Miranda, "Self-Accumulation of Aromatics at the Oil - Water Interface through Weak Hydrogen Bonding," no. 17, pp. 18281–18286, 2010.

[46] S. Abdel-Azeim and M. Y. Kanj, "Dynamics, Aggregation, and Interfacial Properties of the Partially Hydrolyzed Polyacrylamide Polymer for Enhanced Oil Recovery Applications: Insights from Molecular Dynamics Simulations," *Energy and Fuels*, vol. 32, no. 3, pp. 3335–3343, 2018.

[47] P. Raffa, A. A. Broekhuis, and F. Picchioni, "Polymeric surfactants for enhanced oil recovery: A review," *J. Pet. Sci. Eng.*, vol. 145, pp. 723–733, 2016.

[48] V. Sahni, R. M. Dean, C. Britton, D. H. Kim, U. Weerasooriya, and G. A. Pope, "The role of co-solvents and co-surfactants in making chemical floods robust," *Spe 130007*, no. 1976, 2010.

[49] R. G. Prasad, "Enhanced Oil Recovery by using Polymer Flooding in Oil and Gas Industry in Tertiary Recovery," vol. 6, no. I, pp. 2146–2153, 2018.

[50] S. Abbas, A. W. Sanders, J. C. Donovan, and D. Oil, "SPE 165311 Applicability of Hydroxyethylcellulose Polymers for Chemical EOR," no. July, pp. 2–4, 2013.

[51] S. S. Hu *et al.*, "Influence of crude oil components on interfacial dilational properties of hydrophobically modified polyacrylamide," *Energy and Fuels*, vol. 29, no. 3, pp. 1564–1573, 2015.

[52] W. Pu, C. Shen, B. Wei, Y. Yang, and Y. Li, "A comprehensive review of polysaccharide biopolymers for enhanced oil recovery (EOR) from flask to field," *J. Ind. Eng. Chem.*, vol. 61, no. December, pp. 1–11, 2018.

[53] C. Wang, P. Liu, Y. Wang, Z. Yuan, and Z. Xu, “Experimental Study of Key Effect Factors and Simulation on Oil Displacement Efficiency for a Novel Modified Polymer BD-HMHEC,” *Sci. Rep.*, vol. 8, no. 1, pp. 1–9, 2018.

[54] D. A. Z. Wever, F. Picchioni, and A. A. Broekhuis, “Polymers for enhanced oil recovery: A paradigm for structure-property relationship in aqueous solution,” *Prog. Polym. Sci.*, vol. 36, no. 11, pp. 1558–1628, 2011.

[55] M. Laschet, J. P. Plog, C. Clasen, and W. M. Kulicke, “Examination of the flow behaviour of HEC and hmHEC solutions using structure-property relationships and rheo-optical methods,” *Colloid Polym. Sci.*, vol. 282, no. 4, pp. 373–380, 2004.

[56] B. Hess, C. Kutzner, D. Van Der Spoel, and E. Lindahl, “GRGMACS 4: Algorithms for highly efficient, load-balanced, and scalable molecular simulation,” *J. Chem. Theory Comput.*, vol. 4, no. 3, pp. 435–447, 2008.

[57] W. L. Jorgensen, D. S. Maxwell, and J. Tirado-Rives, “Development and testing of the OPLS all-atom force field on conformational energetics and properties of organic liquids,” *J. Am. Chem. Soc.*, vol. 118, no. 45, pp. 11225–11236, 1996.

[58] W. L. Jorgensen and J. Tirado-Rives, “The OPLS [optimized potentials for liquid simulations] potential functions for proteins, energy minimizations for crystals of cyclic peptides and crambin,” *J. Am. Chem. Soc.*, vol. 110, no. 6, pp. 1657–1666, 2005.

[59] S. H. Jamali, T. Van Westen, O. A. Moultos, and T. J. H. Vlugt, “Optimizing Nonbonded Interactions of the OPLS Force Field for Aqueous Solutions of Carbohydrates: How to Capture Both Thermodynamics and Dynamics,” *J. Chem. Theory Comput.*, vol. 14, no. 12, pp. 6690–6700, 2018.

[60] H. J. C. Berendsen, J. R. Grigera, and T. P. Straatsma, “The missing term in effective pair potentials,” *J. Phys. Chem.*, vol. 91, no. 24, pp. 6269–6271, 1987.

[61] M. Castaldi *et al.*, “Transport Properties of the Binary System Glucose - Water at 25 ° C. A Velocity Correlation Study,” vol. 9568, no. 98, pp. 653–657, 1998.

[62] V. R. N. Telis, J. Telis-Romero, H. B. Mazzotti, and A. L. Gabas, “Viscosity of aqueous carbohydrate solutions at different temperatures and concentrations,” *Int. J. Food Prop.*, 2007.

[63] T. Darden, D. York, and L. Pedersen, “Particle mesh Ewald: An N·log(N) method for Ewald sums in large systems,” *J. Chem. Phys.*, vol. 98, no. 12, pp. 10089–10092, 1993.

[64] J. G. E. M. Hess, B., Bekker, H., Berendsen, H.J.C. & Fraaije, “LINCS: A linear constraint solver for molecular simulations. Journal of Computational Chemistry,” *J. Comput. Chem.*, vol. 18, no. 18, pp. 1463–1472, 1997.

[65] A. S. Lemak and N. K. Balabaev, “On the berendsen thermostat,” *Mol. Simul.*,

1994.

[66] R. Martoňák, A. Laio, and M. Parrinello, “Predicting Crystal Structures: The Parrinello-Rahman Method Revisited,” *Phys. Rev. Lett.*, 2003.

[67] J. Brillo, A. I. Pommrich, and A. Meyer, “Relation between self-diffusion and viscosity in dense liquids: New experimental results from electrostatic levitation,” *Phys. Rev. Lett.*, vol. 107, no. 16, pp. 1–4, 2011.

[68] S. Abdel-azeim, “Revisiting OPLS-AA Force Field for the Simulation of Anionic Surfactants in Concentrated Electrolyte Solutions,” 2020.

[69] A. A. Chialvo and L. Vlcek, “Toward the understanding of hydration phenomena in aqueous electrolytes from the interplay of theory, molecular simulation, and experiment,” *Fluid Phase Equilib.*, vol. 407, pp. 84–104, 2015.

[70] Y. Zhang, A. Otani, and E. J. Maginn, “Reliable Viscosity Calculation from Equilibrium Molecular Dynamics Simulations: A Time Decomposition Method,” *J. Chem. Theory Comput.*, vol. 11, no. 8, pp. 35

Chapter 6 Vitae

Name :Mohammed Bazaid

Nationality :Saudi

Date of Birth :2/6/1994

Email :eng.mohbazd@gmail.com

Address :Saudi Arabia, Makkah, Aziziah Distract, Al-Amudi St , Postal code: 24235.

Academic Background :BSc in Mechanical Engineering from King Fahd University of Petroleum and Minerals. Especiallized in Computaitional material sicence, specifically Molecular Dynamics (MD) and Density Functional Theroy (DFT). Expreinced in GROMACS and LAMMPS softwares for MD and moderate knowledge about VASP in DFT. Inerested in applications related to energy.